NOTICE

The quality of this microform is heavily dependent upon the quality of the original thesis submitted for microfilming. Every effort has been made to ensure the highest quality of reproduction possible.

If pages are missing, contact the university which granted the degree.

Some pages may have indistinct print especially if the original pages were typed with a poor typewriter ribbon or if the university sent us an inferior photocopy.

Reproduction in full or in part of this microform is governed by the Canadian Copyright Act, R.S.C. 1970, c. C-30, and subsequent amendments.

AVIS

La qualité de cette microforme dépend grandement de la qualité de la thèse soumise au microfilmage. Nous avons tout fait pour assurer une qualité supérieure de reproduction.

S'il manque des pages, veuillez communiquer avec l'université qui a conféré le grade.

La qualité d'impression de certaines pages peut laisser à désirer, surtout si les pages originales ont été dactylographiées à l'aide d'un ruban usé ou si l'université nous a fait parvenir une photocopie de qualité inférieure.

La reproduction, même partielle, de cette microforme est soumise à la Loi canadienne sur le droit d'auteur, SRC 1970, c. C-30, et ses amendements subséquents.

ISBN 0-315-56045-2

Vibration Isolation Using Hydraulic Mounts With Dual-Phase Damping

Seshadri Venkatesh

A Thesis

in

The Department

of

Mechanical Engineering

Presented in Partial Fulfillment of the Requirements
for the Degree of Master of Engineering at
Concordia University
Montréal, Québec, Canada

December 1989

ABSTRACT

Vibration Isolation Using Hydraulic Mounts With Dual-Phase Damping

Seshadri Venkatesh

Isolators, such as those applied to engine mount for isolation of engine induced vibration demand performance over a wide frequency range. This results primarily from low speed idle shake and high speed unbalance. Conventional rubber-metal mounts or passive hydraulic mounts provide effective isolation in a limited frequency range and are thus considered inadequate. Although, semi-active devices have the potential for improved performance in such applications, a low cost alternative vibration isolation system is investigated.

In this study, the vibration isolation characteristics of a hydraulic mount with a dual-phase damper is investigated for application to mass induced vibration. Hydraulic mounts based on dual-phase damping control offers a compromise between semi-active and passive mount systems. The dual-phase damper, based on relative displacement requires no external power for modulating its orifice for fluid flow and is essentially a passive device. Two types of displacement dependent dual-phase dampers are studied under similar conditions and the vibration isolation performance of the dual-phase dampers is evaluated in terms of transmissibility. The performance characteristics of the

dual-phase dampers are compared to those of the passive hydraulic mounts to demonstrate the superior performance of the dual-phase damped hydraulic mount. For a selected dual-phase damping concept, a prototype was built and tested in the laboratory to carry out performance evaluation and validation of the analytical model.

ACKNOWLEDGEMENTS

I wish to express my deep appreciation and gratitude to my thesis supervisors Dr. S. Sankar and Dr. A.K.W. Ahmed for their dedicated guidance, support, friendship and encouragement during the course of this investigation.

Thanks are due to Dr. S. Rakheja and other faculty members, graduate students and staff of CONCAVE Research Centre and the Department of Mechanical Engineering at Concordia University for their help during the course of this work. Special thanks are due to Mr.Frank Marsman, Mr.Dale Rathwell, Mr.Moses Levy and Mr.R.Ranganathan.

The financial support in the form of research assistantship provided by CONCAVE Research Centre, Department of Mechanical Engineering at Concordia University is gratefully acknowledged.

Finally, I would like to express my appreciation for the personal encouragement provided by my mother, sister, Murthy and other family members.

DEDICATED TO

MY FATHER AMPLE.V.SESHADRI

TABLE OF CONTENTS

CHAPTER 3

SIMULATION RESULTS AND DISCUSSIONS ON DUAL-PHASE DAMPER

CHAPTER 4

EXPERIMENTAL INVESTIGATION

CHAPTER 5

CONCLUSIONS AND RECOMMENDATIONS FOR FUTURE WORK

LIST OF FIGURES

LIST OF TABLES

NOMENCLATURE

Symbol	Description
A_o	area of orifice[m^2]
BDC	bottom dead centre
C, C_1, C_2	damping coefficient[N-s/m]
C_d	coefficient of discharge
C_{eq}	equivalent damping coefficient[N-s/m]
com	compression
DOF	degree of freedom
d	pin diameter[m]
D_o	orifice diameter[m]
D_p	inside diameter of the tube[Fig.4.3]
e	eccentricity[m]
ext	extension
Expt	experimental data
F(t)	excitation force
F_d	damping force[N]
F_k	spring force[N]
F_n	undamped natural frequency of the system[Hz]
F_o	centrifugal force[$me\omega^2$]
K, K_1	spring stiffness[N/m]
K_d	dynamic stiffness[N/m]
K_s	static stiffness[N/m]
L	length of connecting rod[m]
LVD	linear viscous damper

M	mass of the engine[Kg]
m	eccentric mass or unbalanced mass[Kg]
N	spring stiffness ratio[K_1/K]
N^*	spring stiffness ratio[K/K_1]
Q	flow rate[m^3/s]
R	crank radius[m]
r	frequency ratio[ω/ω_n]
Simu	simulation data
T	force transmissibility
TDC	top dead centre
T_{FC}	turbulent flow coefficient[Kg/m]
T_r	magnification ratio[Mx/me]
ω	angular velocity[rad/s]
ω_n	natural frequency of the system[rad/s]
ωt	crank angle
X	sprung mass displacement[m]
X_p	displacement of piston[m]
α_1, α_2	nondimensional displacement
β_1, β_2	nondimensional displacement
Δp	pressure drop across the orifice
ρ	mass density of fluid[Kg/m^3]
τ	period[s]
ζ, ζ_1, ζ_2	damping ratio
ζ_{eq}	equivalent damping ratio

CHAPTER 1

INTRODUCTION AND LITERATURE REVIEW

1.1 General Introduction

Isolation of vibrations in vehicles has continued to be a major area of research, to achieve improved performance. The presence of vibration in vehicles and in particular, vibration resulting from engine leads to undesirable effects such as structural failure, expensive maintenance and human discomfort. An engine which is well mounted is not only pleasant to ride, but also reduces driver's fatigue. Further, in the modern competitive market, consumers are also becoming more aware of the noise and vibration levels inside the vehicle, ride comfort on different types of road surfaces, fuel efficiency and reliability of the vehicle. Hence, all this has stimulated new interest in the study of isolation of engine induced vibration. The primary objective in developing isolators for engine mount is to provide improved performance over a wide frequency range. Such performance cannot be provided by conventional rubber-metal mounts or passive hydraulic mounts. However, a dual-phase damper can provide a compromise not only in performance but also in cost. This investigation looks at a general case of vibration isolation using dual-phase concepts. Dual-phase damper concept is being studied because of its capability to provide low as well as high damping or vice versa. Hence, this concept can be utilized in engine mount applications. In the following sub-sections the vibration characteristics of engine and use of conventional isolators in mount applications are discussed.

1.1.1 Vibration Characteristics of Engine

The emphasis on fuel efficiency has resulted in a trend towards smaller and lighter vehicles powered by four-and six-cylinder engines. However, these smaller engines with lighter and more flexible vehicle frames have led to increased frame vibration. Engine induced vibration transmitted to the passenger through the chassis is an undesirable factor. Thus, in an effort to protect the vehicle and the passengers, the automobile industry uses engine mounts for vibration isolation. The isolator is placed between the engine and the frame. The purpose of the isolator is to reduce the force transmitted to the frame, and in turn to the passengers, by absorbing the force. The isolator or the engine mounting system consists of three or four elastomeric mounts supporting the engine and the gearbox unit. The essential features of a vibration isolator are the resilient load supporting capability [springs] and energy dissipating capability [dampers]. In certain types of isolators, these two functions of load support and energy dissipation may be performed by a single element. In other isolators, the resilient load carrying devices may lack sufficient energy dissipating characteristics. In such cases, separate and distinct energy dissipating devices are provided.

The mounts, in addition to supporting the engine are expected to minimize frame twisting, resist and/or isolate dynamic loads, limit engine motion and provide acceptable service life. The mount selection is based on the performance desired. The vibration isolation in turn depends on a number of factors such as mount location, mount material,

mount size, number of mounts and the like.

The internal combustion engine used in automobiles produce two basic types of vibration, namely [1, 2]*:

1. Vibration due to rotating and reciprocating motions of the moving parts; and
2. Vibration due to periodic variation in the cylinder gas pressure caused by imperfect mixing in the cylinders.

The essential moving elements of an internal combustion engine are: the piston, the connecting rod, and the crankshaft. The purpose of a piston, connecting rod and crankshaft in an internal combustion engine is to convert the heat generated due to combustion of the fuel in the cylinder into reciprocating piston movement and the crankshaft in turn, converts this motion into useful torque. This cyclic operation leads to variation in gas pressure and the acceleration and deceleration of the reciprocating parts generates inertial forces. A general arrangement of a piston, a connecting rod and a crankshaft is illustrated in Fig.1.1 where;

X_p = downward displacement of piston from top,

ωt = crank angle from the top dead center,

R = crank radius, and

L = length of the connecting rod.

---

* Numbers in square brackets designate references at the end of thesis

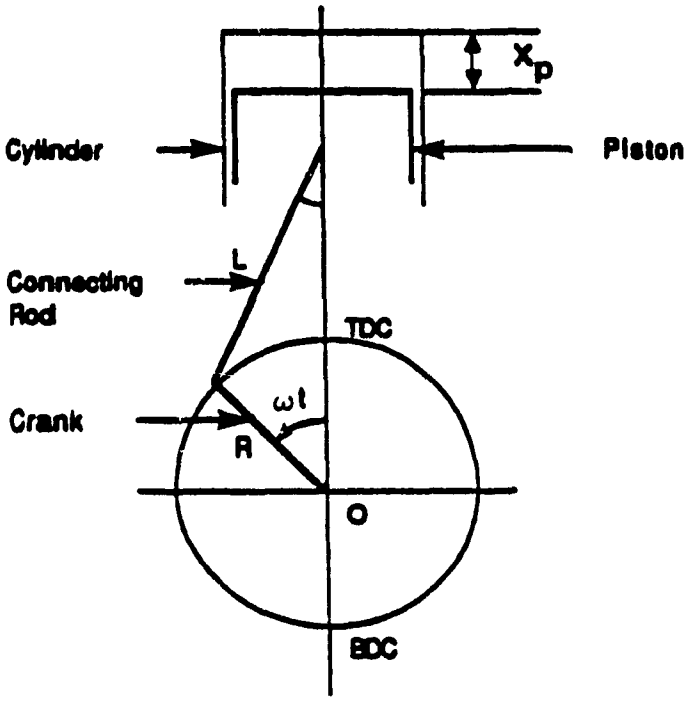

Fig. 1.1 Schematic of crank mechanism

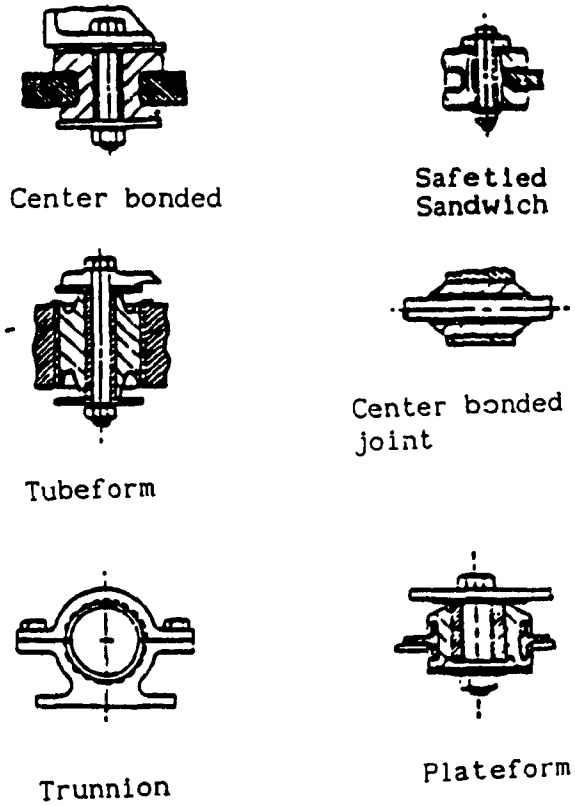

Fig. 1.2 Schematic of typical elastomeric mounts[2]

The gas pressure applied periodically to the piston imposes a force on the piston and the reaction upon the chassis of the engine takes the form of a couple. This couple tries to rotate the engine about an axis parallel to the crankshaft. Similarly, the rotating and reciprocating motion give rise to inertial forces and torques. The inertial force acts along the piston axis as well as perpendicular to the crank and piston axis. Whereas, the inertial torque will act about an axis which is parallel to the crank. The vibrations caused by these forces are transmitted primarily through the engine mounts. Hence, the engine mounts are a critical component as far as the isolation of vibration and noise levels inside the vehicle is concerned. Mount stiffness, location and inclination are some of the factors which are critical for either elimination or reduction of vibration. Consequently, in recent years, importance is given to engine mount technology with the objective of reducing engine induced vibrations.

1.1.2 Conventional Engine Mounts

The most commonly used engine mounts are the rubber mounts. Fig. 1.2 illustrates typical rubber mounts used in automobiles [2]. Rubber mounts have been accepted as standard for many years in automobile industry for vibration isolation because of certain inherent advantages like low modulus of elasticity and their capability to sustain deformation of as much as 1000 percent [3]. After any deformation, it quickly and forcibly restores back to its original dimensions. They are resilient and yet exhibit internal damping.

Further, they can be manufactured to any shape and size and have the capability to adhere to metal inserts or mounting plates. Also, their properties can be changed to obtain predominantly favorable characteristics for a particular application by adding different compounds, however, with some deterioration of other properties. In addition, rubber does not corrode and generally does not require any lubrication. Finally, its low cost, no maintenance, availability and ease of manufacture makes it the right choice for vibration isolation. But studies have shown that engine mounts made of rubber suffer from low damping rates at low excitation frequencies and the stiffness increases with increase in frequency or decrease in temperature [3,4]. Since engine vibration levels are critical during idling speeds [low frequencies], rubber mounts are inadequate for effective isolation of engine isolations.

Finally, the quality of vibration isolation depends on the type of engine mount. The criteria for selecting the best type of engine mount depends on a number of factors as discussed previously. To achieve the goal of minimizing the effect of engine vibration, one can modify the engine suspension. Accordingly, hydraulic mounts were developed. At low frequencies, the hydraulic mounts provide higher damping than the conventional rubber mounts. However, in case of hydraulic mounts, because of a fixed orifice the damping properties are fixed, irrespective of the force transmitted. With this type of hydraulic mount, the goal of isolating the vibration over a wide frequency range is not fulfilled. This has led to the search for alternate mount system. It is clear that the desirable requirement for an engine mount is the

performance over wide frequency range. This can be achieved utilizing a semi-active or even better, an actively controlled suspension system for the engine mount. However, a semi-active or an active system has a significant price tag in terms of initial cost, power requirement as well as maintenance. Such concepts are therefore, not a practical or viable solution for engine mount or similar applications. The solution perhaps lies in utilizing a passive dual-phase damper which is slightly more complex than the hydraulic mounts. In the following sections, a detailed review of the previous studies on hydraulic engine mount is presented so as to develop the scope of the present investigation.

1.2 State-of-the-Art and Literature Review

An examination of previously published literature in the area of vehicle system vibration clearly reveals that although vibration is one of the most widely studied subject, little attention has been directed towards the isolation of engine induced vibrations.

During the past several years, extensive research has been initiated on passive, semi-active and active vehicle suspension in order to improve the ride quality, handling, and stability of vehicles[5-12]. In these studies, the engine induced vibration was however not considered as one of the factors responsible for poor ride quality. It has been found that the frame vibration is very significant at engine idle speeds, which for a four cylinder engine is in the range of 10 to 20Hz[13].

The use of rubber mounts for engine support can be traced back to the time when vehicles were first developed. These mounts in different shapes and forms can still be found in the majority of vehicles on the road today mainly due to the fact that they are highly cost effective with reasonable performance. In the early 60's, Butyl rubber was used for making rubber mounts because of its high damping characteristic which was necessary to control the idle shake of an engine. Later on, natural rubber replaced Butyl rubber because of certain advantages like low damping in the high frequency range and slower deterioration characteristics resulting in longer life. The engine mounts have to resist high temperature. Normally the temperature in the engine compartment will vary between 100 to 200^{o} F. Further, due to cyclic deformation of rubber, enormous amount of heat will be generated which makes the rubber soft, resulting in its early failure. The dynamic loads transmitted to the chassis depends on the stiffness of the mounts and good isolation can be achieved by simply having softer mounts. But by softening the conventional rubber mounts, other problems such as engine displacement will be encountered; that is, if mounts are very soft and the vehicle travels on rough roads, very large clearances should be provided in order to make room for large amplitudes of vibration. Further, the mounts will not last long because the large displacements will reduce the strength of the rubber. Hence in order to overcome the above problem, a stiff and highly damped mount must be used. But high level of damping always brings in high dynamic stiffness. This will result in a conflict between vibration isolation and rattle space. The above drawbacks along with its poor isolation characteristics at low frequencies (or idling) has led to the search for an alternate mount

system.

Schmitt and Leingang[2] have discussed the sources of vibration in internal combustion engines. They have also listed a number of factors that are to be considered while developing engine mounts. A brief description of various types of rubber mounts and their installation was presented.

Racca[14] has given an overview of the various factors that are to be considered while selecting elastomeric isolators for vibration isolation in the case of off-highway vehicles. Halvorsen[15] has described the design of rubber isolation systems for vibration isolation in automobiles. He has reviewed various methods that are available to study the dynamic properties of rubber. He has studied the influence of temperature and frequency on the stiffness and damping characteristics of rubber isolators.

The most recent development in the engine mount technology is the introduction of hydraulic mounts. A number of individual manufacturers have developed a variety of hydraulic mounts with similar basic principles, but with minor modifications in design and appearance. Figs. 1.3(a) to 1.3(f) illustrate some of the recently introduced hydraulic mounts. The hydraulic mount performance depends on mount geometry, orifice size, rubber type and the damping fluid. Generally, an antifreeze solution is used as the damping fluid.

The passive hydraulic mount was first introduced by Marc

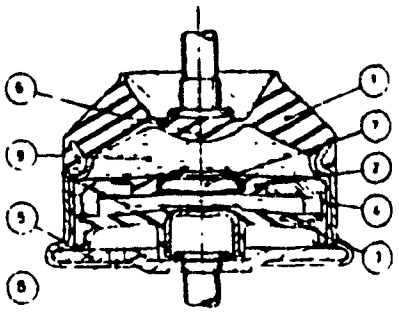

Fig. 1.3(a) Schematic of hydraulic mount[13]

1. Main spring 2. Secondary spring 3. Auxillary spring
4. Damping channel 5. Closing plate 6. Rubber buffer
7. Reaction pad 8. Support columr 9. Viscous fluid

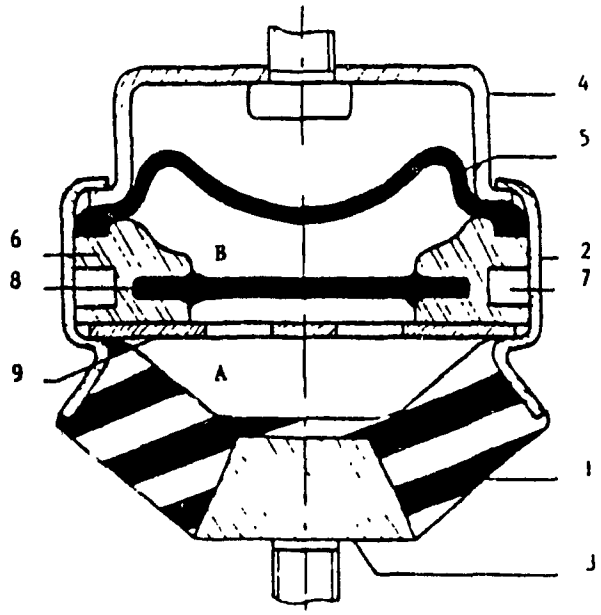

Fig. 1.3(b) Schematic of hydraulic mount[16]

1. Main rubber element 2 & 3. Metallic parts 4. Cover
5. Membrane bellow 6. Diaphragm 7. Circular channel
8. Elastic membrane 9. Perforated disc. A & B: Chambers

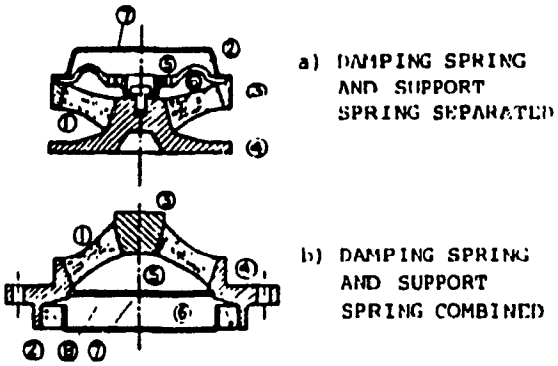

Fig. 1.3(c) Schematic of hydraulic mount[17]

1 Suspension spring 2. Damping spring 3. Outer ring
4. Attachment flange 5. Upper chamber 6. Lower chamber
7. Orifice 8. Inner plate

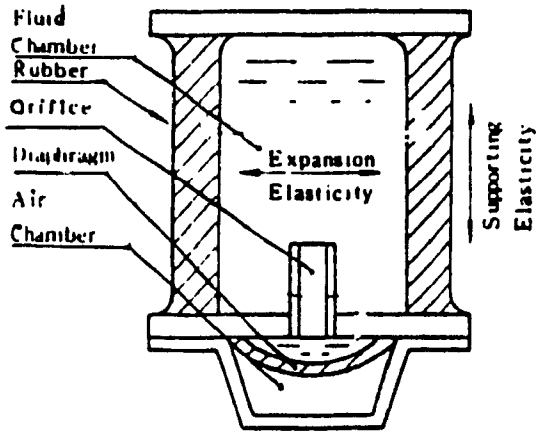

Fig. 1.3(d) Schematic of hydraulic mount[18]

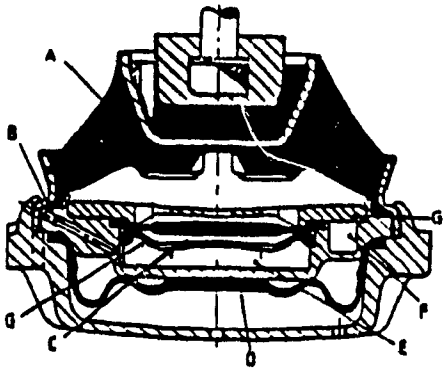

Fig. 1.3(e) Schematic of hydraulic mount[21]

A. Top element B. Air vent C. Diaphragm D. Bellow E. Air space F. Damping Orifice G. Snubber plates

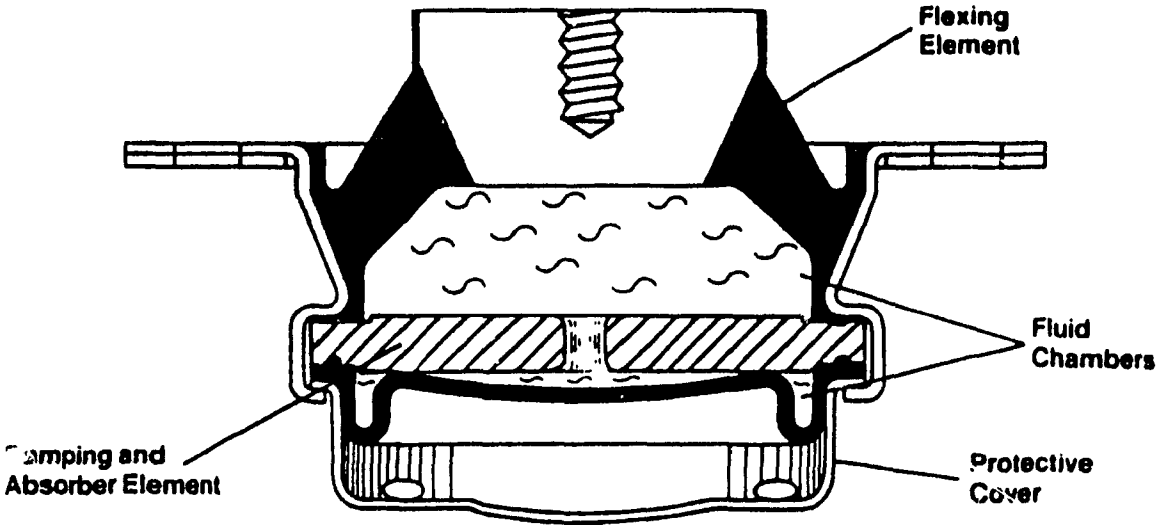

Fig. 1.3(f) Schematic of hydraulic mount[22]

Bernuchon[16]. These mounts were developed to overcome the conflict between vibration isolation and engine bounce. These mounts can have a softer rubber than that used in conventional rubber mounts resulting in better isolation. The fluid in the chamber provides the necessary damping to overcome the engine bounce. The main components of the passive hydraulic mounts are the primary rubber element which support the engine load and also acts as a piston to pump an incompressible fluid between two internal chambers connected by an orifice. These mounts are called passive mounts because they do not require any external power and can dissipate and temporarily store energy. These mounts produce a resistive force against any input force independent of the rate at which the force is applied.

On the other hand, active hydraulic mounts have the capability to supply energy when desired as well as dissipate energy. In active systems, the ideal force generator replaces the passive damper. This extraordinary vibration isolation capability of an active vibration control system is attributed to the active force that is dependent on the system response and/or excitation variables. The active vibration control system, in order to provide the best isolation requires an external energy source, controllers and sophisticated control system with a large number of sensors. Hence, an ideal active vibration control system can be described as one in which the damping force is generated by an actuator with the help of external power, and modulated by a sophisticated force controlling device. Thus the controlled actuator is a servomechanism that has the capability to absorb or generate the energy that is necessary to minimize the force transmitted. All these

add up to the cost and make the system expensive, complex, bulky and less reliable. Hence, the application of active vibration control systems are limited to cases where performance gains outweigh the above disadvantages.

A compromise between a passive and active hydraulic mount can be achieved using a semi-active hydraulic mount. The concept of semi-active vibration isolation using active damper was introduced for vehicle suspension by Karnopp and Crosby[6]. According to them, the performance of semi-active control system approaches that of an active control system. The semi-active control does not require any external power. Here, the damping forces are generated in a damper by modulating its orifice area. The semi-active control requires only low level electric power for signal processing and for valve actuation. In a semi-active system the ideal force generator will be substituted by a damper, whose damping coefficient C can be varied over a high bandwidth. Thus, a semi-active system generates damper forces passively and these can be modulated continuously by a very small external power source. When the damper force and the required force are equal and are of same sign, the damper will be on, and if they are of opposite sign, it is off, meaning that no force will be generated. The performance of a semi-active system can approach the performance of a fully active system, if one judiciously chooses the semi-active control strategy.

As pointed out earlier, the technology sophistication and cost associated with semi-active suspension with controller cannot be justified for applications such as engine mounts in vehicles. As a

result, majority of researchers have been directing there attention on improved low cost passive devices.

Clark[13] has analyzed a passive hydraulic mount by modelling as a three-degree-of-freedom elastically coupled linear viscous damper system. He investigated the optimum performance level of his model for engine induced vibration and road inputs. He observed that large stiffness ratio helps to achieve low frequency isolation, by lowering the peak transmissibility values. But this will be at the cost of high frequency isolation. He concluded that the best isolation is provided by very soft mounts. On the other hand, increased stiffness is required for acceptable fatigue life. Hence the optimum stiffness rate and damping value will be different for different input conditions and the overall performance depends on the particular vehicle being studied.

Marc Bernuchon[16] compared the performance of conventional rubber mounts with passive hydraulic mounts. The passive hydraulic mount was represented by a single-degree-of-freedom model for a sinusoidal input excitation of constant amplitude. An experimental study was also presented. Based on his study he concluded that, in rubber mounts the dynamic stiffness increases with the increase in frequency. However, the maximum value of the dynamic stiffness was lower when hydraulic mount was used. This was attributed to the fact that the hydraulic mount behaved as a vibration absorber. Also, there was substantial improvement in the acoustic levels when hydraulic mounts were used. The improvement was of the order of 5 to 6 db.

Corcoran and Ticks[17] studied passive hydraulic mount by modelling it as a single-degree-of-freedom model with an elasto-damper in parallel with a linear spring with the objective of overcoming engine bounce, idle shake and noise inside the vehicle. Field trials were conducted on a six-cylinder in-line and V-engines. From their experimental study they found that there was a 5 db decrease in the noise level when hydraulic mounts was used.

Masaru Sugino[18] developed and studied the hydro-elastic engine mount. He describes his mount as a velocity amplifying dynamic damper, because the mass of the fluid inside the orifice is increased due to velocity amplification and thus increases the damping effect. His study was aimed at reducing the engine shake due to base excitation. He concluded that the resonant frequency of fluid inside the orifice should match the engine shake frequency when the orifice is closed.

Fowler[19] has proposed three different types of fluidlastic mount models. He has studied the influence of having a short and a long orifice between the top and bottom chamber of a fluidlastic mount. The first model was a mount with short orifice and he observed that by having a short orifice, the stiffness will vary gradually and the damping will be more pronounced. Hence, by having a short orifice it will be possible to provide damping over an operating frequency range. In his second model he replaced the short orifice by a long orifice or inertia track [A tube of known length and cross sectional area. The tube is called inertia track because it guides the fluid flow between the top and bottom chambers]. He observed that the long orifice is useful where

a high level of damping is necessary over a narrow band. In his third model, he introduced a decoupler along with the inertia track. He found that the decoupler provides high damping at large amplitudes and low frequency and low damping at low amplitudes and high frequency.

Shoureshi and Graf[20] proposed a continuous type, semi-active hydraulic mount system. The model was analyzed by making three assumptions: the frame is rigid; the fluid is incompressible and newtonian; and the nonlinear model can be linearised. Experiments were also conducted. The results indicated that the orifice area and injection pressure influence vibration isolation. They found that there was more than 20 db noise reduction when semi-active control was adapted.

The semi-active hydraulic mount suggested by West[21], utilizes vacuum to alter the mount characteristics. Accordingly, an external vacuum pump is used to control the diaphragm movement in the mount. By varying the vaccum level in the air space, he found that the damping level varies. A high level of vacuum produced high damping over a wide range of frequency and switching off the vacuum reduced the damping.

Mizuguchi et al[23] have tried to introduce an active control system to improve engine mount performance. They have developed a hydraulic mount with an orifice and a port. The fixed orifice is always left open and the opening and closing of the port is electronically controlled using a rotary solenoid. They found that by controlling the opening and closing of the port the damping and stiffness

characteristics of the mount can be varied resulting in better performance of the vehicle.

Yukihiko et al[24] have developed an active control system using an electro dynamic linear actuator, a controller and a power amplifier which drives the actuator. The active force generated by the actuator compensates the engine torque resulting in reduced vibration of the car body. Their experimental study showed that there was a 16 db reduction in vibration near the driver's seat.

Marjoram[25] has incorporated hydraulic mounts for vibration isolation in cabs. He has studied the effect of internal pressurization on the performance of engine mounts. He found that the suspended mass can be partially supported by pressurization, which in turn would reduce the strain on the primary support rubber.

Taylor[26] has given a general overview of hydraulic mount by considering four different models. He has studied a viscous damped hydraulic mount and then studied the influence of having a short and long orifice between the top and bottom chamber. He concludes that by having a short orifice, it is possible to decide damping over a wide frequency range. On the other hand, the long orifice, also called as inertia track are used where high level of damping is necessary over a narrow band. In the last model, a decoupler is introduced to bring into effect the decoupler effect.

The performance of a dual-phase viscous damped isolator system was

investigated for shocks by Snowdon[27]. According to him a dual-phase damper is expected to have a constant damping ratio equal to either ζ_1 or ζ_2 depending on whether the relative velocity across the damper terminals is either small or large. For intermediate velocities there will be a linear transition from one extreme value of the damping ratio to the other. He studied the system response by subjecting it to rounded pulse, rounded step and oscillatory step inputs at the base. From the study, he concluded that this type of isolator system is capable of bringing down the maximum values of absolute displacement and acceleration compared to systems with a linear viscous damper.

The response of a shock mount with dual-phase damping was investigated by Venkatesan and Krishnan[28 and 29]. The system was subjected to harmonic input. Here, the damping ratio was a function of the absolute value of the relative displacement. They concluded that by varying the damping parameters it is possible to reduce vibration transmissibility in the low frequency as well as high frequency range. They also studied the effect of introducing a dual-phase damper in an aircraft landing gear with the intention to minimize the peak acceleration transmitted to the aircraft structure.

Guntur and Sankar[30] have analyzed the performance of a single degree of freedom non-linear shock mount with six different types of dual-phase damping arrangement. The shock mounts were subjected to two displacement inputs, namely rounded pulse and oscillatory step. The performance was evaluated based on the maximum acceleration transmitted with respect to the shock severity factor.

1.3 Scope of the Present Study

A proper engine mount selection helps in several ways namely, they not only eliminate or reduce shock, noise and vibration but are also helpful in extending the fatigue life of other components, reducing the product downtime by minimizing maintenance and repair, improving the overall product performance and last but not least improves the safety and comfort of the driver and passengers. From a review of recent studies, it is evident that the performance of isolator for a mount can be evaluated with reasonable results by utilizing a single-degree-of-freedom model of a mass-spring-damper system. This approach has been taken in several studies on rubber and hydraulic mounts[13, 16, 17, 19 and 20].

The review of previous studies on engine mounts has further shown that the performance of isolators in such cases are generally evaluated through the maximum force transmitted to the frame and through the relative displacement across the mounting. The scope for improving the performance of either conventional rubber mounts or passive hydraulic mounts over a wide frequency range is limited. In overcoming certain drawbacks of a passive hydraulic mount, a practical and viable alternative is the dual-phase damping concept. This has the potential for improvement over a conventional passive device. Also, limited studies has been carried out on dual-phase damping. However, its potential for mount application has not been investigated. Furthermore, the concept has not been validated or evaluated through experiments.

Hence, in this study the performance of a hydraulic mount with dual-phase damping will be studied using a single-degree-of-freedom model to explore its potential in improving the vibration isolation performance in a mount application. Such a damping system has been selected due to its simplicity and practicality in implementation on majority of the vehicles. Furthermore, the model, depending on system parameters is valid for all vehicle systems including off-road vehicles, recreational vehicles as well as any machinery supported on a fixed base. The investigation is carried out using analytical models of various mount configuration with two types of displacement dependent dual-phase dampers. For a selected concept a prototype is built and tested in the laboratory.

Chapter 2, presents a detailed description of three different types of hydraulic mounts. This is followed by a description of the concept of dual-phase damping. Then two different types of dual-phase dampers are presented. In Type I dual-phase damper, the damping ratio is high, when the displacement is low and then the damping decreases with the increase in displacement. In Type II dual-phase damper the damping ratio is low when the displacement is low and increases with an increase in displacement. Finally, a method to determine the equivalent damping ratio is discussed.

In chapter 3, the results of introducing a dual-phase damper in place of a passive damper in a two-element and a four-element model is presented. Further, a parametric study on Type II two-element model is carried out. Finally the results from the study on two-element and

four-element models are compared with each other and with the visco-elastic model developed by Clark[13].

In chapter 4, the development of the damper, test procedure and results from the tests are presented. The test results are presented in two phases. In phase I the force-displacement characteristics of the damper are evaluated. In phase II, acceleration transmissibility and relative displacement ratio results are presented. Finally, the analytical results are compared to those obtained from experiment.

Finally in chapter 5, the conclusions and the recommendations for future work are presented.

CHAPTER 2

FORMULATION OF EQUATIONS OF MOTION FOR HYDRAULIC MOUNT MODELS

2.1 Introduction

The study is aimed at a detailed investigation of dual-phase damper as an isolator for machineries, such as an engine in a vehicle. The system input in such cases are primarily from unbalance and is introduced as mass induced vibrations. Ideally, to carryout vibration analysis realistically for an engine mount system, it should be modelled with three or four mounts and should include bounce, pitch as well as roll motions. However, introducing details of the problem in a study that is aimed at a new concept of isolation may lead to inaccurate or misleading interpretation of results pertaining to the influence of various parameters within the new concept. For initial investigation it is often more useful to consider simple models with detailed study of the concept and its isolation performance. The model considered in this investigation is that of a simple isolator with mass induced vibration input due to unbalance. Different isolation configuration with two types of dual-phase damping are considered. The models are sufficiently general, and can be applied to mounts for any rotating machinery.

In the following sub-sections, three different types of hydraulic isolators with the same basic parameters are presented and discussed. Following this, a detailed description of dual-phase damping characteristics is discussed with sketches to realize the above

characteristics. Finally, the method of determining the equivalent damping ratio for non-linear dual-phase damping considered in this study is presented.

2.2 Description of a Viscous Damped Hydraulic Mount Model

Fig. 2.1 illustrates a schematic of a single-degree-of-freedom, directly coupled, viscous damped hydraulic mount model. The mount consists of two elements, a linear spring K in parallel with a linear viscous damper C. The following four basic assumptions are made in order to accept the models developed. They are:

1. There is no input from the base, input is due to unbalance only.
2. The hydraulic fluid is incompressible.
3. The temperature effects on the fluid is negligible and
4. The base is fixed.
5. Isolator is constrained to move along vertical coordinate.

The equation of motion of the passive SDOF isolator illustrated in Fig. 2.1 can be written as

$$M\ddot{X} + C\dot{X} + KX = F_o e^{i\omega t} = F[t] \qquad (2.1)$$

This can be reduced to a non-dimensional form,

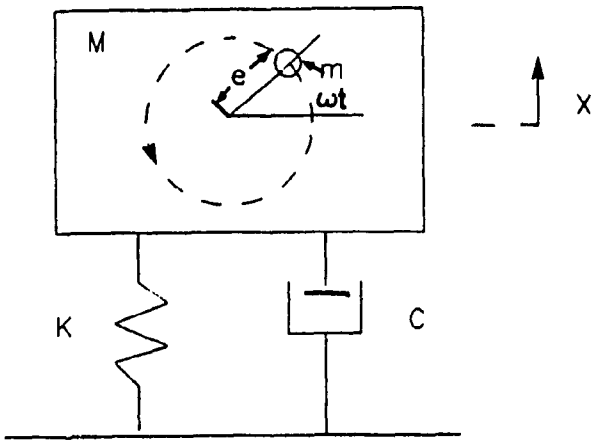

Fig. 2.1 Schematic of a two element passive mount

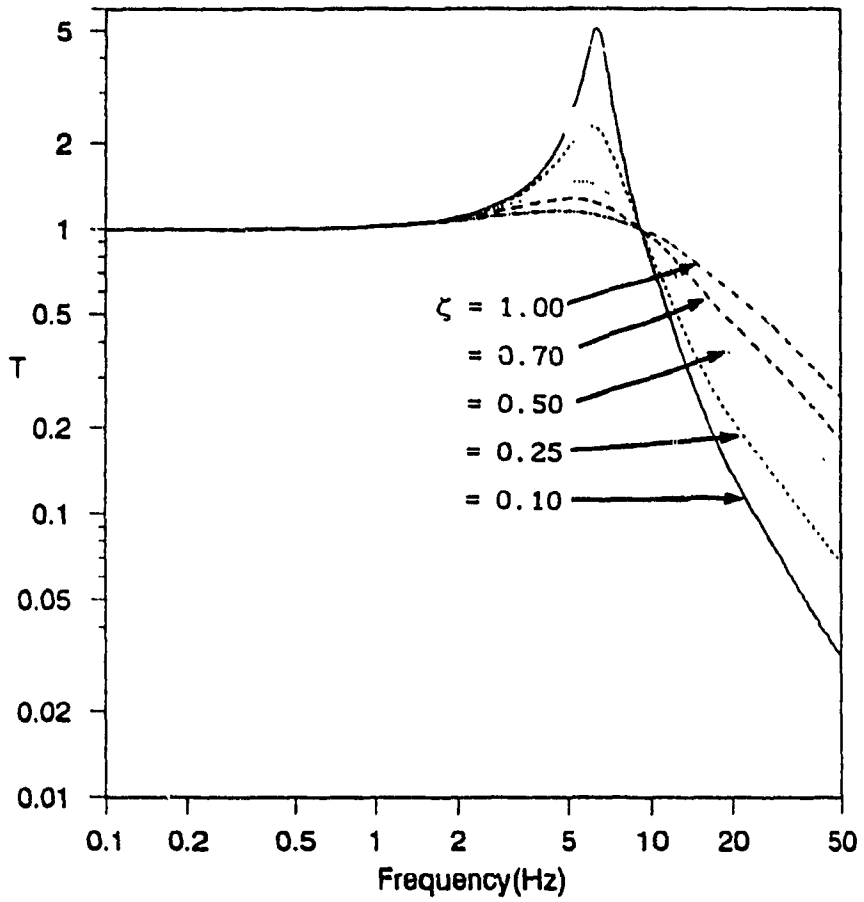

Fig. 2.2 Force transmissibility of a two-element passive mount

$$\frac{MX}{me} = T_r = \frac{r^2}{\sqrt{(1 - r^2)^2 + (2\zeta r)^2}} \qquad (2.2)$$

where

$\ddot{X}$ = the absolute acceleration of the mass

$\dot{X}$ = the absolute velocity of the mass

X = the absolute displacement of the mass

M = mass of the engine [240 kg]

K = the primary hydraulic mount stiffness [400 kN/m]

C = the damping setting of the hydraulic mount

$\omega_n = \sqrt{K/M}$, the undamped natural frequency of the system in rad/s

F_n = undamped natural frequency (6.5 Hz)

F[t] = excitation force = $F_o e^{i\omega t}$

$F_o = me\omega^2$, the Centrifugal force

m = eccentric mass

e = eccentricity = Stroke/2 (for engines)

ω = angular velocity of m

$\zeta = C/2\sqrt{KM}$, the viscous damping ratio

T_r = Magnification ratio

$r = \omega/\omega_n$

The quantities within brackets are the assumed values for M and K which represent a four-cylinder engine on a hydraulic mount[13].

The vibration isolation can be characterized by force transmissibility (where force transmissibility is defined as the ratio of the force transmitted to the magnitude of input force). Hence for the

passive mount system discussed above, the force transmissibility T is given by,

$$\frac{F_{tr}}{F_o} = T = \frac{\sqrt{1 + (2\zeta r)^2}}{\sqrt{(1 - r^2)^2 + (2\zeta r)^2}} \qquad (2.3)$$

where F_{tr} = amplitude of the transmitted force

Fig. 2.2 illustrates the force transmissibility vs frequency plot for the given engine mount parameters, and for various values of damping ratio, ζ. This plot shows the basic performance characteristics of most passive mounts. It can be observed from the above plot that, high damping values give good isolation in the resonant range at the expense of poor high frequency performance. However, low damping gives good isolation at high frequencies but poor performance in the resonant range and the transmissibility will be less than one if one operates the system at a frequency ratio greater than $\sqrt{2}$ [31].

2.3 Description of Hydraulic Mount Modelled as an Elastically Coupled Viscous Damper

The schematic diagram of a hydraulic mount with elastically coupled viscous damping is illustrated in Fig. 2.3. This is a three-element combination of an isolator having a damper with damping ratio ζ and two springs of stiffness K and K_1. This model was proposed by Clark[13] in

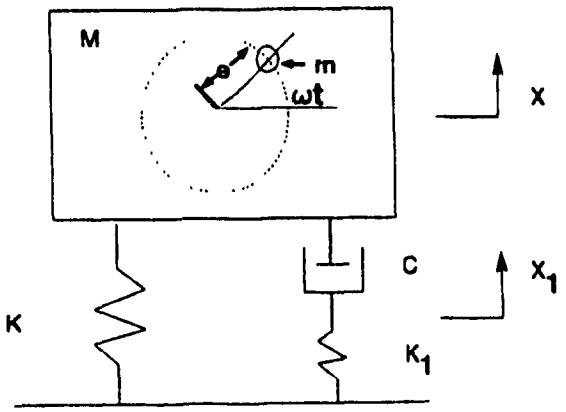

Fig. 2.3 Schematic of a three-element passive mount

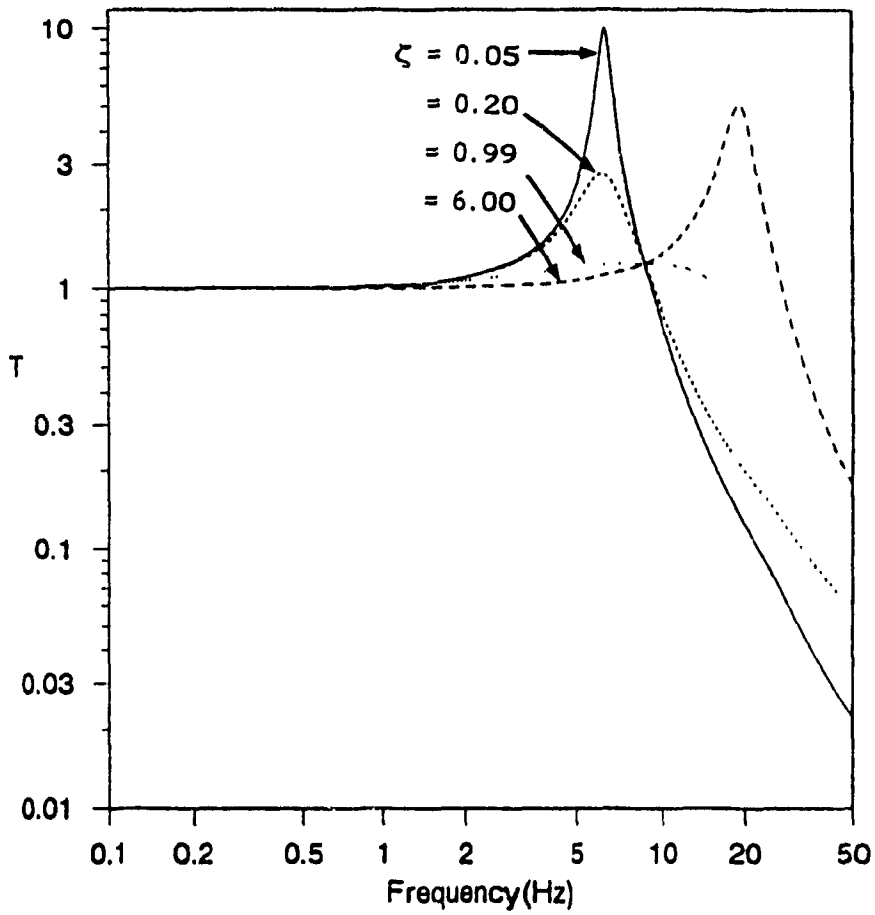

Fig. 2.4 Force transmissibility of a three-element passive mount for various values of damping ratio, with N = 8

an investigation of an isolator for engine vibration. The following are the equations of motion for the hydraulic mount shown in Fig. 2.3,

$$M\ddot{X} + C[\dot{X} - \dot{X}_1] + KX = F_o e^{i\omega t} = F[t] \tag{2.4}$$

Since the spring K_1 and the damper C are in series, the spring force is equal to the damping force,

$$K_1 X_1 = C[\dot{X} - \dot{X}_1] \tag{2.5}$$

Since the motion $X_1[t]$ and X[t] are harmonic, the above equations can be solved by the mechanical impedance method. So, the force transmitted is the sum of the forces transmitted through the springs K_1 and K. Thus, the general force transmissibility equation of the three-element mounting is given by,

$$T = \frac{\sqrt{1 + \left[2\zeta r\left(\frac{N+1}{N}\right)\right]^2}}{\sqrt{(1-r^2)^2 + \left[2\zeta r\left(\frac{N+1-r^2}{N}\right)\right]^2}} \tag{2.6}$$

where, N = stiffness ratio of the springs = K_1 / K

Figs. 2.4 and 2.5 illustrate the force transmissibility versus frequency plots for various values of the stiffness ratio N and for a wide range of damping ratio values. In order to understand the behaviour of the three-element mount, the extreme range possibilities of N = 0 to N = ∞ as well as ζ = 0 to $\zeta = \infty$ can be analyzed. Clark [13] has studied

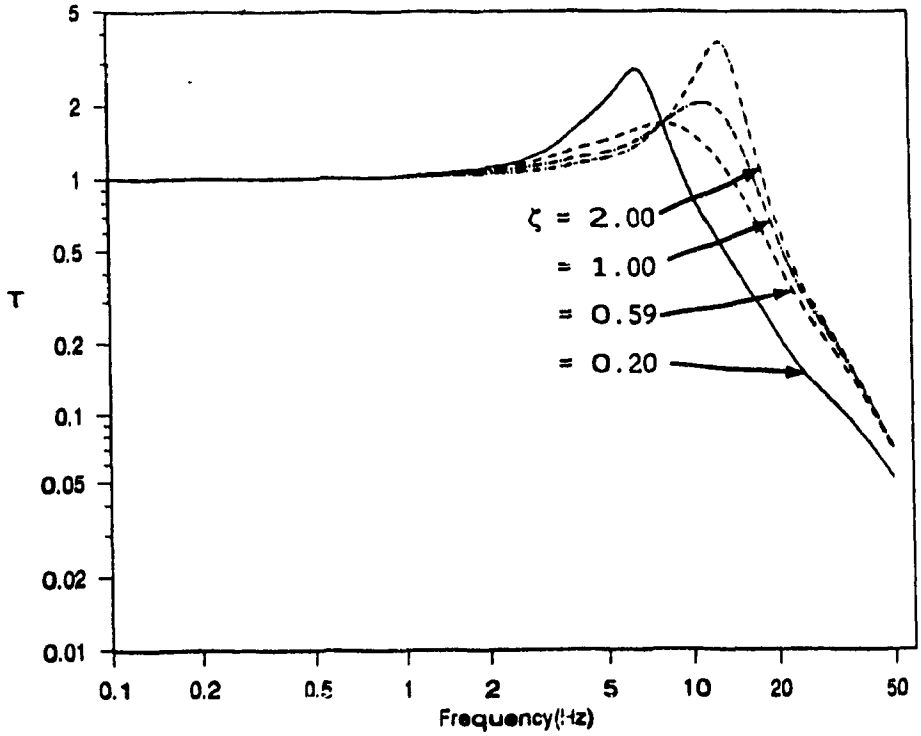

Fig. 2.5 Force transmissibility of a three-element passive mount for various values of damping ratio, with N = 3

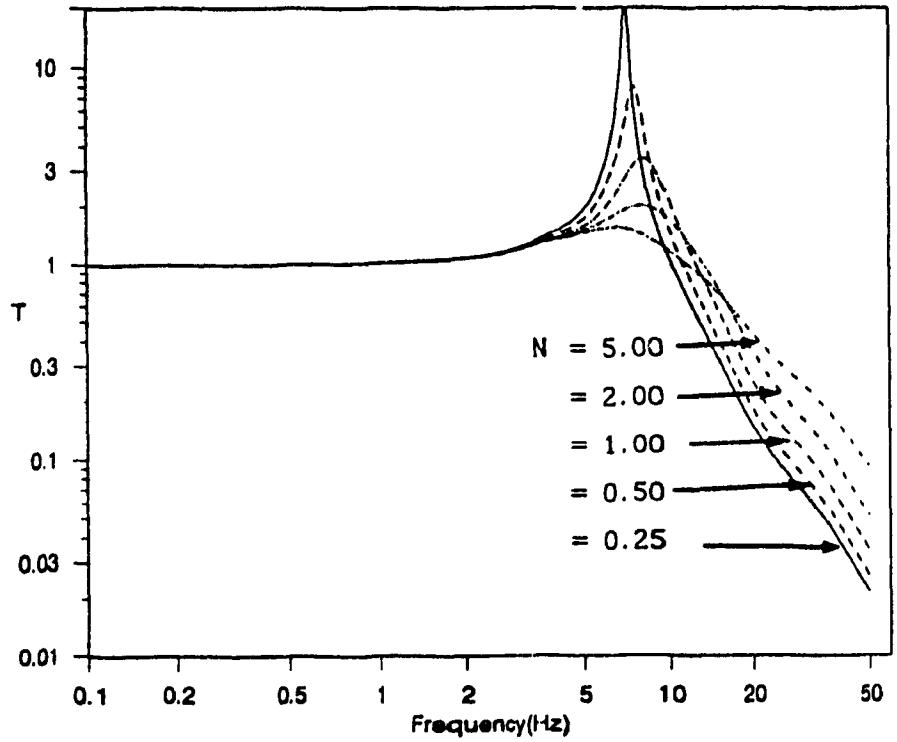

Fig. 2.6 Force transmissibility of a three-element passive mount for various values of stiffness ratio, with ζ=0.5

the effect of increasing the damping ratio value for a constant stiffness ratio.

Referring to Figs. 2.4 and 2.5, keeping the stiffness ratio N fixed and by varying the damping ratio ζ it was found that at the two extreme values of no damping and high damping the three-element model performance is poor in the resonant range. But it can be observed from the above figures that as damping ratio increases, the resonant transmissibility initially decreases, and then passes through a common point and then increases with increase in damping. The transmissibility curve with a peak value corresponding to the common point will be tuned with the optimum damping necessary for that particular system to overcome resonance. This results in an optimally tuned hydraulic mount with a known stiffness ratio and a damping ratio.

Similarly, another factor that could be discussed is the effect of stiffness ratio. Keeping the damping ratio constant and by increasing the stiffness ratio N, the performance of the three-element mount improves in the resonant range but deteriorates in the high frequency range. This is illustrated in Fig. 2.6. Hence it can be concluded that a very small stiffness ratio will result in poor performance in the resonant range but extremely good performance in the high frequency range.

2.4 Description of a Four-Element Hydraulic Mount Model

The schematic diagram of a four-element hydraulic mount model is

illustrated in Fig. 2.7. It is a combination of two springs of stiffness K and K_1 and two viscous dampers having damping ratios ζ and ζ_1 respectively.

The equation of motion for the four-element hydraulic mount with elastically coupled viscous damper is given by,

$$M\ddot{X} + C\,[\,\dot{X} - \dot{X}_1\,] + KX + C_1\dot{X} = F_o\, e^{i\omega t} = F[t] \qquad (2.8)$$

Since the spring K_1 and the damper C are in series, the spring force is equal to the damping force,

$$K_1 X_1 = C\,[\,\dot{X} - \dot{X}_1\,] \qquad (2.9)$$

The general force transmissibility equation of a four-element mount in dimensionless form is given by,

$$T. = \frac{F_{tr}}{F_o} = \frac{K\,K_1}{DELT}\left[\left(1 - 4\,\zeta\,\zeta_1 r^2\,N^*\right]^2 + \left(2\zeta r\,(1 + N^*)\right)^2\right]^{0.5} \qquad (2.10)$$

where

$$DELT = K\,K_1\left\{\left[\left(1 - r^2 - 4r^2\zeta\,\zeta_1 N^*\right)^2 + \left(2r\left(\zeta(N^*+1-r^2N^*) + \zeta_1\right)\right)^2\right]\right\}^{0.5} \qquad (2.11)$$

where, $r = \omega/\omega_n$, $2\zeta r = C\omega/K$, $2\zeta_1 r = C_1\omega/K$, N^* = stiffness ratio = K/K_1 with K_1 = 340 kN/m, K = 400 kN/m, and ω_n = 40.82rad/s

Fig. 2.8 illustrates the force transmissibility plot for various

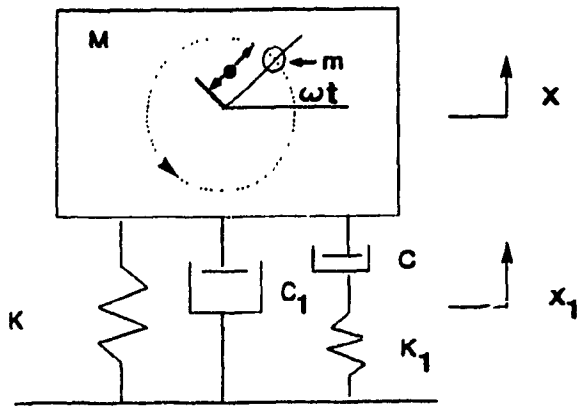

Fig. 2.7 Schematic of a four-element passive mount

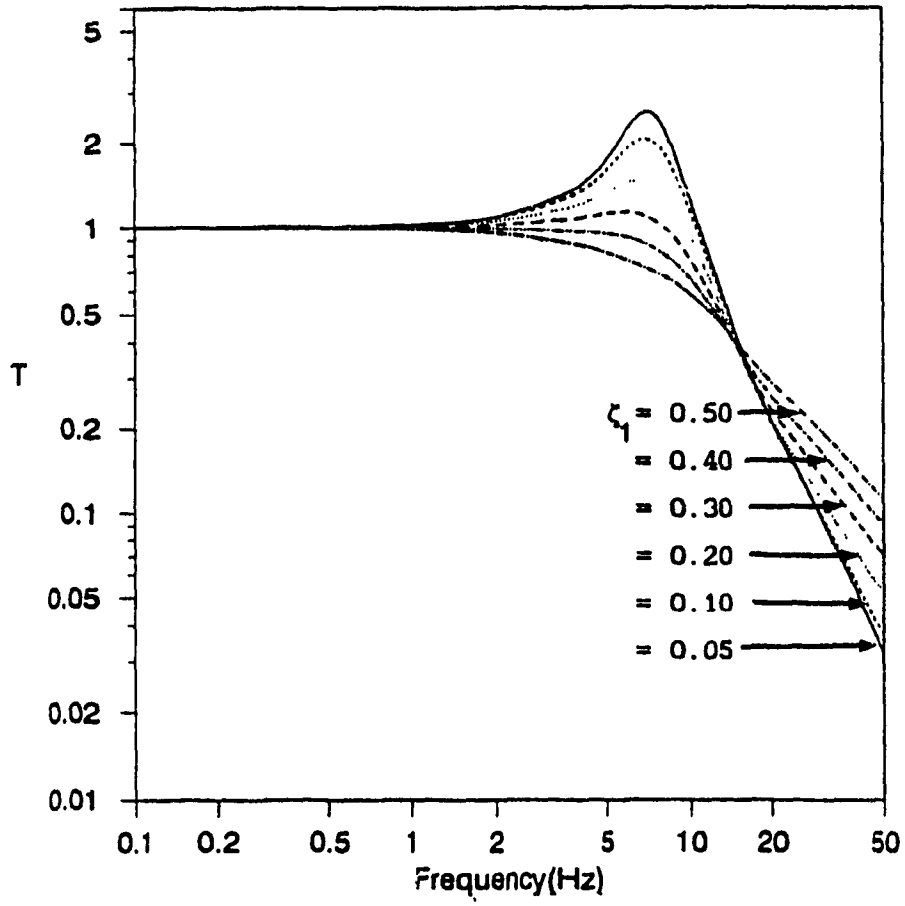

Fig. 2.8 Force transmissibility of a four-element passive mount with $N^* = 1.17$, C = 5.094 kN-s/m

values of damping ratio, ζ_1. It can be observed from the plot that an increase in damping ratio value will result in a decrease in transmissibility near resonance, while the high frequency performance deteriorates.

2.5 Description of the Concept of Dual-Phase Damper

The schematic of a non-linear hydraulic mount model with dual-phase damping is illustrated in Fig. 2.9. It is represented as a spring-mass system with a variable damper constrained to move in the vertical direction and excited by the mass induced vibration caused due to rotating unbalance.

The equation of motion for this non-linear single-degree-of-freedom model is given by

$$M\ddot{X} + F_d + F_k = F[t] = F_o e^{i\omega t} \qquad (2.12)$$

where X = displacement of the mass

F_d = non linear damping force = $C_{eq}\dot{X}$,

F_k = spring force = KX

Since the equation of motion of the hydraulic mount with dual-phase damping is a non-linear differential equation, the analysis becomes more complex and general methods of solution cease to exist. Hence no closed form solution is available, unless the nonlinear equation is linearised. Here the performance evaluation in the frequency domain is carried out

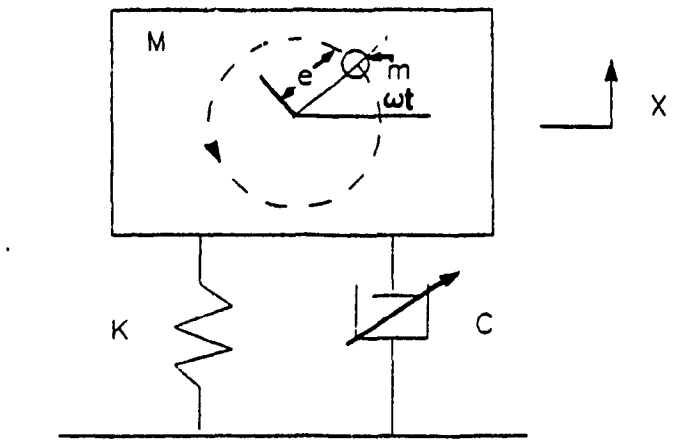

Fig. 2.9 Schematic of a non-linear mount with dual-phase damping

using linearised set of equations. The linear analysis allows computation of the system response in the frequency domain using transfer function which provides a clear and concise description of the mount behaviour. Further, linear approximation of non-linear elements may be considered appropriate for systems subjected to small disturbances [linear range]. However, if the situation asks for a more complete understanding of the qualitative and quantitative behaviour of the system then it is necessary to include non-linear effects. Hence, in order to obtain a linear differential equation, an equivalent damping coefficient must be determined. Once the equivalent damping ratio is obtained the system equation can be solved by computer simulation. The equivalent damping force is found by equating the total energy dissipated per cycle of vibration by the non-linear damper to that of an equivalent viscous damper experiencing the same harmonic displacement across the damper. In this model, depending on the absolute displacement value, the damping ratio ζ takes on different values.

As mentioned earlier, this investigation considers two types of dual-phase damping characteristic. In both cases, damping is a non-linear function of displacement and hence is a displacement dependent dual-phase damper. They are referred to as Type I and Type II dual-phase dampers in the thesis for convenience. Generally, the dual-phase dampers are expected to have a constant damping ratio equal to either ζ_1 or ζ_2 depending on the magnitude of displacement across the damper is either small or large. For intermediate displacements there will be a linear transition from one extreme value of the damping ratio to the other.

The schematic diagram illustrated in Fig. 2.10 explains the Type I dual-phase damping characteristic. Here the damping ratio ζ changes in value from ζ_1 to ζ_2 as the displacement across the damper increases from α_1 to β_1. Since $\zeta_1 > \zeta_2$, for small displacements the damping ratio ζ will be equal to ζ_1[high] and for large displacements ζ will be equal to ζ_2[low]. For intermediate displacements, the damping ratio ζ will vary between ζ_1 and ζ_2.

Similarly, the schematic diagram shown in Fig.2.11 describes the Type II dual-phase damping characteristic. Here for small displacements the damping ratio ζ will be equal to ζ_1[low] and for large displacements ζ will be equal to ζ_2 [high]. For intermediate displacements, the damping ratio ζ will vary between $\zeta_1$and ζ_2.

Generally, the dual-phase damper starts off with a known damping ratio, ζ_1 upto a known displacement α_1 or α_2,(depends on whether Type I or Type II is considered) indicating that orifice opening is fixed for small displacements in the range 0 to α_1 or 0 to α_2. For displacements in the range α_1 to β_1 or α_2 to β_2 damping ratio ζ will vary linearly, depending on the orifice opening. The variable flow will start either at α_1 or α_2 and ends either at β_1 or β_2. Finally the dual-phase damper reaches a known damping ratio ζ_2 beyond β_1 or β_2.

The most attractive aspect for a displacement dependent dual-phase damper considered in this investigation is that they can be realized by utilizing a metering pin shaped to achieve a given characteristic. In such systems, dual-phase damping characteristic can be achieved without

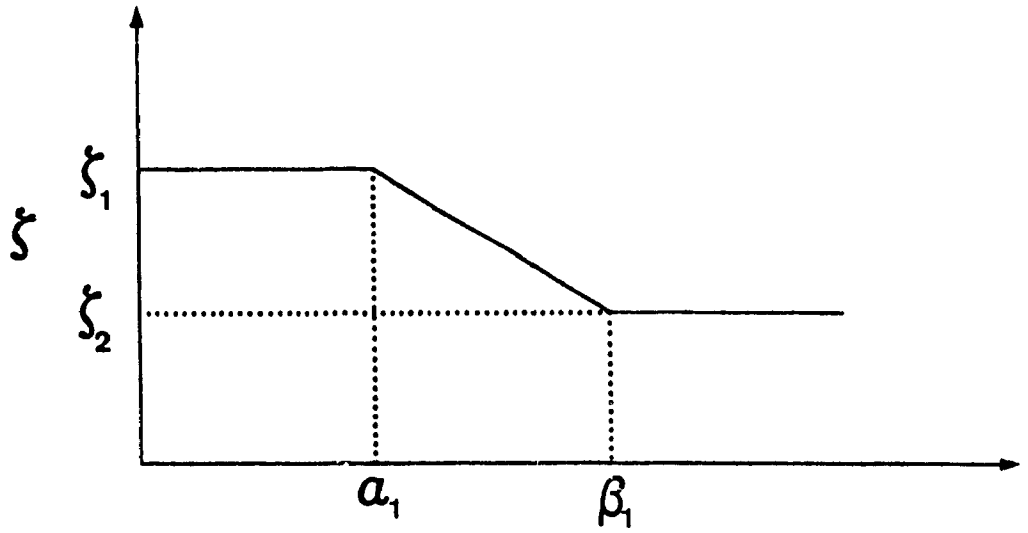

Fig. 2.10 Configuration of Type I Dual-Phase Damper with $\zeta_1 > \zeta_2$

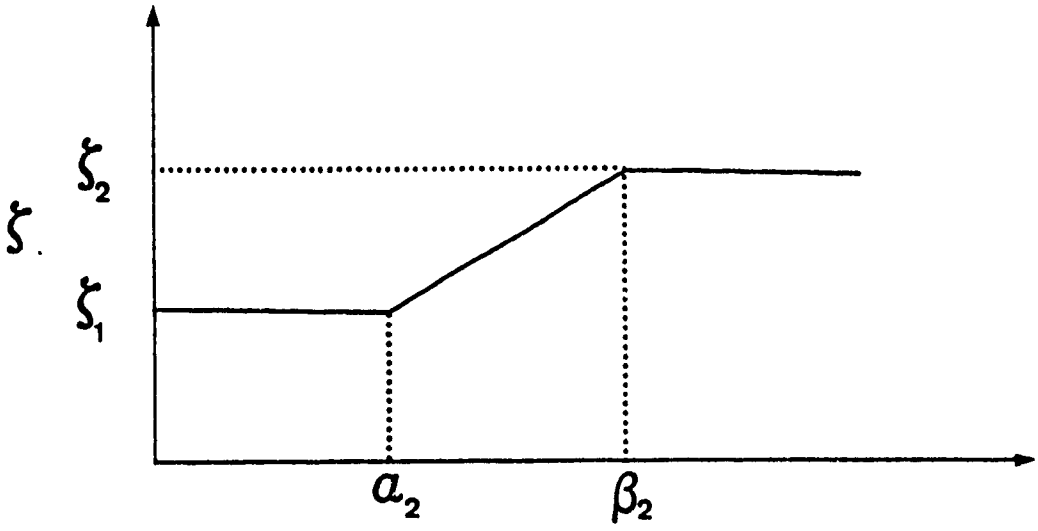

Fig. 2.11 Configuration of Type II Dual-Phase Damper with $\zeta_1 < \zeta_2$

the requirement of external power source, essentially keeping the device a passive one. The Type I dual-phase damping characteristic(Fig.2.10) proposed in this investigation can be realized by an arrangement shown in Fig.2.12. Fig.2.13 presents an arrangement that can reproduce the characteristics of a Type II dual-phase damper shown in Fig.2.11. The damping characteristic in either case is represented by the position of the pin inside the cylinder.

2.6 Determination of Equivalent Damping Ratio

The common technique adopted to determine the vibration response of any mechanical system depends on its linearity. A linear system is one, that obeys the principle of superposition and will exhibit a direct relationship between input and output. When a sinusoidal excitation is applied to a system, then for a linear system, both the excitation and the system response are sinusoidal of the same frequency. However, the technique adopted to evaluate response behaviour of a non-linear system is not as straight forward as that for a linear system since it does not obey the principle of superposition and there is no direct relationship between input and output. Consequently, the non-linear system has to be solved using direct integration techniques on a digital computer. The drawback of this approach is the extensive computing involved in obtaining frequency response. This has resulted in the search of alternate methods to solve non-linear systems. One of the methods is to linearise the non-linear system by finding an equivalent linear system which accurately exhibits the non-linear characteristics displayed by the non-linear element[s] in the system. In the present situation, the

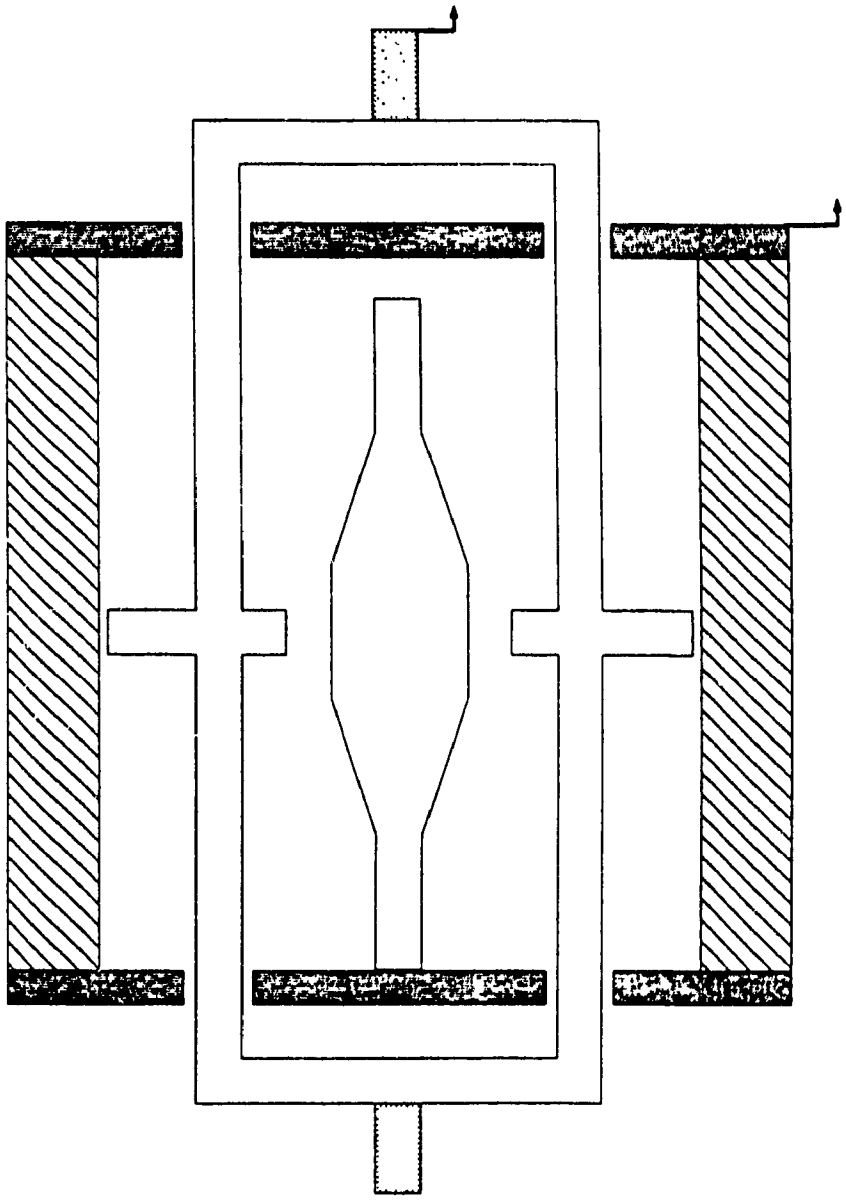

Fig. 2.12 Damper arrangement to reproduce dual-phase damping characteristic when $\zeta_1 > \zeta_2$

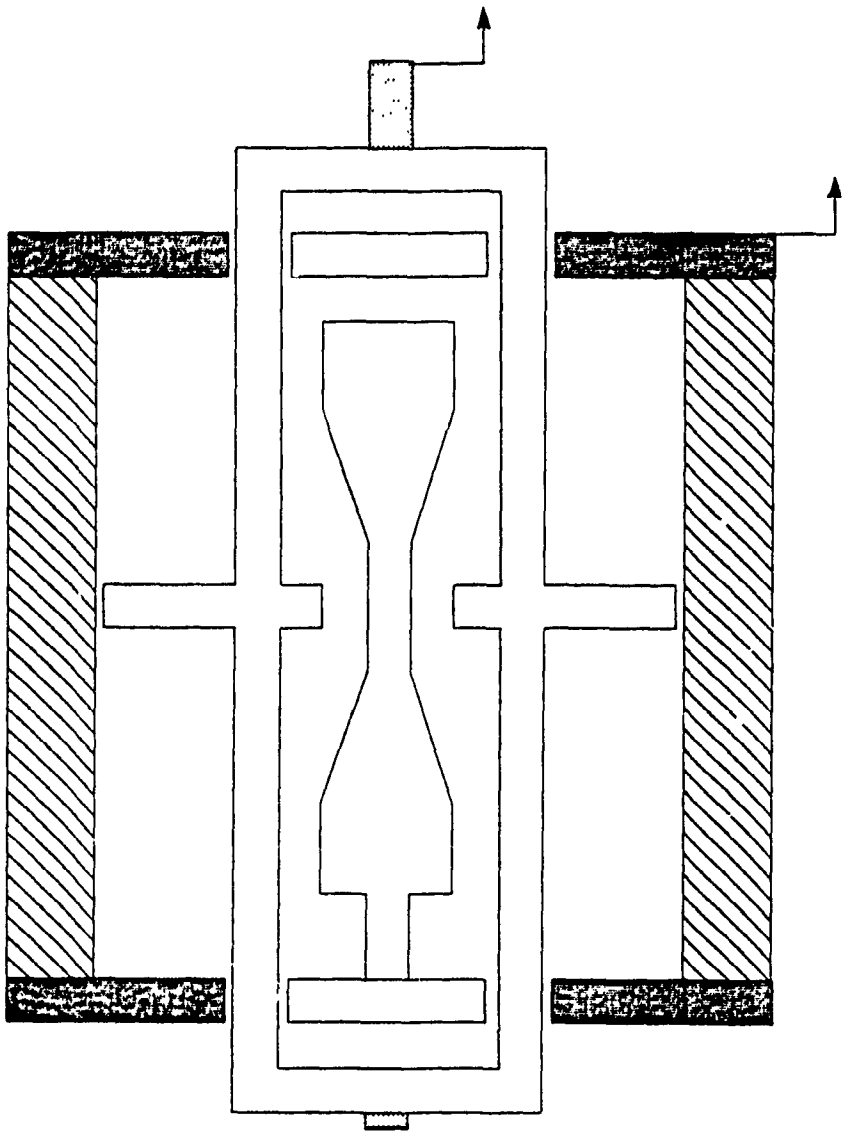

Fig. 2.13 Damper arrangement to reproduce dual-phase damping characteristic when $\zeta_1 < \zeta_2$

non-linearity is exhibited by the dual-phase damper. Consequently, an equivalent damping ratio has to be determined. So, the concept of equivalent viscous damping developed by Jacobson [32] is used. Accordingly, it involves the approximation of a non-linear damping force by an equivalent viscous damping force. That is, the energy W_d dissipated (the term dissipate is used to mean the conversion of energy from one form to another) per cycle of vibration by the non-linear damping element is equated to the energy dissipated by an equivalent viscous damper. Thus, the general equation for the energy lost per cycle in an equivalent viscous damper is:

$$W_d = \oint_0^{\tau} F_d \, dx \tag{2.14}$$

where $F_d = C_{eq}\dot{X}$, τ = period = $\frac{2\pi}{\omega}$

substituting for F_d, the energy dissipated per cycle becomes

$$W_d = \oint_0^{\tau} C_{eq}\dot{X} \, dx = \int_0^{\tau} C_{eq}\dot{X}^2 \, dt = C_{eq}X^2\omega^2\int_0^{\tau}\cos^2[\omega t - \phi] \, dt$$

$$W_d = \pi \, \omega \, C_{eq} \, X^2 \tag{2.15}$$

As mentioned earlier, the dual-phase damper can perform in at least three regions, and depending on that, the τ value will vary. Consider Figs. 2.10 and 2.11. When the displacement is less than or equal to α_1 or α_2, then the corresponding equivalent viscous damping ratio is given by:

$$\zeta_{eq} = \zeta_1 \tag{2.16}$$

If the displacement lies beyond β_1 or β_2, then ζ_{eq} can be found by integrating equation 2.14 and equating it to equation 2.16 to obtain equation 2.17.

$$\zeta_{eq} = \frac{4}{\pi}\left[\zeta_1 P_1 + R_2 P_3 + R_1 T_r P_2 + \zeta_2 P_4\right] \tag{2.17}$$

where

$$P_1 = \left[\frac{\sin 2\omega t_1}{4} + \frac{\omega t_1}{2}\right]; \quad P_2 = \left[\frac{\cos^3 \omega t_1 - \cos^3 \omega t_2}{3}\right]$$

$$P_3 = \left[\frac{\sin 2\omega t_2}{4} - \frac{\sin 2\omega t_1}{4}\right]; \quad P_4 = \left[\frac{\pi}{4} - \frac{\omega t_2}{4} - \frac{\sin 2\omega t_2}{4}\right]$$

$$R_1 = \left[\frac{\zeta_1 - \zeta_2}{\alpha_1 - \beta_1}\right]; \quad R_2 = \left[-R_1 \alpha_1 + \zeta_1\right]$$

$$\sin \omega t_1 = \frac{\alpha_1}{T_r}, \quad \sin \omega t_2 = \frac{\beta_1}{T_r}$$

On the other hand, if the displacement is between α_1 and β_1 or between α_2 and β_2, which is nothing but the non-linear region, then the relation to determine the equivalent damping ratio is given by

$$\zeta_{eq} = \frac{4}{\pi}\left[\zeta_1 P_1 + R_1 T_r P_5 + \zeta_2 P_6\right] \tag{2.18}$$

where

$$P_5 = \left[\frac{\cos^3 \omega t_1}{3}\right] \quad \text{and} \quad P_6 = \left[\frac{\pi}{4} - \frac{\omega t_1}{2} - \frac{\sin 2\omega t_1}{4}\right]$$

Once ζ_{eq} value is known for a particular frequency, then the corresponding transmissibility for a system with dual-phase damping can be determined by substituting for ζ in appropriate equation depending on the system considered.

2.7 Summary

In this chapter three different types of hydraulic mounts with passive damping were presented along with their equations of motion and results. The general characteristics of a dual-phase damper was presented with sketches to realize them. In addition, two types of dual-phase dampers and the procedure to solve the non-linear differential equation using equivalent damping ratio was discussed. In the following chapter, the performance of engine mount with dual-phase damping is discussed.

CHAPTER 3

SIMULATION RESULTS AND DISCUSSIONS ON DUAL-PHASE DAMPER

3.1 Introduction

In the previous section a detailed description of the isolator system with two-elements, three-elements and four-elements was given. This was followed by a description of the non-linear dual-phase damper and a method for determining the equivalent damping ratio for the dual-phase damper system considered. In this chapter, a critical evaluation of vibration isolation characteristics of hydraulic mounts with two different kinds of dual-phase damping is compared with that of viscous damping, for both two-element and four-element isolator systems discussed in chapter two. Next, the influence of damping parameters on the isolation performance is studied. A parametric study is also carried out to examine the influence of dual-phase parameters on the equivalent damping ratio as excitation frequency is varied. The vibration isolation performance in all cases is evaluated in terms of force transmissibility ratio.

3.2 Two-Element Hydraulic Mount Model

3.2.1 Type I Dual-Phase Damper

A hydraulic mount with two-element is referred to a system presented in Fig.2.1 in section 2.2. In evaluating dual-phase damper the viscous damper is replaced by a variable damper capable of providing

three possible damping ratios ζ_1, ζ_2 and intermediate values between ζ_1 and ζ_2. For the Type I dual-phase damper the parameters selected are ω_n = 40.82 rad/s, ζ_1= 0.5 or 0.9 and ζ_2= 0.1. Figs. 3.1-3.4 show the force transmissibility vs frequency plots of the system with Type I dual-phase damper and the passive system with linear viscous damper[LVD]. It can be observed from the figure that, for all cases high damping provides good isolation in the low frequency range but performs poorly in the high frequency range. However, lower damping provides good isolation at high frequencies, but performs poorly in the low frequency region. So, a decrease in damping increases the resonant transmissibility and decreases the high frequency transmissibility. In the figure the force transmissibility for dual-phase damping is also shown for different α_1 and β_1 values. It can be clearly seen that a dual-phase damping has a compromising performance in the low frequency as well as high frequency range. It can also be observed from the plots that as β_1 value is increased, the dual-phase damper performs well in the resonant range but the high frequency performance deteriorates. Similarly, an increase in α_1 value will improve the performance in the low and resonant range and result in poor performance in the high frequency range. Further, from the transmissibility plot on Fig. 3.4 it can be seen that an increase in damping results in an improvement in the resonant transmissibility, but also increases the high frequency transmissibility, similar to that of a linear viscous damping.

Figs. 3.5 and 3.6 show the variation of equivalent damping ratio with frequency for Type I dual-phase damper. It can be observed from the above figure that the equivalent damping ratio value is influenced by

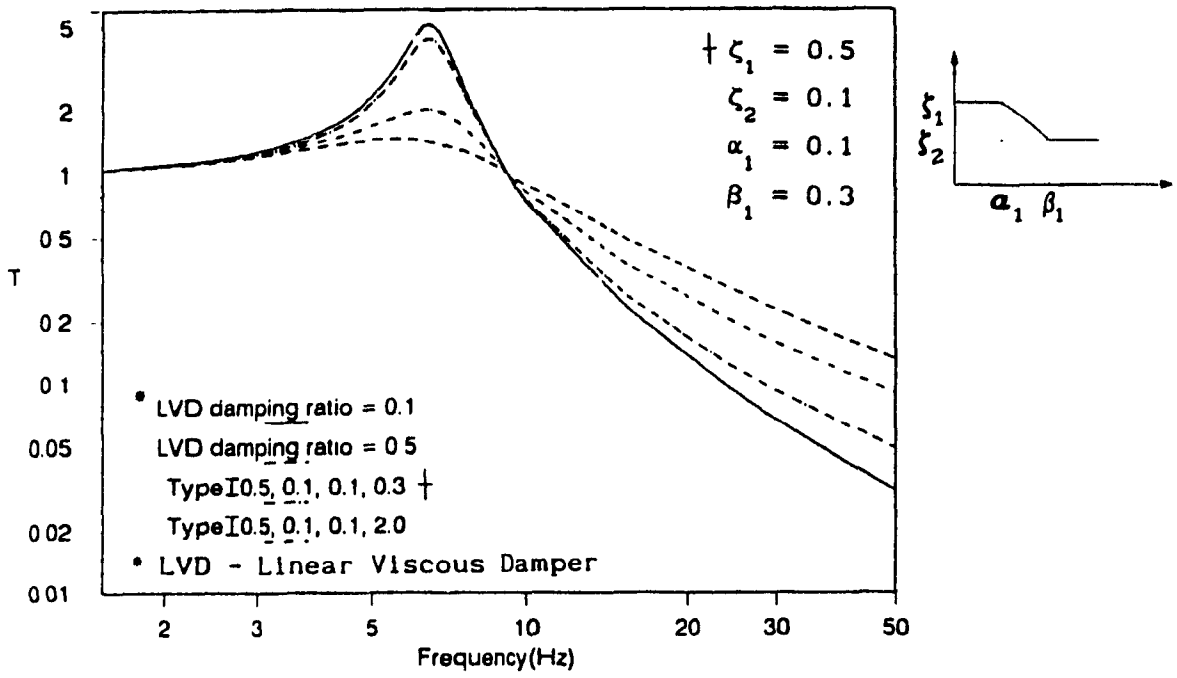

Fig. 3.1 Force Transmissibility comparison of Type I Dual-phase Damper with passive mount for α_1 = 0.1, and β_1 = 0.3 and 2.0

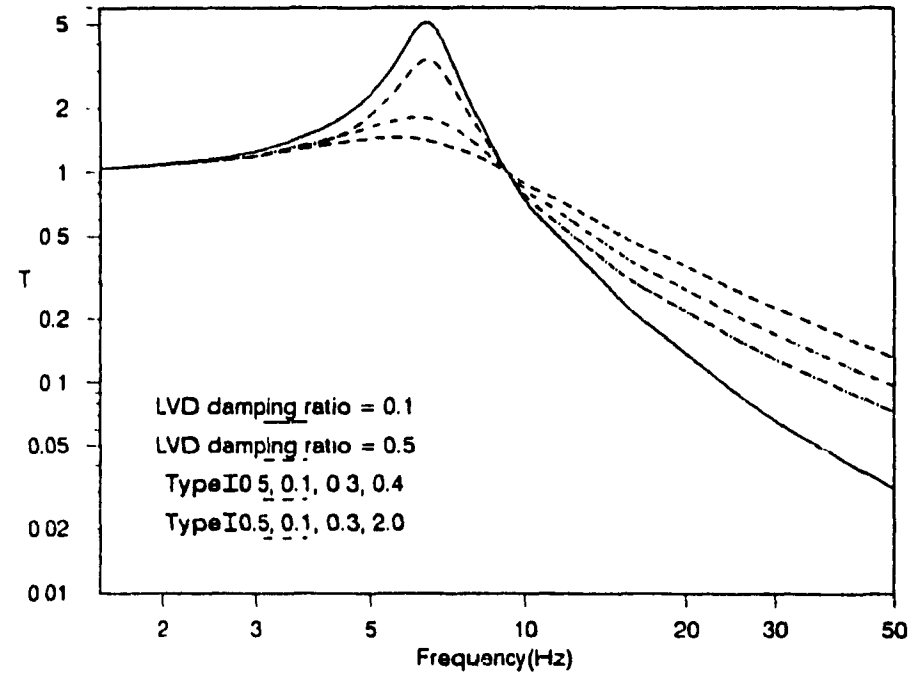

Fig. 3.2 Force Transmissibility comparison of Type I Dual-phase Damper with passive mount for α_1 = 0.3, and β_1 = 0.4 and 2.0

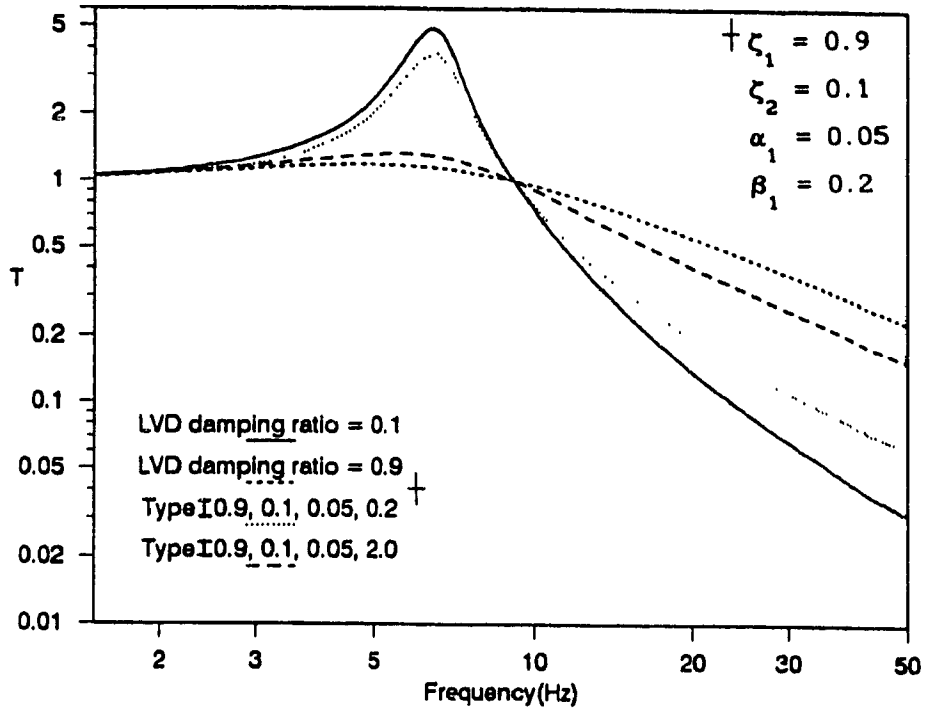

Fig. 3.3 Force Transmissibility comparison of Type I Dual-phase Damper with passive mount for α_1 = 0.05, and β_1 = 0.2 and 2.0

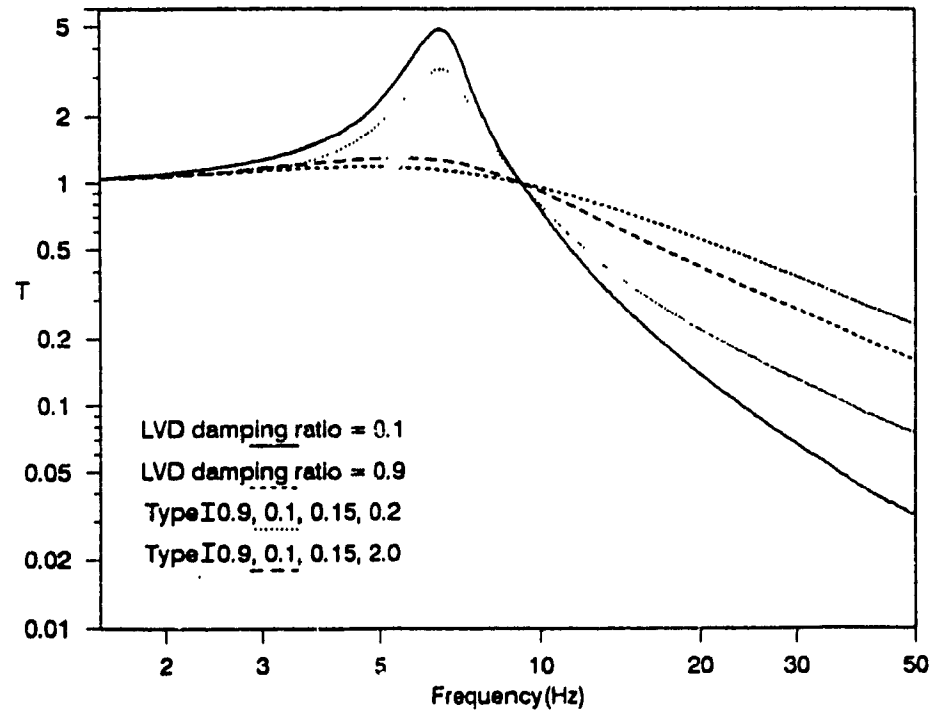

Fig. 3.4 Force Transmissibility comparison of Type I Dual-phase Damper with passive mount for α_1 = 0.15, and β_1 = 0.2 and 2.0

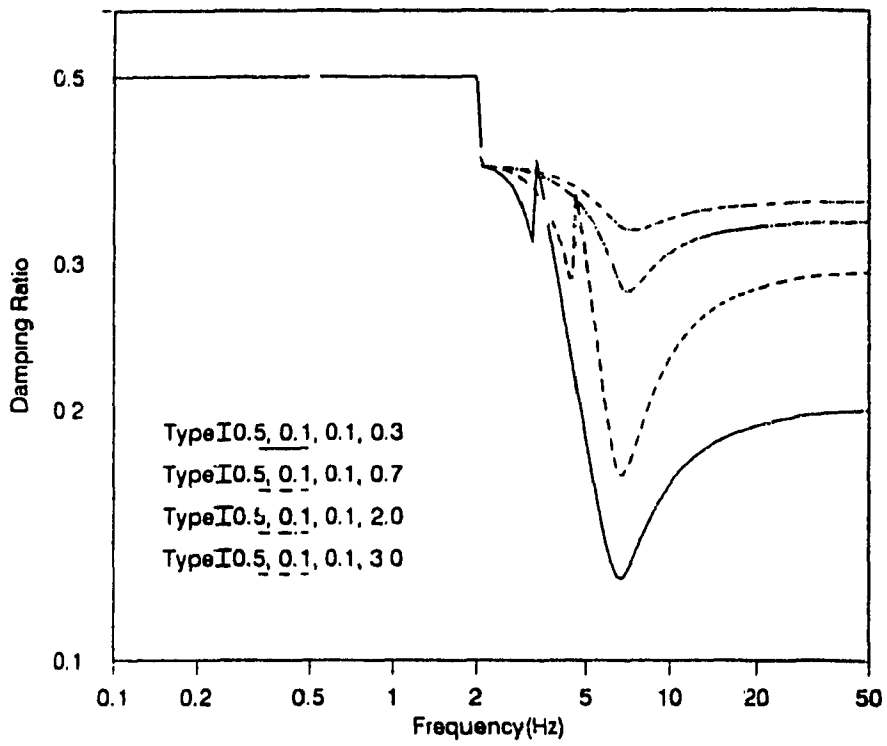

Fig. 3.5 Influence of excitation frequency on equivalent damping ratio for Type I Dual-phase Damper as β_1 is varied(α_1 = 0.1)

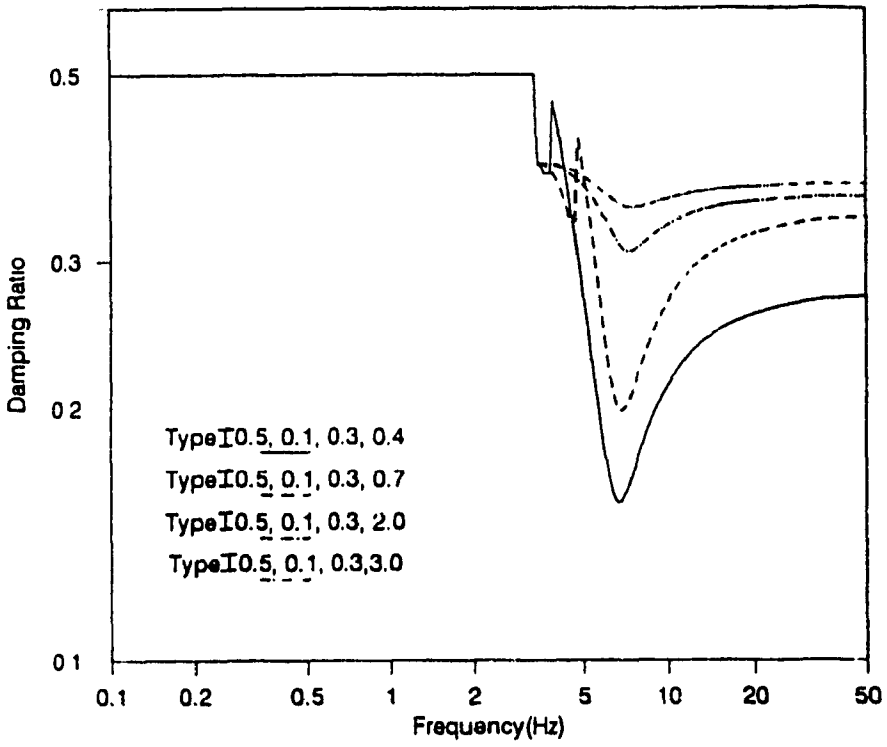

Fig. 3.6 Influence of excitation frequency on equivalent damping ratio for Type I Dual-phase Damper as β_1 is varied(α_1 = 0.3)

the variations in α_1 and β_1 values. In general, the damping ratio remains constant and equal to the high damping value of the dual-phase damper for low frequencies. The damping ratio approaches a minimum near resonance and then increases as frequency is increased. However, the magnitude of change in damping ratio depends on the value of α_1 and β_1. The damping ratio is low near resonance when α_1 and β_1 values are low and any increase in β_1 value will result in an increase in damping ratio value in the resonant range. This results in an improved performance in the resonant frequency range with performance deteriorating in the high frequency range. Further, an increase in α_1 value will also result in high damping. Thus this type of dual-phase damper has the capability to perform well in the resonant range when the difference between α_1 and β_1 values are wide. However, its performance will deteriorate in the high frequency range.

3.2.2 Type II Dual-Phase Damper

In the investigation of two-element hydraulic mount model with Type II dual-phase damper, the linear viscous damper of the system(Fig.2.1) is replaced by the dual-phase damper with Type II characteristics(Fig.2.11). The parameters selected for this system are ω_n = 40.82 rad/s, ζ_1 = 0.1 and ζ_2 = 0.5 or 0.9. Figs. 3.7-3.11 show the force transmissibility vs frequency plots of Type II dual-phase damper and a passive hydraulic mount with LVD. It can be observed from the figure that, high damping provides good isolation in the low frequency range but performs poorly in the high frequency range and low damping provides good isolation at high frequency but performs poorly in the low

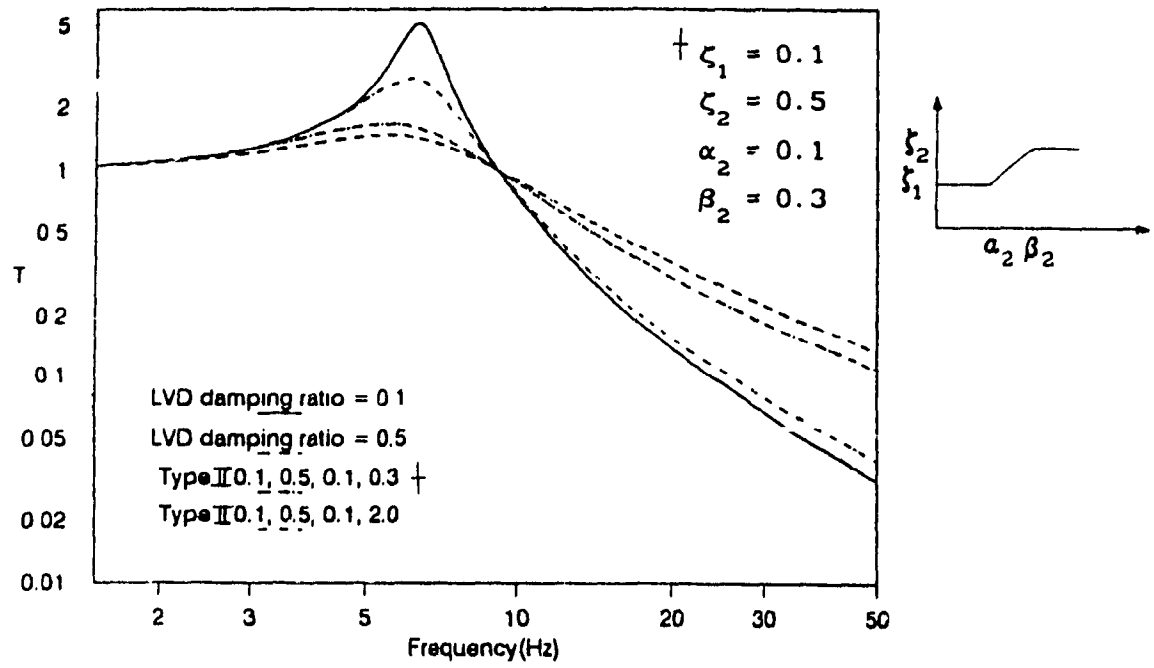

Fig. 3.7 Force Transmissibility comparison of Type II Dual-phase Damper with passive mount for α_2= 0.1, and β_2= 0.3 and 2.0

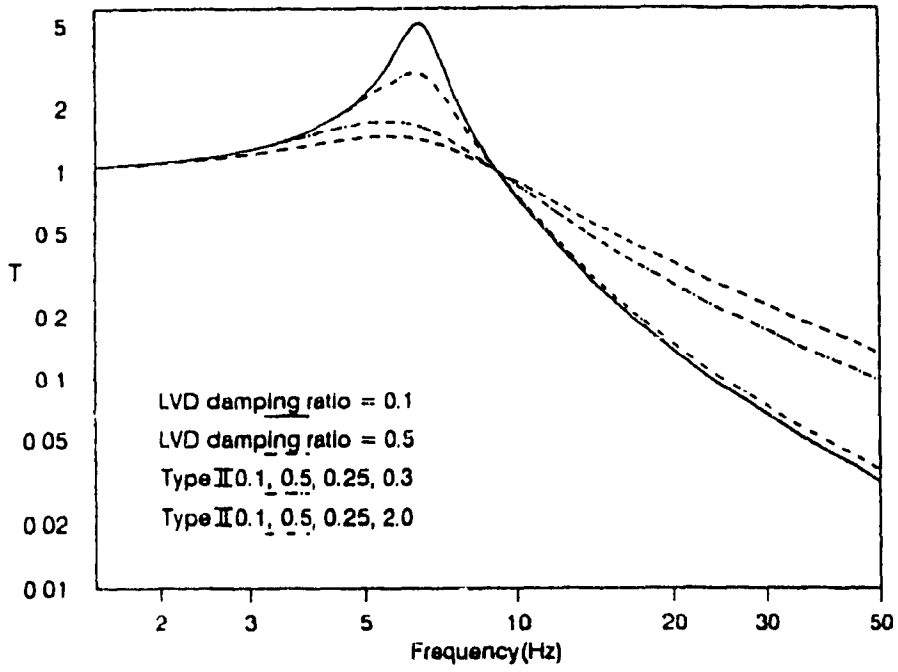

Fig. 3.8 Force Transmissibility comparison of Type II Dual-phase Damper with passive mount for α_2= 0.25, and β_2= 0.3 and 2.0

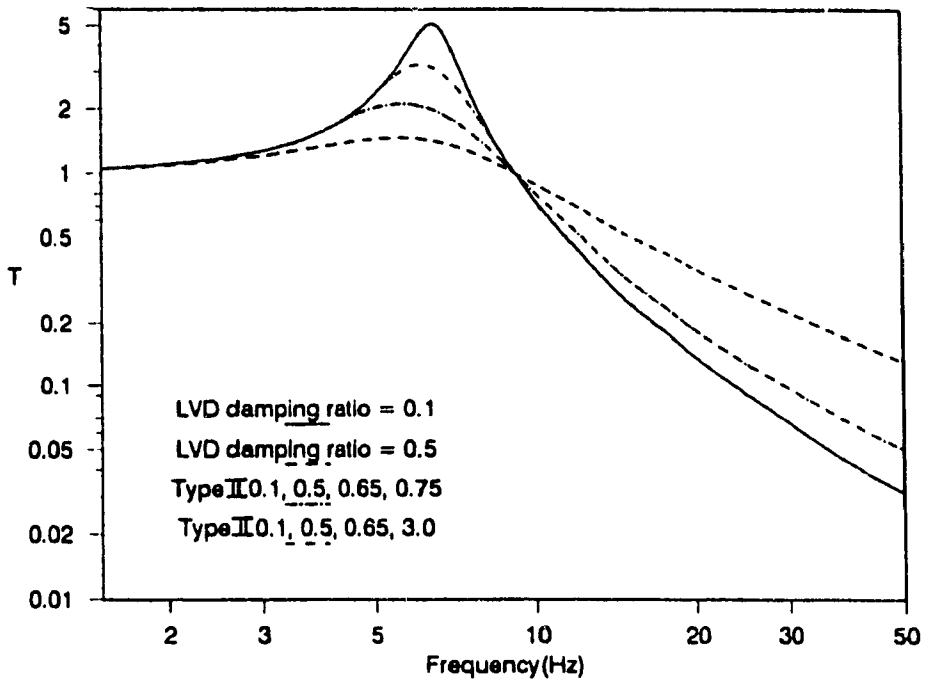

Fig. 3.9 Force Transmissibility comparison of Type II Dual-phase Damper with passive mount for α_2= 0.65, and β_2= 0.75 and 3.0

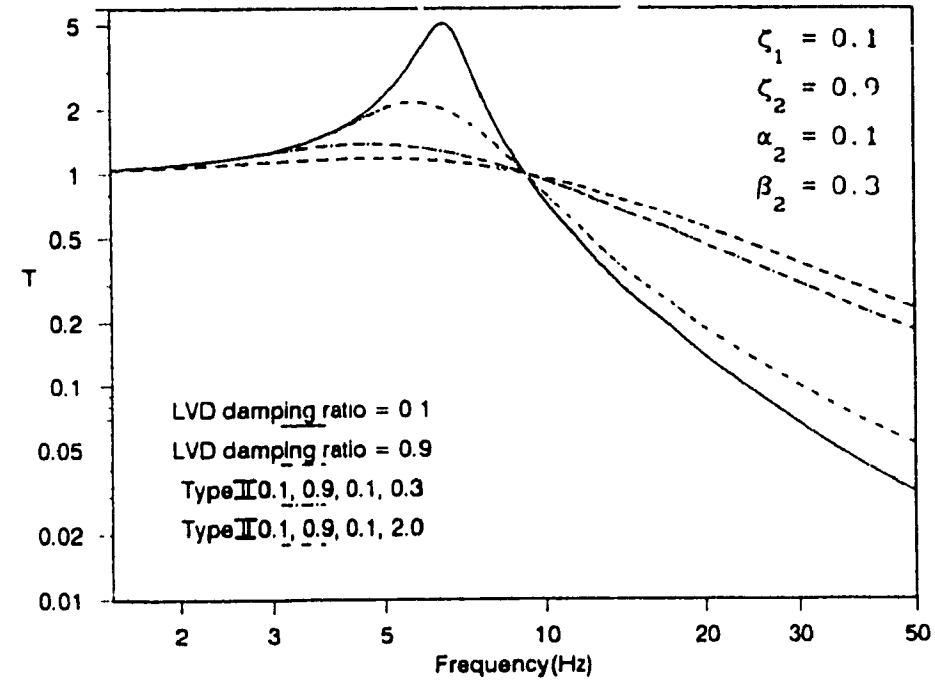

Fig. 3.10 Force Transmissibility comparison of Type II Dual-phase Damper with passive mount for α_2= 0.1, and β_2= 0.3 and 2.0

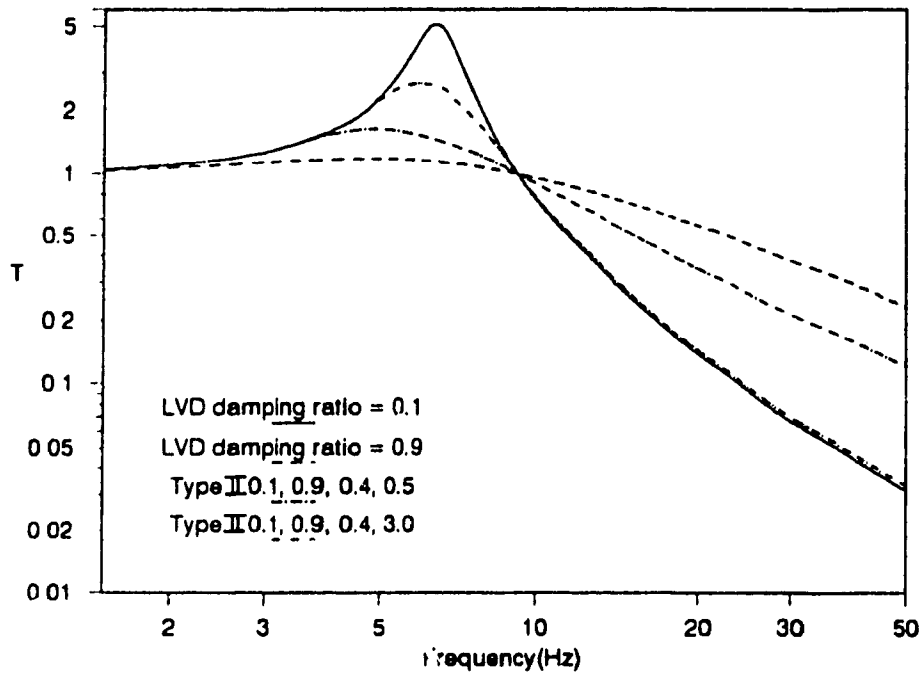

Fig. 3.11 Force Transmissibility comparison of Type II Dual-phase Damper with passive mount for α_2= 0.4, and β_2= 0.5 and 3.0

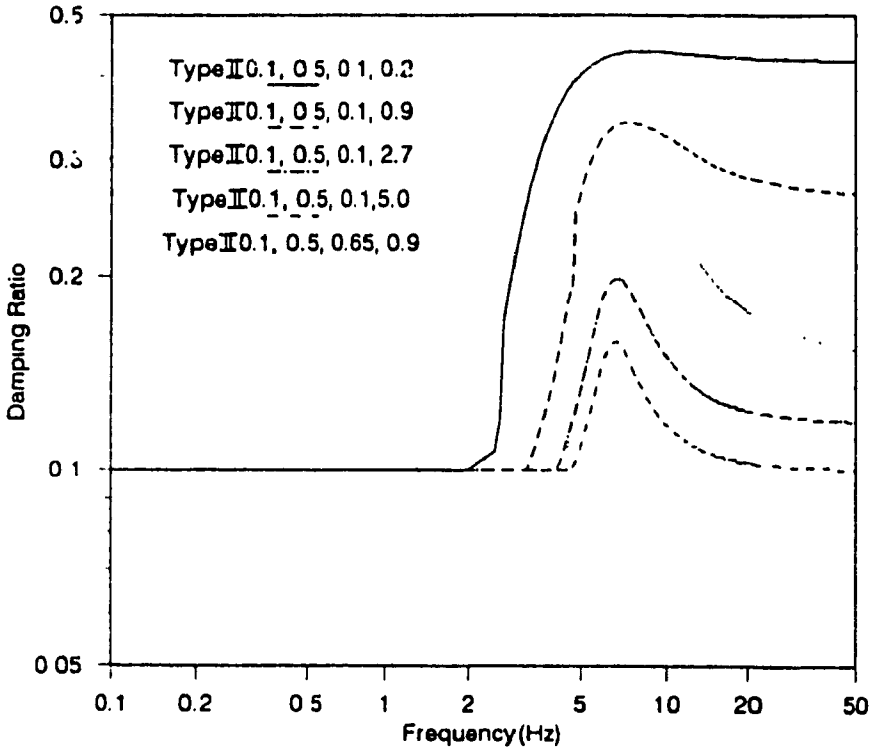

Fig. 3.12 Influence of excitation frequency on equivalent damping ratio for Type II Dual-phase Damper as β_2 is varied(α_2=0.1)

frequency region. In the figure, the performance of a dual-phase damper for different α_2 and β_2 values is also shown. It can be clearly seen that when dual-phase damping is introduced in place of viscous damper there is substantial reduction in transmissibility in the low as well as high frequency range. It can also be seen from the plots that, an increase in β_2 value will result in a decrease in high frequency transmissibility, however at the resonant frequency the transmissibility increases. The high frequency transmissibility decreases with increasing α_2 and β_2, however at the resonant and low frequencies, the transmissibility increases. If ζ_2 is increased, the low frequency and resonant frequency transmissibility decreases, and on the high frequency side the transmissibility increases.

The results presented in Figs. 3.12-3.14 illustrate the behaviour of equivalent damping ratio with variation in α_2 and β_2 values. In general, as frequency is increased, the damping ratio remains constant and equal to the low damping value of the dual-phase damper for low frequencies. The damping ratio approaches a maximum near resonance and then decreases as frequency is increased. The magnitude of this change in damping ratio, however depends on the value of α_2 and β_2. The figures clearly show that damping is high when α_2 and β_2 values are close and any increase in β_2 value will reduce the damping ratio value. Also, the characteristics of this type of damper will be influenced by α_2 value and it can be seen from the figures above that an increase in α_2 value will lower the damping in the resonant range resulting in poor performance in the resonant region and improved performance in the high frequency region.

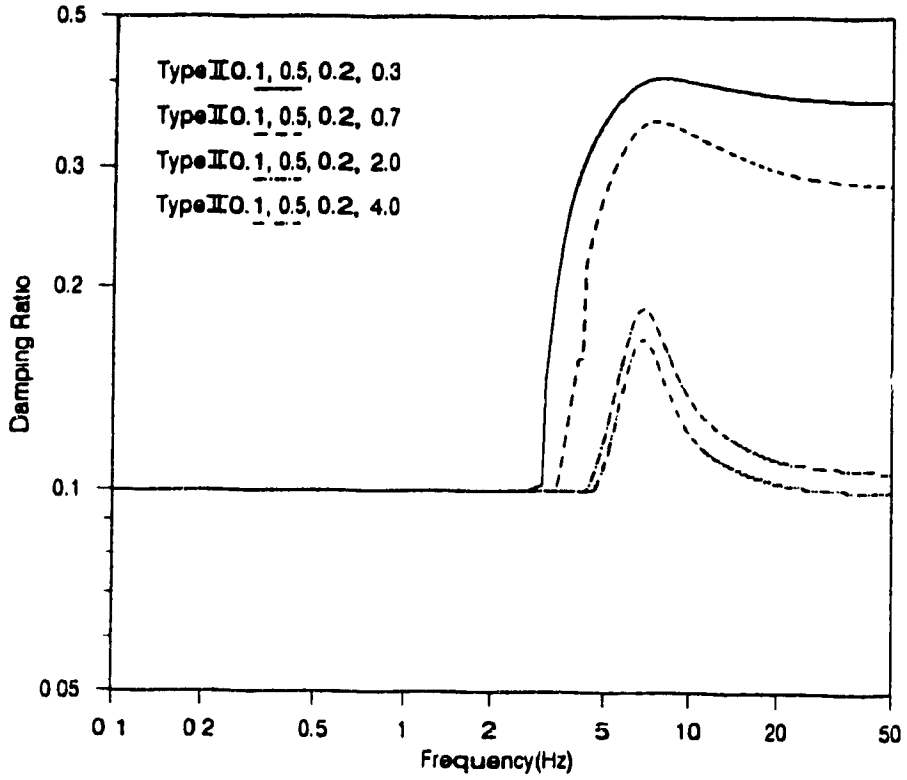

Fig. 3.13 Influence of excitation frequency on equivalent damping ratio for Type II Dual-phase Damper as β_2 is varied(α_2=0.2)

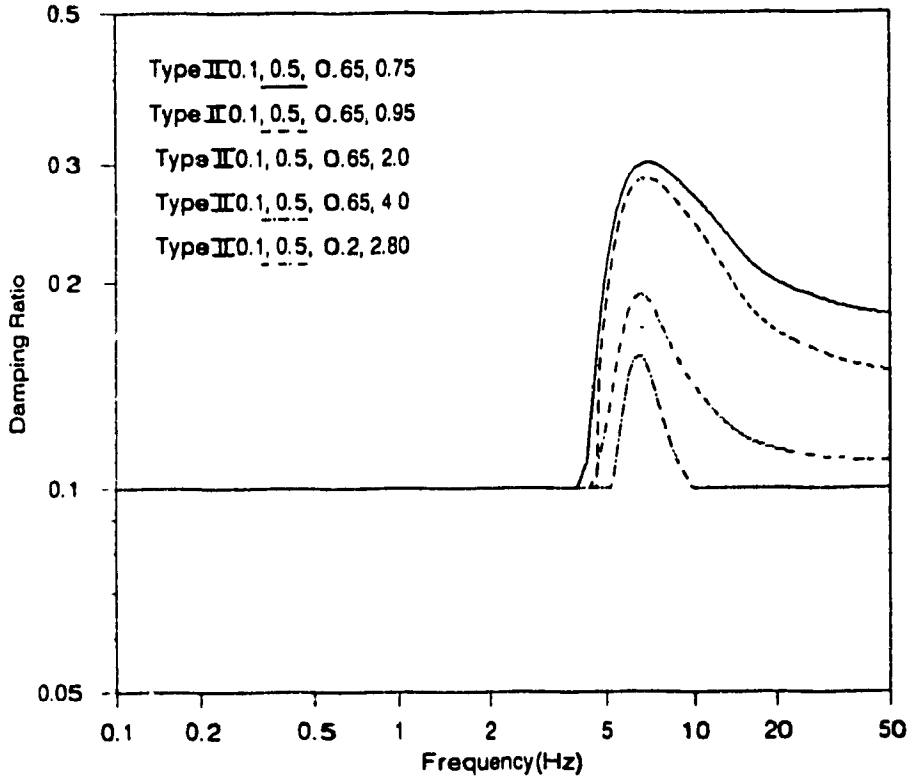

Fig. 3.14 Influence of excitation frequency on equivalent damping ratio for Type II Dual-phase Damper as β_2 is varied(α_2=0.65)

3.3 Four-Element Hydraulic Mount Model

3.3.1 Type I Dual-Phase Damper

Four-element hydraulic mount refers to the system presented as Fig.2.7 in section 2.4. Here the conventional damper is replaced by a dual-phase damper. Figs. 3.15 and 3.16 illustrates the response of four element hydraulic mount model with Type I dual phase damper for various α_1 and β_1 values. The parameters selected are ω_n = 40.82 rad/s, ζ_1= 0.5 or 0.9, ζ_2= 0.1 and N^* = 1.17. Examining the plots of constant damping ratios, it is seen that for low damping ratio the high frequency transmissibility decreases while it markedly increases the resonant transmissibility. The opposite occured for high damping ratio where high frequency transmissibility markedly increased, while there was substantial reduction in the resonant transmissibility. While the Type I dual-phase damper performance was intermediate between the two extreme damping ratios with a performance almost close to that of low damping ratio value in the high frequency range. Further, it was observed that an increase in α_1 value resulted in an improvement in the resonant range but poorer performance in the high frequency range. Examining Figs. 3.17 and 3.18, which is nothing but the variation of equivalent damping value with change in α_1 and β_1 values. It is clearly visible that small α_1 and β_1 values will markedly improve the performance of the damper in the high frequency region with poor performance in the resonant region because of low damping. But an increase in β_1 value resulted in a better performance in resonant region with poor performance in high frequency region. Similarly, an increase in α_1 value resulted in a significant improvement in resonant region with the performance deteriorating in

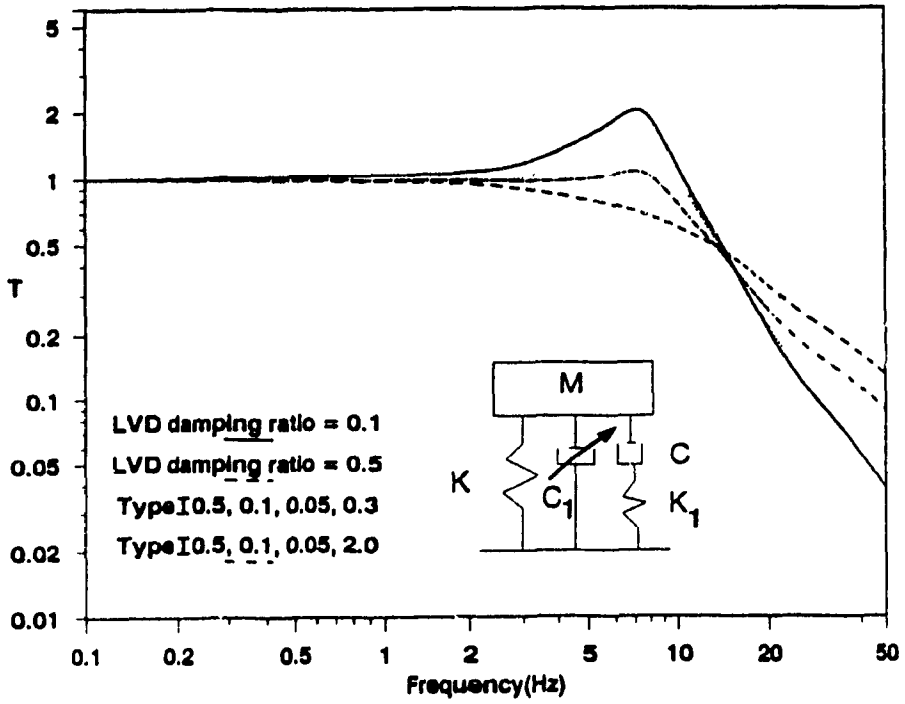

Fig. 3.15 Force Transmissibility comparison of Type I Dual-phase Damper with passive mount for α_1= 0.05, and β_1= 0.3 and 2.0 in a Four-Element model

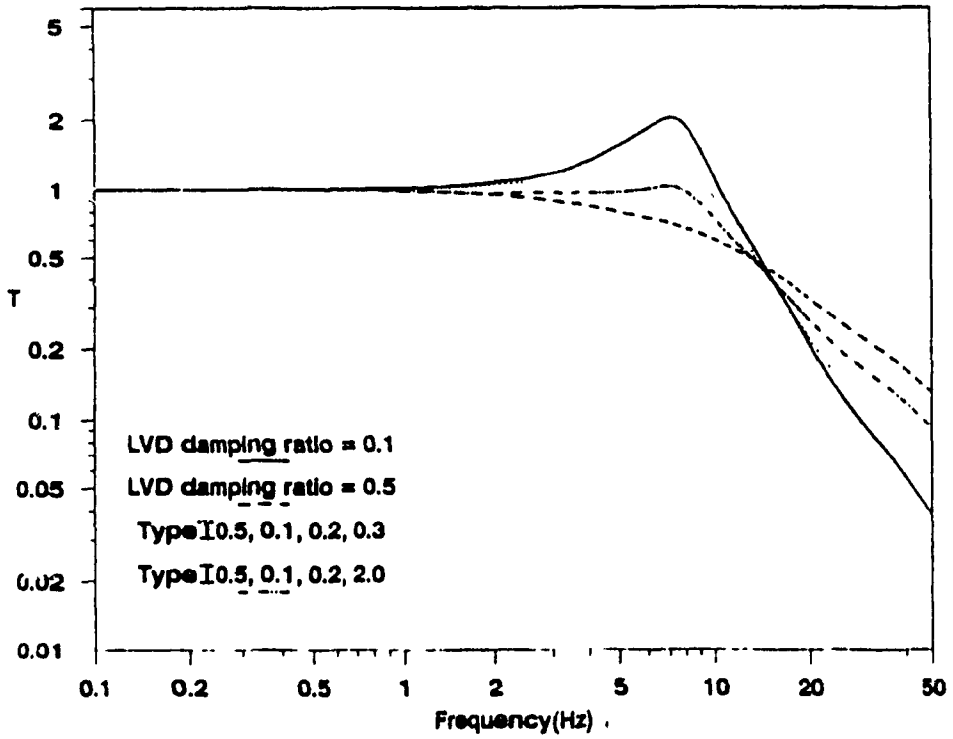

Fig. 3.16 Force Transmissibility comparison of Type I Dual-phase Damper with passive mount for α_1= 0.2 and β_1= 0.3 and 2.0 in a Four-Element model

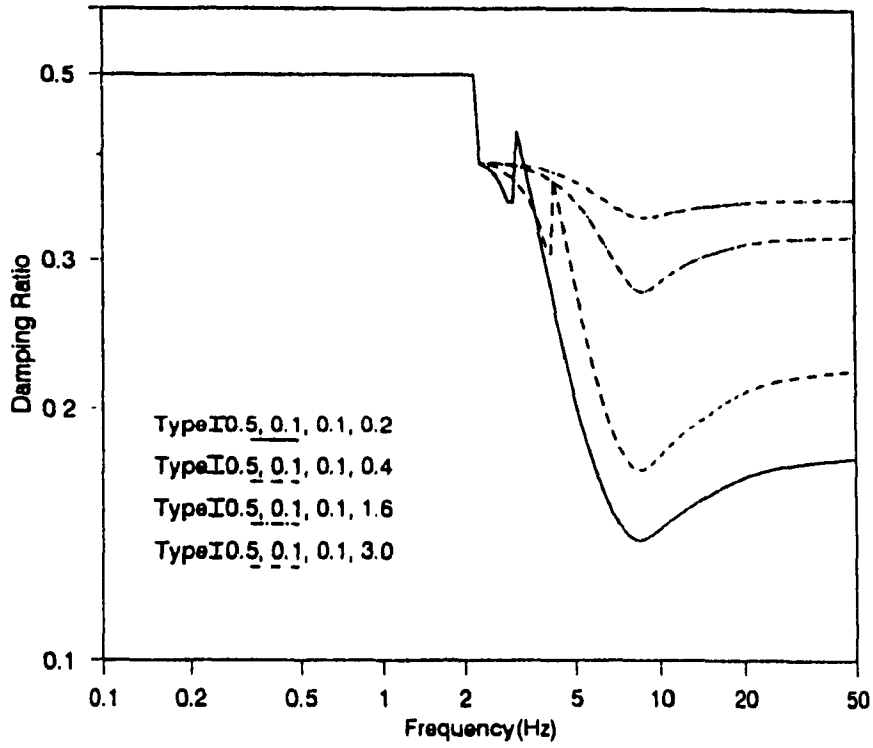

Fig. 3.17 Influence of excitation frequency on equivalent damping ratio for Type I Dual-phase Damper as β_1 is varied(α_1=0.1) in a Four-Element model

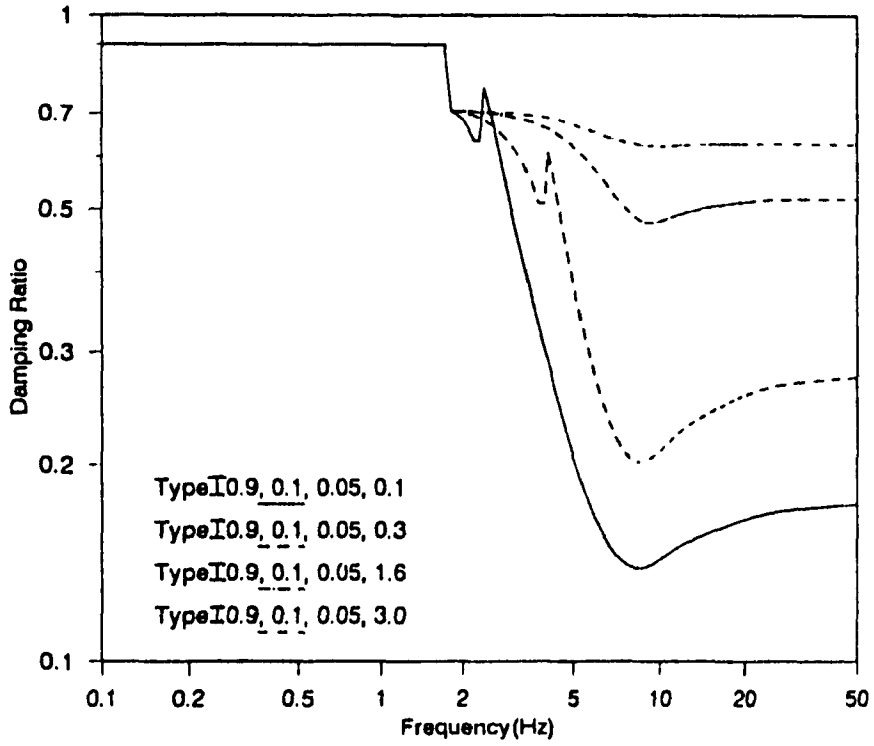

Fig. 3.18 Influence of excitation frequency on equivalent damping ratio for Type I Dual-phase Damper as β_1 is varied(α_1=0.05) in a Four-Element model

high frequency region.

3.3.2 Type II Dual-Phase Damper

Figs. 3.19 and 3.20 illustrates the response of a four-element hydraulic mount with Type II dual-phase damper for various α_2 and β_2 values. It is found by examining the plots of constant damping ratios, that for low damping ratio the resonant transmissibility is high even though the high frequency transmissibility is considerably low. However, at high damping values, the transmissibility increased with increasing frequency in the high frequency range but, the opposite occured in the resonant range. But a Type II dual-phase damper performs well in the resonant and high frequency range when compared to four-element hydraulic mount with constant damping. Further, it was found that α_2 and β_2 values influenced the performance of the dual-phase damper in the low as well as high frequency range. It was observed that an increase in either α_2 or β_2 value improved the performance in the high frequency range at the cost of resonant frequency performance. Similarly, an increase in damping resulted in an improvement in the resonant range but the performance deteriorated in the high frequency range. Figs. 3.21 and 3.22 depicts the influence of α_2 and β_2 values on damping ratio. It is very significant from the above figures that, as β_2 value is increased the damping ratio value will be low, resulting in a significant drop in transmissibility in the high frequency region with an increase in transmissibility in resonant region. Similarly, an increase in α_2 value will also improve the performance in high frequency region.

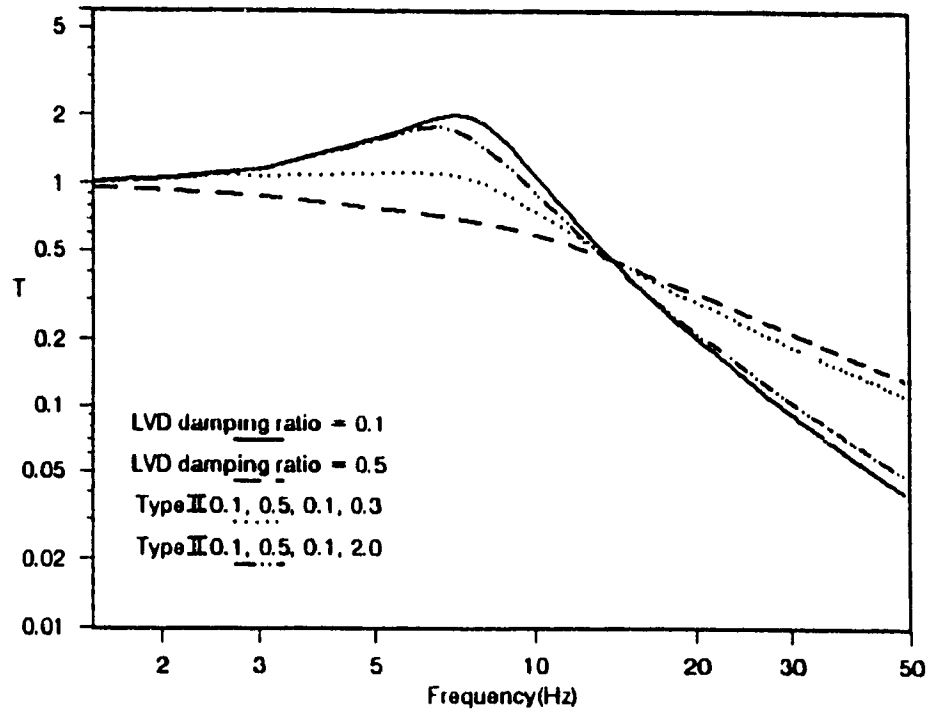

Fig. 3.19 Force Transmissibility comparison of Type II Dual-phase Damper with passive mount for α_2= 0.1, and β_2= 0.3 and 2.0 in a Four-Element model

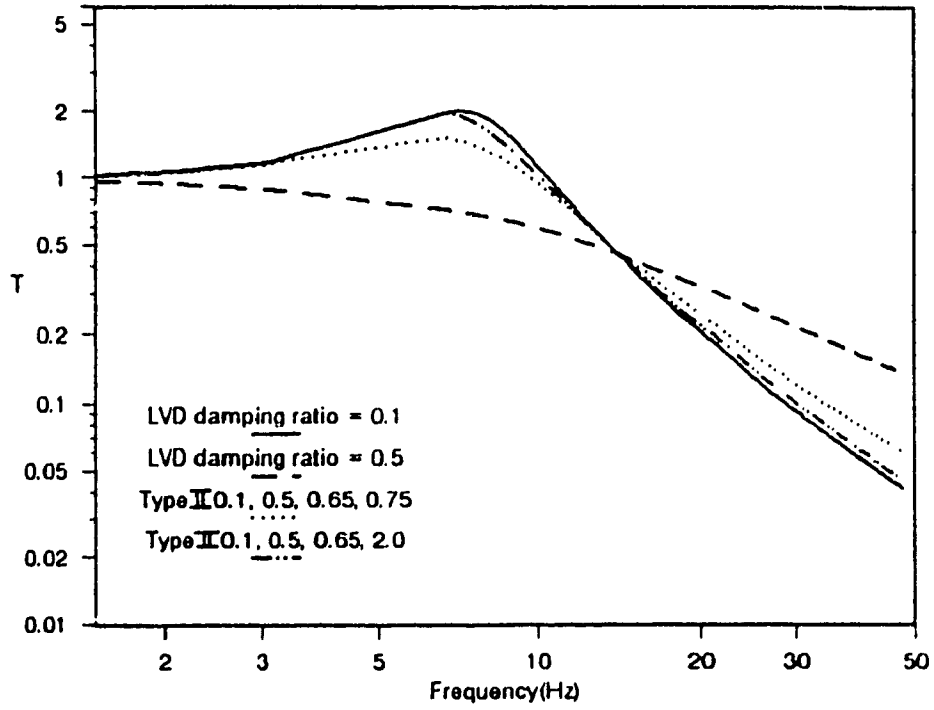

Fig. 3.20 Force Transmissibility comparison of Type II Dual-phase Damper with passive mount for α_2 = 0.65, and β_2 = 0.75 and 2.0 in a Four-Element model

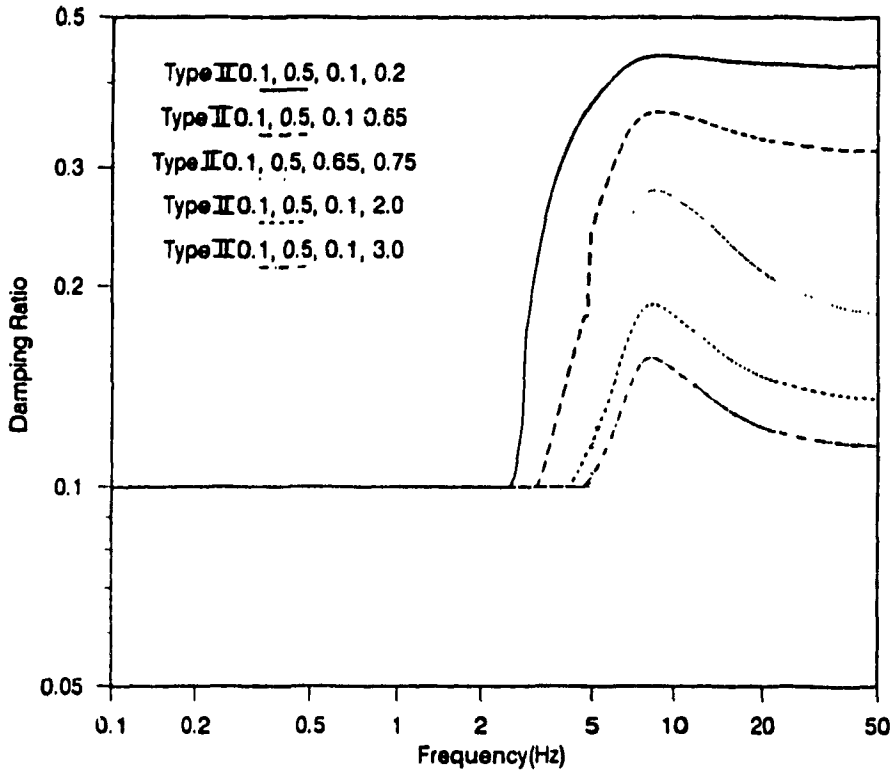

Fig. 3.21 Influence of excitation frequency on equivalent damping ratio for Type II Dual-phase Damper as β_2 is varied(α_2=0.1) in a Four-Element model

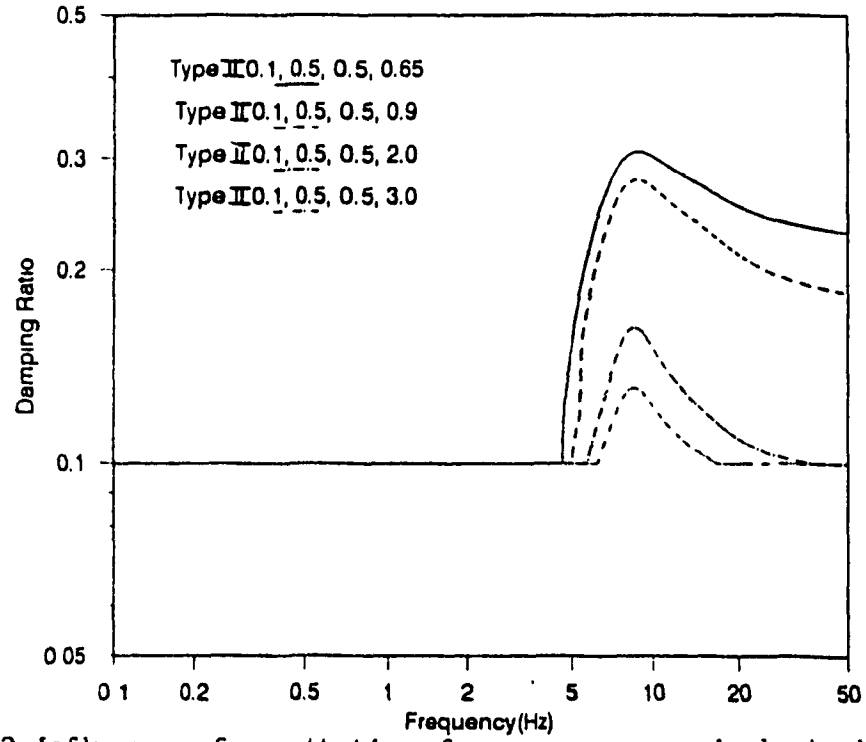

Fig. 3.22 Influence of excitation frequency on equivalent damping ratio for Type II Dual-phase Damper as β_2 is varied(α_2=0.5) in a Four-Element model

3.4 A Parametric study of a Type II dual-phase damper in a two-element model

In this section, Type II dual-phase damper is considered for detailed parametric study, as it was found to perform better for isolator applications. The Type II dual-phase damper was further considered for experimental investigation to validate the analytical study.

For Type II dual-phase damper, the results showing damping ratio versus frequency in Figs. 3.12-3.14 in general indicate that damping ratio remains constant until certain frequency is reached, then it increases initially and then decreases as frequency is increased. This characteristic is influenced by values of α_2 and β_2 which are primary design parameters for such a damper.

This section presents results to show the influence of α_2 and β_2 on the damping characteristics of Type II dual-phase damper. In particular, the influence of α_2 and β_2 on :

1. the value of maximum f for which damping ratio remains constant;
2. maximum damping ratio near resonance; and
3. damping ratio for $f = 3f_n$

Figs.3.23-3.24 show the influence of α_2 and β_2 on f/f_n corresponding to initial constant damping. It was found that with increase in β_2 value the maximum frequency at which the system starts to

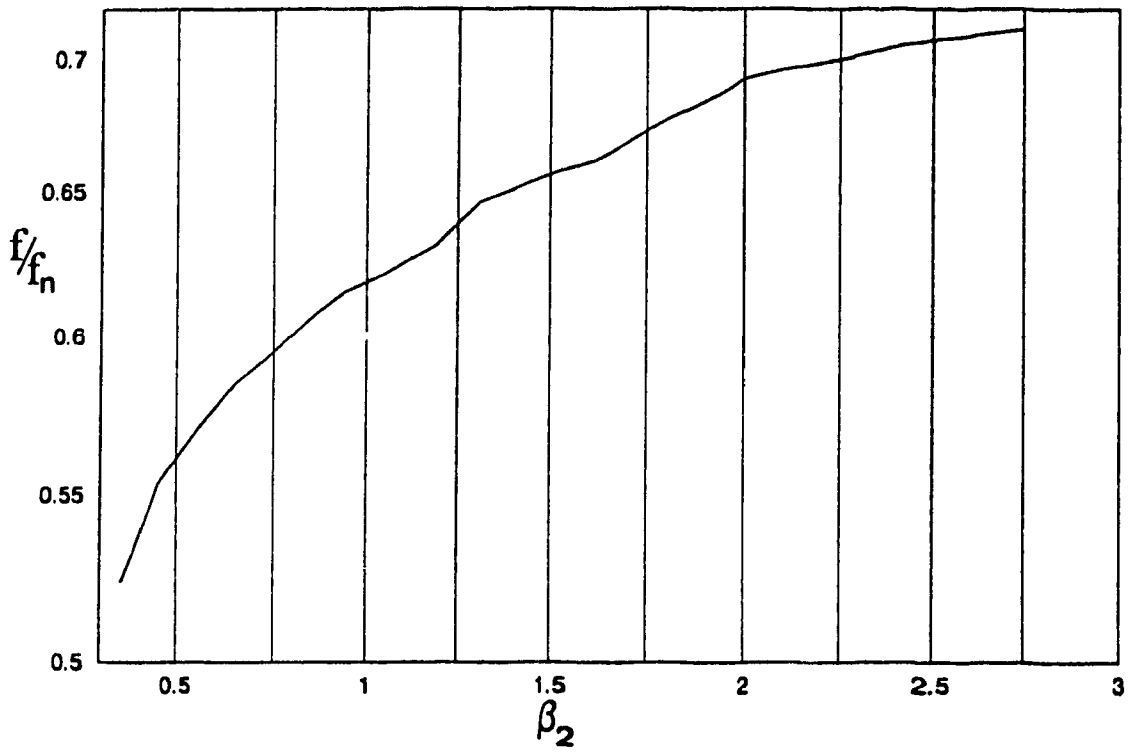

Fig. 3.23 Influence of β_2 on the maximum frequency corresponding to constant minimum damping ratio. $\zeta_1 = 0.1$, $\zeta_2 = 0.5$, $\alpha_2 = 0.3$

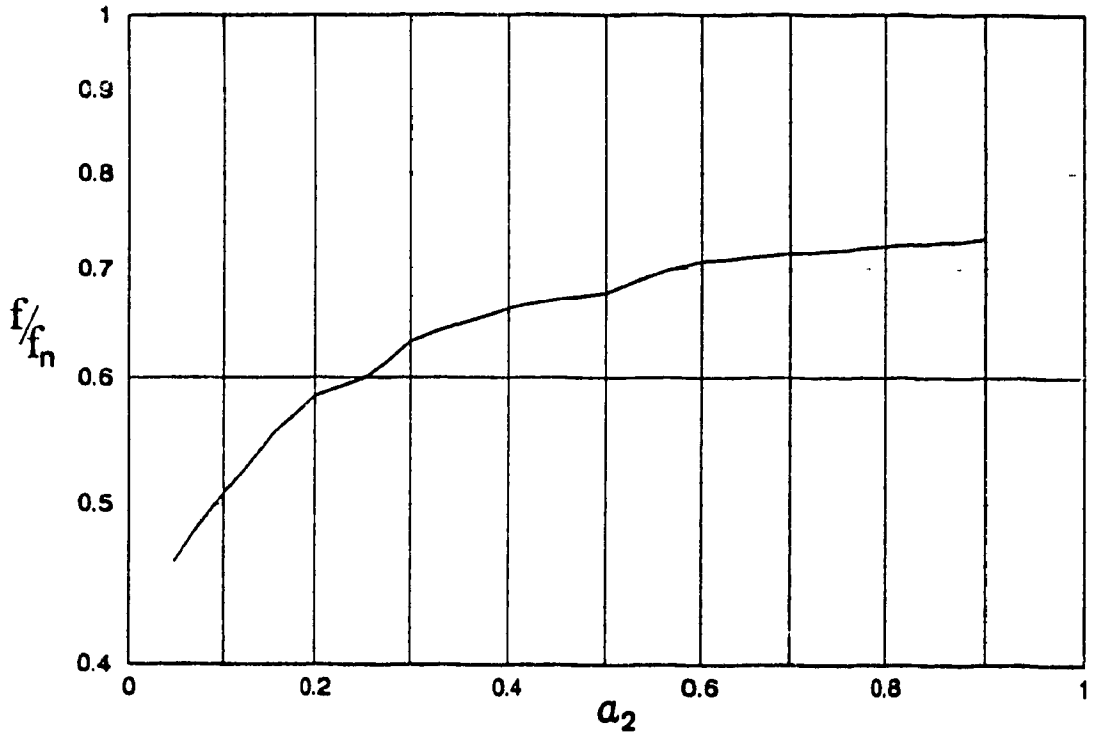

Fig. 3.24 Influence of α_2 on the maximum frequency corresponding to constant minimum damping ratio. $\zeta_1 = 0.1$, $\zeta_2 = 0.5$, $\beta_2 = 1.0$

deviate from a constant equivalent damping ratio increases, indicating that, the system will be dominated by a constant damping value for a longer duration of frequency range. This in turn indicates that the performance at the resonance will deteriorate with increase in β_2 value for a fixed α_2 value. A similar study was made to predict the performance of the system for constant β_2 value and for various α_2 values. Similar to the previous case, it was found that an increase in α_2 value increased the range of frequency in which the damping ratio remained constant.

When the frequency is increased beyond the constant damping ratio range the damping ratio peaks. The influence of α_2 and β_2 on the peak damping ratio is shown in Figs.3.25 and 3.26. It is found that, by increasing the parameter β_2 for a fixed value of α_2, the peak damping ratio will decrease with increase in β_2 value. As in the previous case a similar study was made to predict the performance of the system for constant β_2 value for variation in α_2 values. The results show that an increase in α_2 value results in a shift in the frequency at which peak damping ratio is obtained, and thus results in a decrease in peak damping ratio.

Finally, when $f = 3f_n$ is reached, the damping ratio value for Type II dual-phase damper decreases below the peak value. The influence of α_2 and β_2 on ζ_{eq} for $f = 3f_n$ is shown in Figs.3.27 and 3.28 respectively. The results show that by increasing α_2 and β_2, the damping ratio value shows a decreasing trend. This indicates that the damping ratio will be reduced at high frequency and thus resulting in an improved performance.

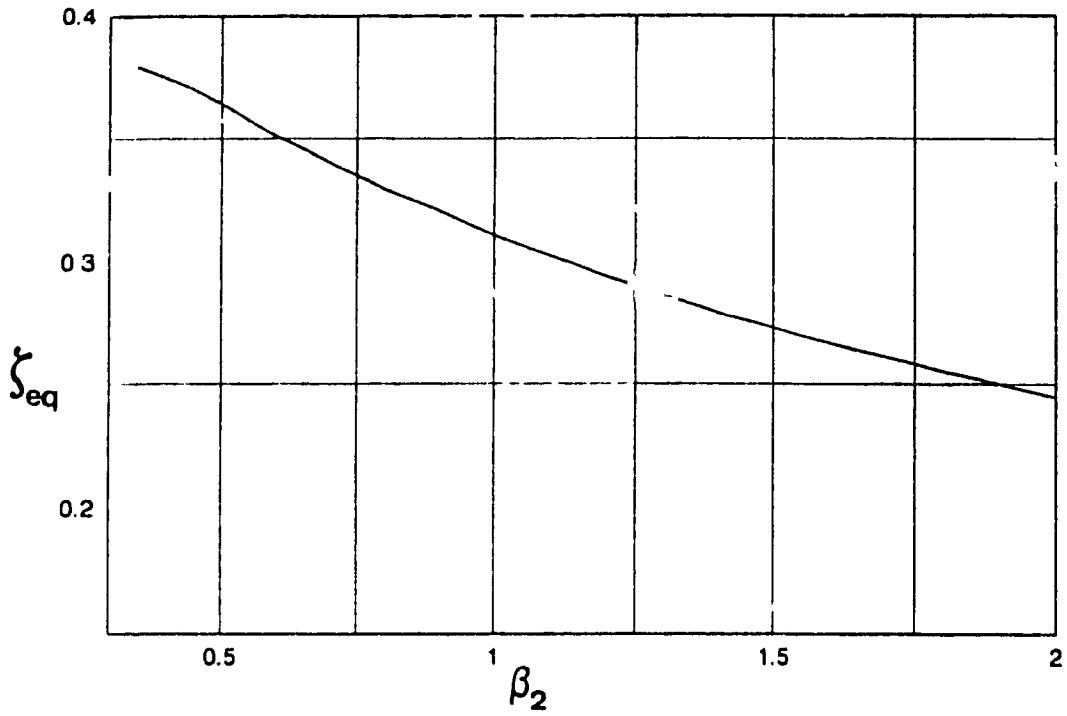

Fig. 3.25 Influence of β_2 on peak damping ratio
$\zeta_1 = 0.1$, $\zeta_2 = 0.5$, $\alpha_2 = 0.3$

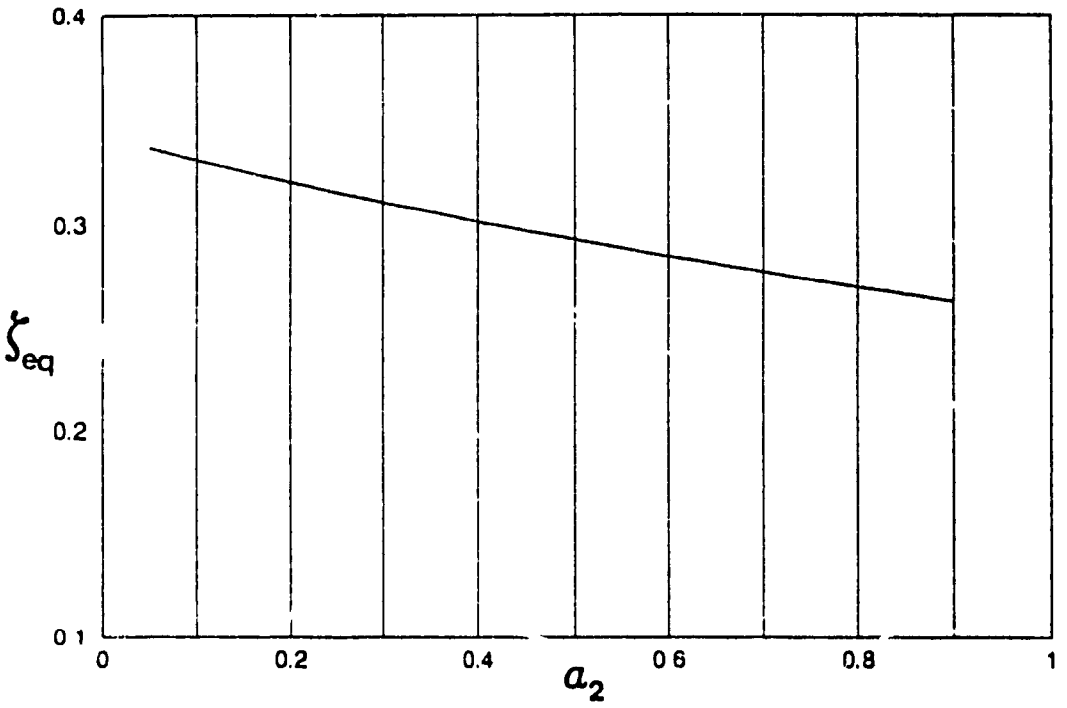

Fig. 3.26 Influence of α_2 on peak damping ratio
$\zeta_1 = 0.1$, ζ_2 [illegible], $\beta_2 = 1.0$

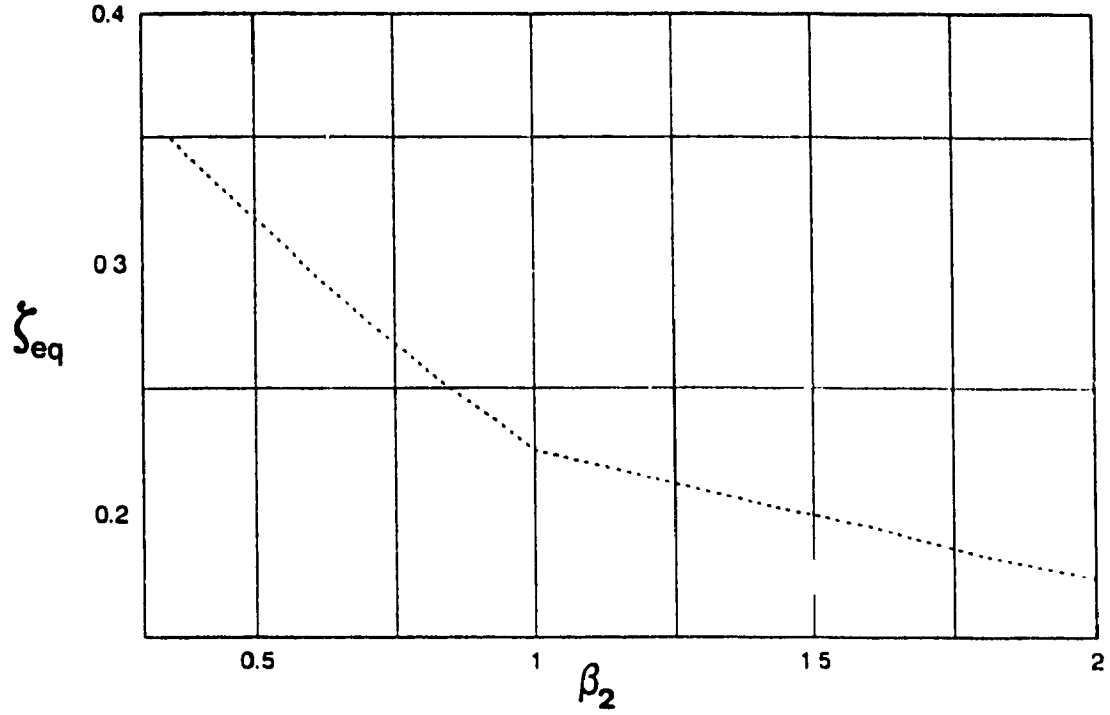

Fig. 3.27 Influence of β_2 on ζ_{eq}. $f = 3f_n$
$\zeta_1 = 0.1$, $\zeta_2 = 0.5$, $\alpha_2 = 0.3$

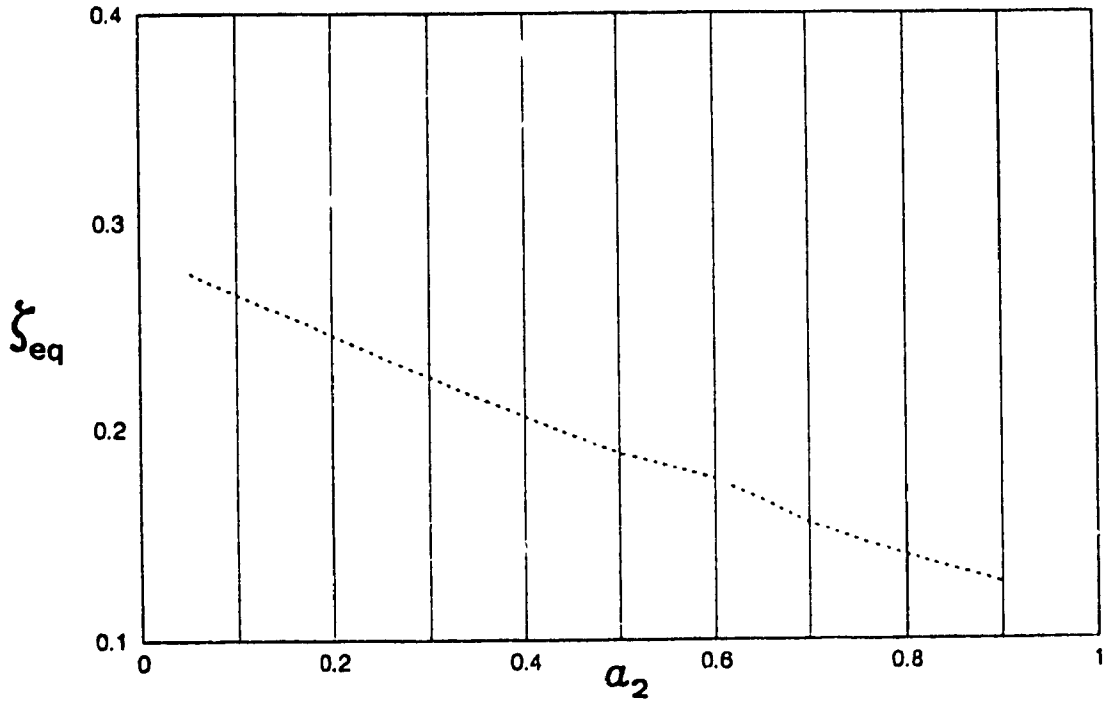

Fig. 3.28 Influence of α_2 on ζ_{eq}. $f = 3f_n$
$\zeta_1 = 0.1$, $\zeta_2 = 0.5$, $\beta_2 = 1.0$

The results presented in this section are useful in selecting the parameters α_2 and β_2 for a specific isolator application. One should attempt to choose α_2 and β_2 such that ζ_{eq} is maximum for or near f_n and that ζ_{eq} is minimum possible for $f>3f_n$. However, as the results indicate they are conflicting requirements. When a Type II dual-phase damper is used, for example, smaller value of α_2, and β_2 close to α_2, results in maximum ζ_{eq} at f_n (desirable) and at $f >> f_n$ (undesirable), and larger α_2 with β_2 very much greater than α_2 results in lower ζ_{eq} at f_n (undesirable) and at $f >> f_n$ (desirable). Due to these conflicts a compromise is needed in selecting α_2 and β_2 depending on the isolation requirement.

From this study, it is also evident that a change in the damping characteristics could be possible through use of a profiled metering pin instead of a piecewise linear pin considered in this study.

3.5 Discussions on Simulation Results

The performance characteristics that will be discussed are some of the major one's that must be taken into account in the evaluation of the hydraulic mount with dual-phase damper. The hydraulic mounts developed by [13, 16, 17] allow the use of softer mounts for better vibration isolation and the internal fluid damping overcomes the engine bounce problem. But the main drawback of these mounts is that they can be tuned only to a particular frequency of interest as specified by the customer. The damping effect for a particular frequency can be obtained by

adjusting the orifice opening connecting the two chambers and by using fluids of different viscosities. On the other hand, a dual-phase damper provides the user with a flexibility to operate the mount at a high or low levels of damping depending on the frequency range. This in turn provides the benefit of tuning the mount over a wide range of frequency. Based on the results presented in this section, following conclusions can be drawn: First, in the low frequency range, the performance of Type I and Type II dual-phase dampers and hydraulic mount with elasto damper by Clark[13] were better than that of hydraulic mounts with linear viscous damper. This is illustrated in Fig. 3.29. Second, among the 2 different types of dual-phase dampers studied, the Type II dual-phase damper is superior both in the high as well as low frequency range as long as α_2 and β_2 values are close. Thus, at low values of absolute displacements the damping ratio should be low [here ζ_1 = 0.1] and at high values of absolute displacements the damping ratio should be high [here ζ_2 = 0.5]. The study on the four-element model also have provided some interesting results. In this case, introduction of Type I dual-phase damper in place of passive damper resulted in an improvement in the high frequency range and the performance also improved in the resonant range when α_1 value was increased. However, when Type II dual-phase damper was introduced, the performance was superior in the resonant range with reasonable improvement in the high frequency range, when difference between α_2 and β_2 were small. Here, an increase in α_2 value resulted in superior performance in high frequency range. Finally, comparing the two-element and four-element models with Type II damper it can be observed from Fig. 3.30 that the four-element model out performs the two element model throughout the frequency range.

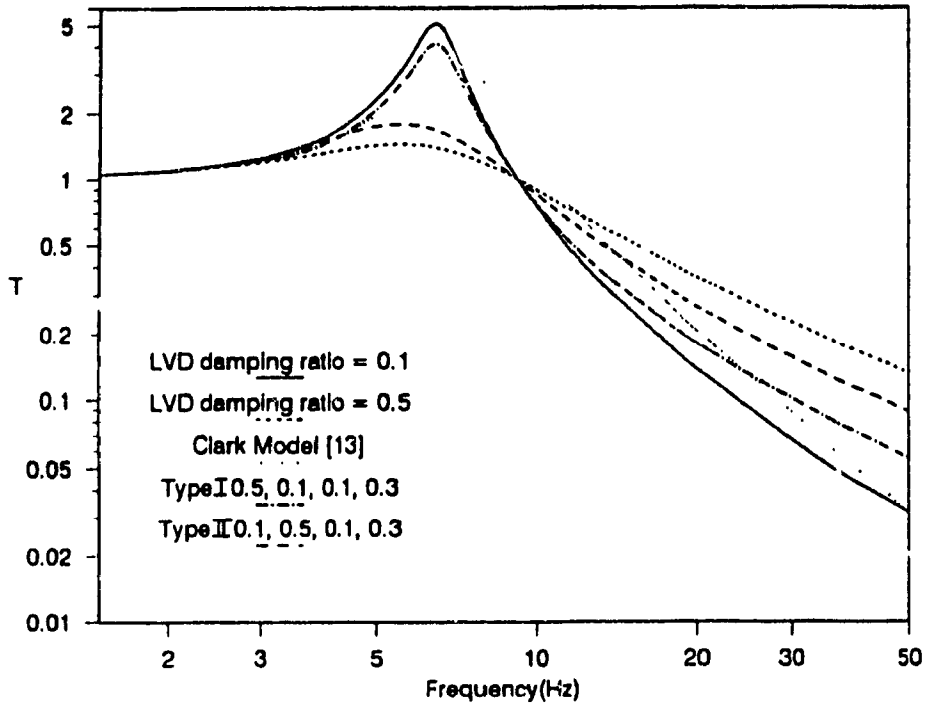

Fig. 3.29 Force Transmissibility comparison of various mount models

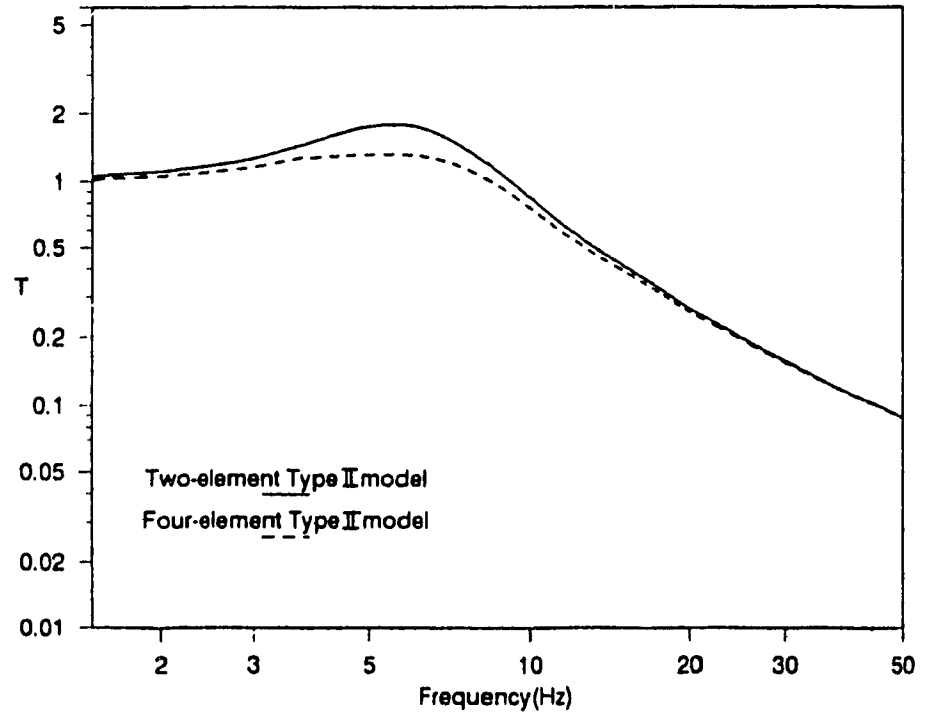

Fig. 3.30 Force Transmissibility comparison of Type II Dual-phase dampers for ζ_1=0.1, ζ_2=0.5, α_2=0.1 and β_2=0.3

Therefore the four-element, Type II dual-phase damper is the best performer among the two models proposed. The two-element, Type II model has performance characteristics that are as good as four-element, Type II model in the low as well as high frequency range. Hence it can be inferred that, the dual-phase damper systems combine the good low frequency performance of highly damped passive systems with good high frequency performance of passive systems with light damping. Thus, when the desired performance cannot be obtained with passive systems and if superior performance using active control system is not a necessity then the simple hydraulic mount system using Type II dual-phase dampers is recommended.

3.6 Summary

Results of the study on two models of hydraulic mounts with two types of dual-phase dampers are presented for different values of damping ratios and displacements. The merits and demerits of each type in comparison with passive mounts are also discussed.

CHAPTER 4

EXPERIMENTAL INVESTIGATION

4.1 Introduction

In the previous sections, analytical studies have been presented to predict the performance of dual-phase dampers for their vibration isolation performance. But, in order to validate the analytical predictions, so that the scheme is feasible for general industrial use, experimental verification is very much necessary. Hence, here the experimental performance of a prototype dual-phase damper and constant orifice dampers are presented and compared with analytical predictions. The analytical studies presented indicates that Type II dual-phase damper combines the good characteristics of high damping near resonance and low damping at high frequency. Consequently, Type II dual-phase damper was selected for experimental investigation.

4.2 Development of the Prototype Damper

A prototype damper with flexibility to adopt as either a constant orifice damper or as a dual-phase damper was developed at Concave Research Centre. The flexibility was possible because of the metering pins used. A large scale construction using plexiglass was selected for the prototype to facilitate visual observation and for ease of variation in parameters.

In order to develop the prototype damper, the fluid flow

characteristics through the orifice must be known. The flow can be either laminar or turbulent. In laminar flow, the fluid flows in layers or laminas and the damping force is generated due to the shearing of the fluid. However in turbulent flow the fluid has irregular motion and the damping force is generated due to fluid flow through an orifice. In the prototype damper, the fluid flow occurs through annular space between the pin and the orifice plate. Thus, the flow is assumed turbulent. The characteristic equation for turbulent flow through an orifice is:

$$Q = C_d A_o \left[2(\Delta p)/\rho\right]^{0.5} \tag{4.1}$$

where C_d = discharge coefficient

A_o = area of orifice

Δp = pressure drop across the orifice

ρ = mass density of the fluid

and the damping force F_d is given by[35]:

$$F_d = T_{FC} V^2 \tag{4.2}$$

where

$$T_{FC} = A_p \frac{\rho}{2} \left[\frac{A_p}{C_d A_o} \right]^2$$

$$A_p = \frac{\pi}{4}\left[D_p^2 - D_o^2\right] \quad \text{and} \quad A_o = \frac{\pi}{4}\left[D_o^2 - d^2\right]$$

where T_{FC} = turbulent flow coefficient

V = relative velocity across the damper

D_p = inside diameter of the tube[Fig. 4.3]

D_o = orifice diameter

d = pin diameter

Here the turbulent flow coefficient is assumed to be same for both compression and extension since the volume of the displaced liquid is assumed to be same in compressic· and extension. Also, the effect of temperature, air column and o-ring friction is neglected.

A prototype of Type II dual-phase damper with a damping characteristic as shown in Fig.4.1 was designed. A constant amplitude of 50.8mm(2") peak to peak and α_2 and β_2 values of 0.25 and 0.45 respectively gave the relative displacement value of 12.5mm and 22.7mm respectively.

The damper was designed with flexibility to adopt one of three metering pins, in which two pins correspond to two constant values of damping and the third pin provided the dual-phase characteristic. Fig.4.2 shows the schematic of the three pins used for the test along with their dimensions. The dimensions were determined based on turbulent flow conditions. Metering pin # 1 corresponds to low damping, pin # 2 corresponds to high damping. while pin # 3 provides low, high and also variable damping depending on the displacement of the pin across the orifice plate. The calculation for orifice and pin dimension in the design of prototype was aimed at achieving an a ٤e value of C_1 = 165Ns/m and C_2 = 292Ns/m for low and high constant orifice damping and the two damping values for dual-phase damper. The orifice plate is

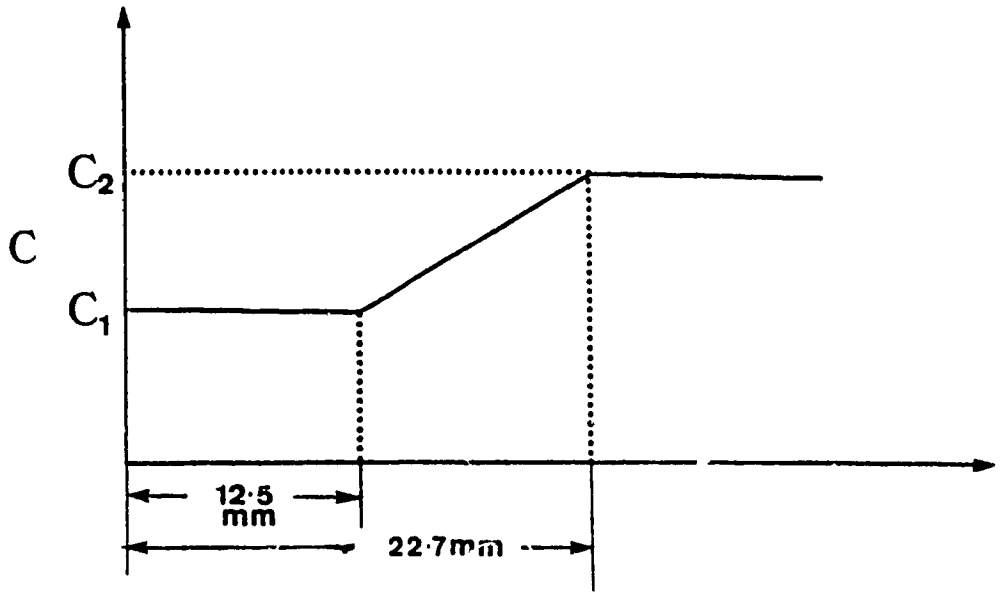

Fig.4.1 Damping characteristics of prototype dual-phase damper with C_1 = 165Ns/m and C_2 = 292Ns/m, α_2= 0.25 and β_2=0.45

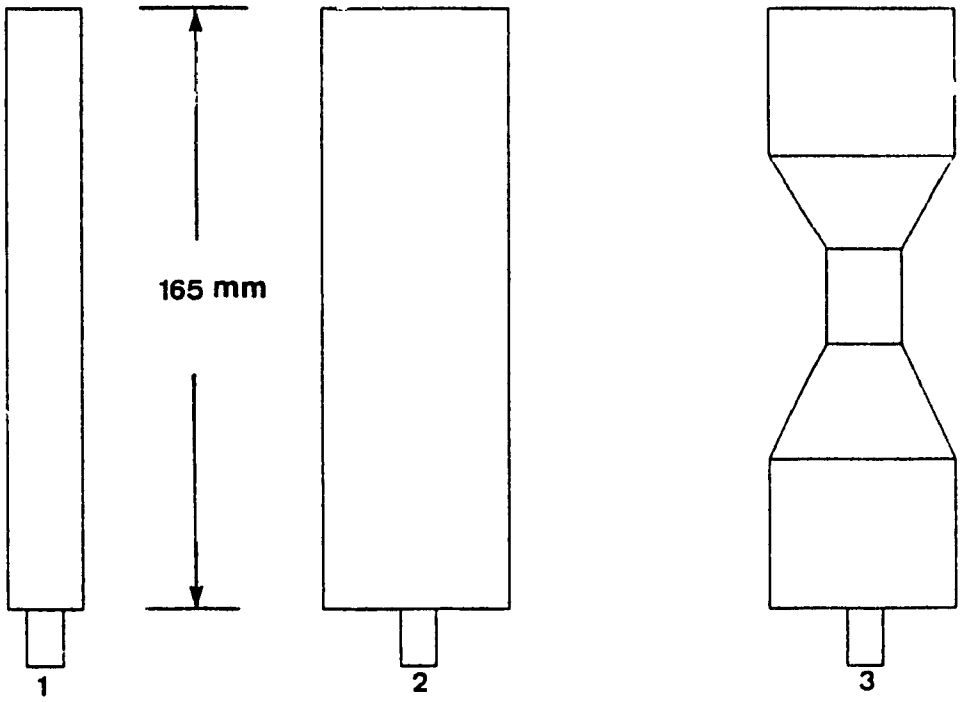

Fig. 4.2 Metering pins for experimental study
1. Low damping pin (diameter=8mm)
2. High damping pin (diameter=17.92mm)
3. Dual-phase damping pin

screwed to the base of the fixed plexiglas tube while the pin is screwed to the bottom of the plexiglas tube connected to the shaker. Vent holes were provided on the top cover of the damper to minimize air spring effect. This is illustrated in Fig.4.3. When the shaker moves up and down, the oil flow across the orifice plate will create the necessary damping depending on the type of pin used.

Testing of the developed prototype damper was carried out in two phases. The objective of phase I was to investigate the Force-Displacement characteristics of the damper. Phase II of the experiment deals with the determination of transmissibility for a mass-spring system using the developed prototype damper. The primary objective in phase II was to validate the analytical results and evaluate the performance of dual-phase damper in comparison to constant orifice damping.

4.3 Phase I: Damper Characteristics

As mentioned in the previous section, the objective of phase I was to determine the damping force developed by the damper for the three metering pins for various frequencies so as to obtain the necessary system parameters for phase II testing.

4.3.1 Test Rig for Phase I

The test rig for phase I consisted of a hydraulic actuator, the prototype damper and a load cell as presented in the pictorial view of

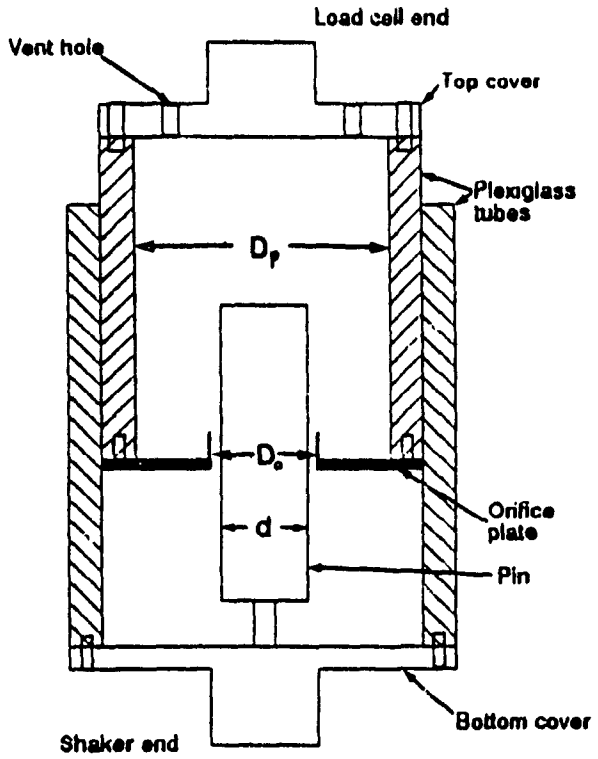

Fig.4.3 Schematic of the prototype damper

Figs. 4.4(a) and 4.4(b). The excitation was provided by the Lab Series 10000 hydraulic actuator manufactured by the LAB division of Mechanical Technology Inc., New York, which has the capability to provide stroke of ± 76.2mm(±3"). Sinusoidal displacement input of 0.5Hz to 4Hz were used. The load cell of 2 ton capacity, manufactured by Kyowa of Japan was used to measure the damping force. The Kyowa unit has the capability to produce reliable signals from DC levels because it makes use of a strain gauge piezoresistance circuit with ± 2V AC bridge excitation. The voltage from the strain amplifier of the load cell was displayed on a strip chart recorder and also on a Philip 5035 series oscilloscope. On the oscilloscope, the X-Y display mode was used with displacement and damping force plotted on the X and Y axis, respectively. Using a polaroid camera the displayed Force-Displacement plot was also recorded.

4.3.2 Test Procedure and Results of Phase I

All tests were carried out for a peak to peak input displacement of 50.8mm(2"). Phase I of the experiment was performed in two stages. In the first stage, the damping force developed by the constant orifice metering system, comprising of metering pin #1 (low damping) and pin #2 (high damping) was tested. During operation, fluid is forced through the constant orifice passage, which in turn will produce the necessary resistive force. Finally, the metering pin with dual-phase damping characteristic was tested. Here, the effective orifice area varies as the damper is stroked. Thus, the orifice area is progressively reduced as metering pin diameter increases due to tapered profile and reaches a maximum as displacement goes beyond β_2 value. In all the three cases,

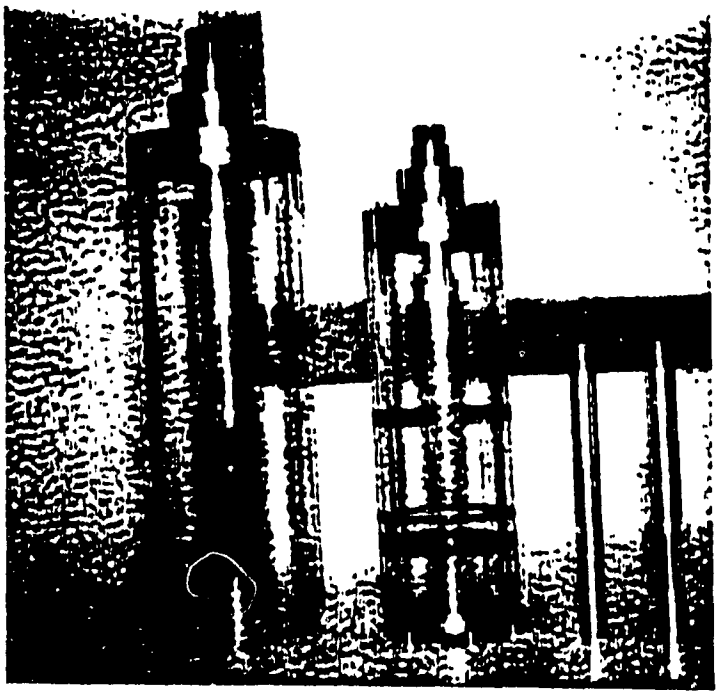

Fig.4.4(a) Components of experimental prototype damper

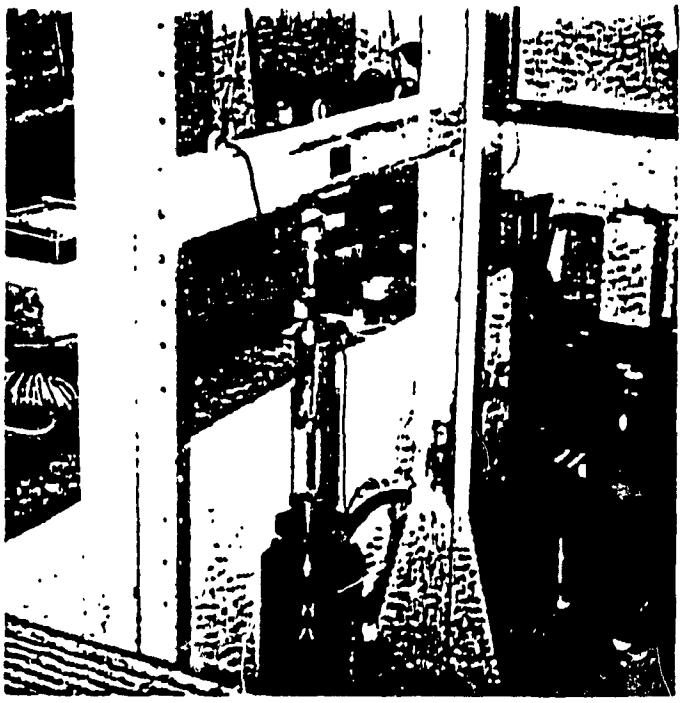

Fig.4.4(b) Experimental setup for force-displacement testing of prototype damper

the damping force developed was measured on a strip chart recorder, as well as on an oscilloscope as Lissajous plots. The Lissajous plots, obtained for all 3 pins in the frequency range of 0.5Hz to 4Hz are presented in the Appendix. These results are useful in evaluating the average damping force and energy dissipation per cycle as frequency is varied.

From the Lissajous plots, the damping force during compression and extension strokes are obtained. Then the result as average damping force as a function of frequency is calculated and presented in Fig.4.5. The method for evaluating average damping force is presented at the end of the Appendix. A curve for dry run to estimate the non-hydraulic effects is also presented. From the curve (Fig.4.5 corresponding to dry run) it is apparent that there is some air damping present for low frequency and air spring effect at high frequencies. It can be observed from the figure that the damping force initially increases with increase in frequency in all the three cases and then decreases with increase in frequency. When the metering pin corresponding to high damping was used, the damping force increased rapidly with increase in frequency. But when the metering pin corresponding to low damping was used, the damping force increased only gradually with frequency. However, when the metering pin corresponding to dual-phase damping characteristic was used, the damping force initially increased with increase in frequency(followed high damping for low frequencies) and then starts to decrease with increase in frequency(followed low damping for high frequencies).

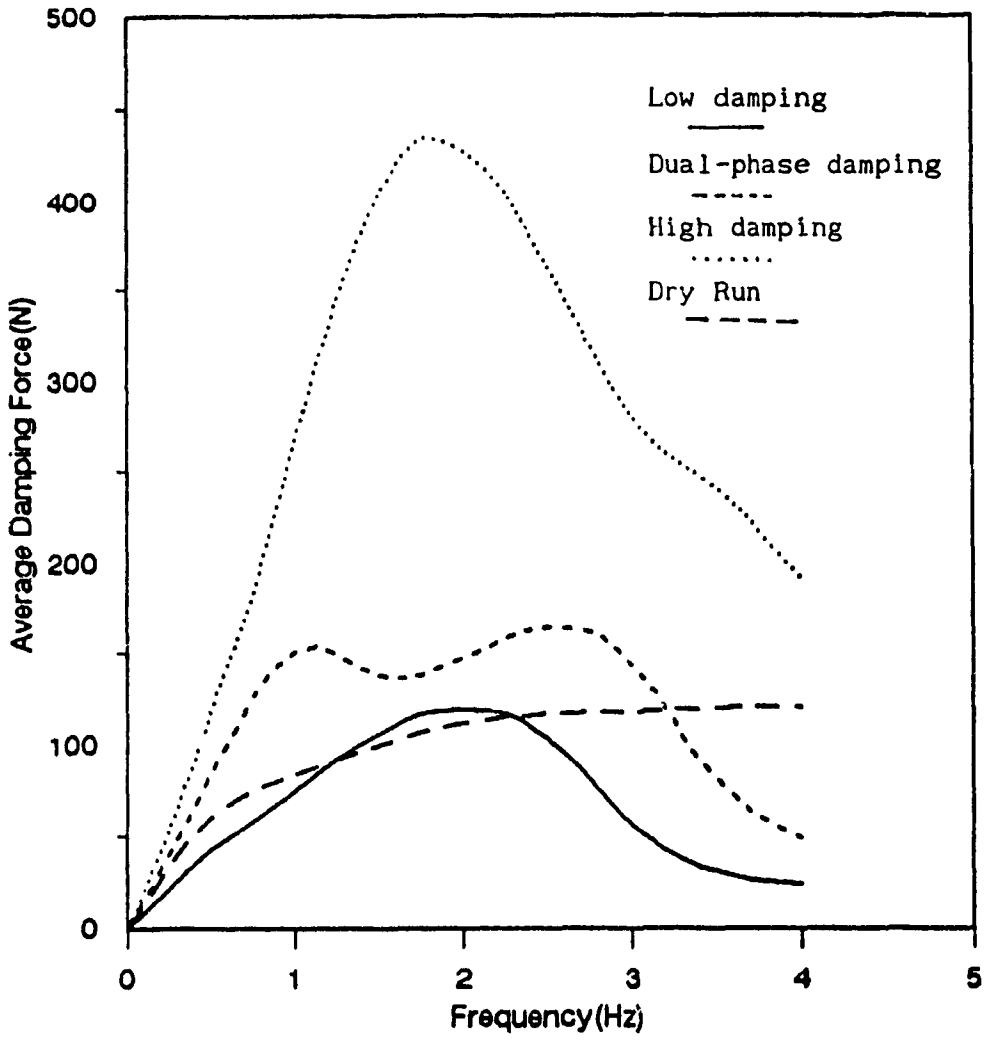

Fig.4.5 Experimental average damping force as frequency is varied

Similarly, from the experimental Lissajous plots at various frequencies, equivalent damping coefficients(C_{eq}) is computed by equating the area inside the Lissajous loop to the energy dissipated per cycle in a viscous damper. The result as equivalent damping coefficient versus frequency is shown in Fig.4.6. The results show that, the damping coefficient of the dual-phase damper approaches high damping value for low frequencies and low damping value for high frequencies. The results further show that the equivalent damping coefficient in all the three cases reduces significantly as frequency is increased. Once again for dual-phase case, the damping coefficient approaches high damping for low frequencies and low damping for high frequencies.

4.4 Phase II: Isolation Characteristics

The objective of phase II was to determine the experimental damping ratio, acceleration transmissibility and relative displacement ratios for three runs using the three pins. Determination of damping ratio was found necessary in order to validate the experimental results analytically. Test results were obtained for a frequency range of 0.5Hz to 5Hz, and each run was performed twice to ensure repeatability of the experiment.

4.4.1 Test Rig

In contrast to phase I of the experiment, where only the damper was tested, in phase II a complete spring-mass-damper system was built to study the performance of Type II dual-phase damper, and to validate the

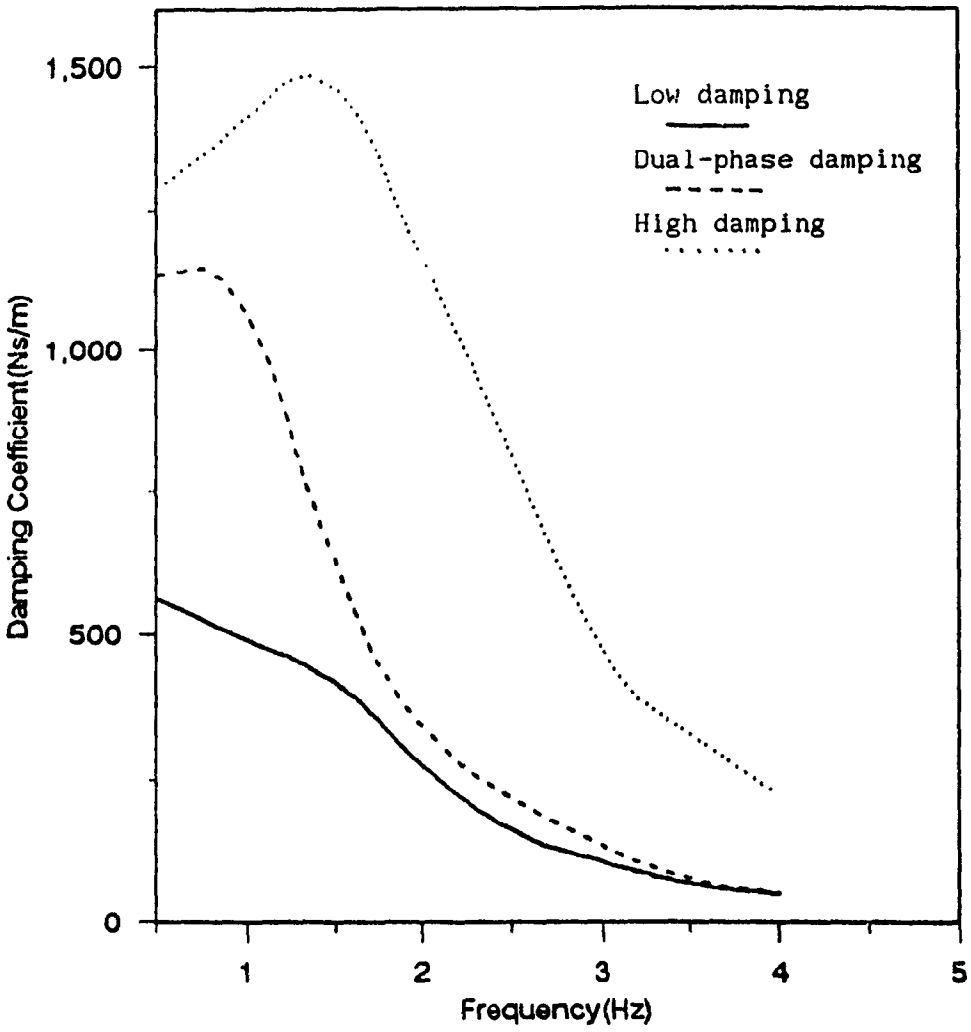

Fig.4.6 Equivalent damping coefficient based on experimental energy dissipation for different excitation frequency

analytical model. Hence, commercially available springs capable of providing stiffness of about 13660 N/m(78 lb/in) was used as spring. Steel plates with a total mass of about 74.90 kg was attached to the top of the damper unit as mass. Four Thomson linear bearings, attached to the platform on the inertial frame was used as guide to the mass which moves up and down along with the actuator. A schematic of the setup is shown in Fig. 4.7.

Commercially available instrumentation components were used to measure the input and mass accelerations and relative displacement for various frequencies. The instrumentation used were:

- two piezoelectric accelerometers (Type 4370) and two charge amplifiers (Type 2651) manufactured by B & K were used to measure the acceleration of the mass and the actuator,

- a Linear Variable Differential Transformer, often known as LVDT (Type 3000 DC-DC) manufactured by Durham Instruments was used to measure the relative displacement between the mass and the actuator, and

- a 4 channel strip chart recorder manufactured by Gould Inc., Cleveland Ohio, U.S.A. was used to record the signals.

4.4.2 Test Procedure and Results of Phase II

4.4.2.1 Determination of Damping Ratio

The primary objective in this part of the testing was to determine

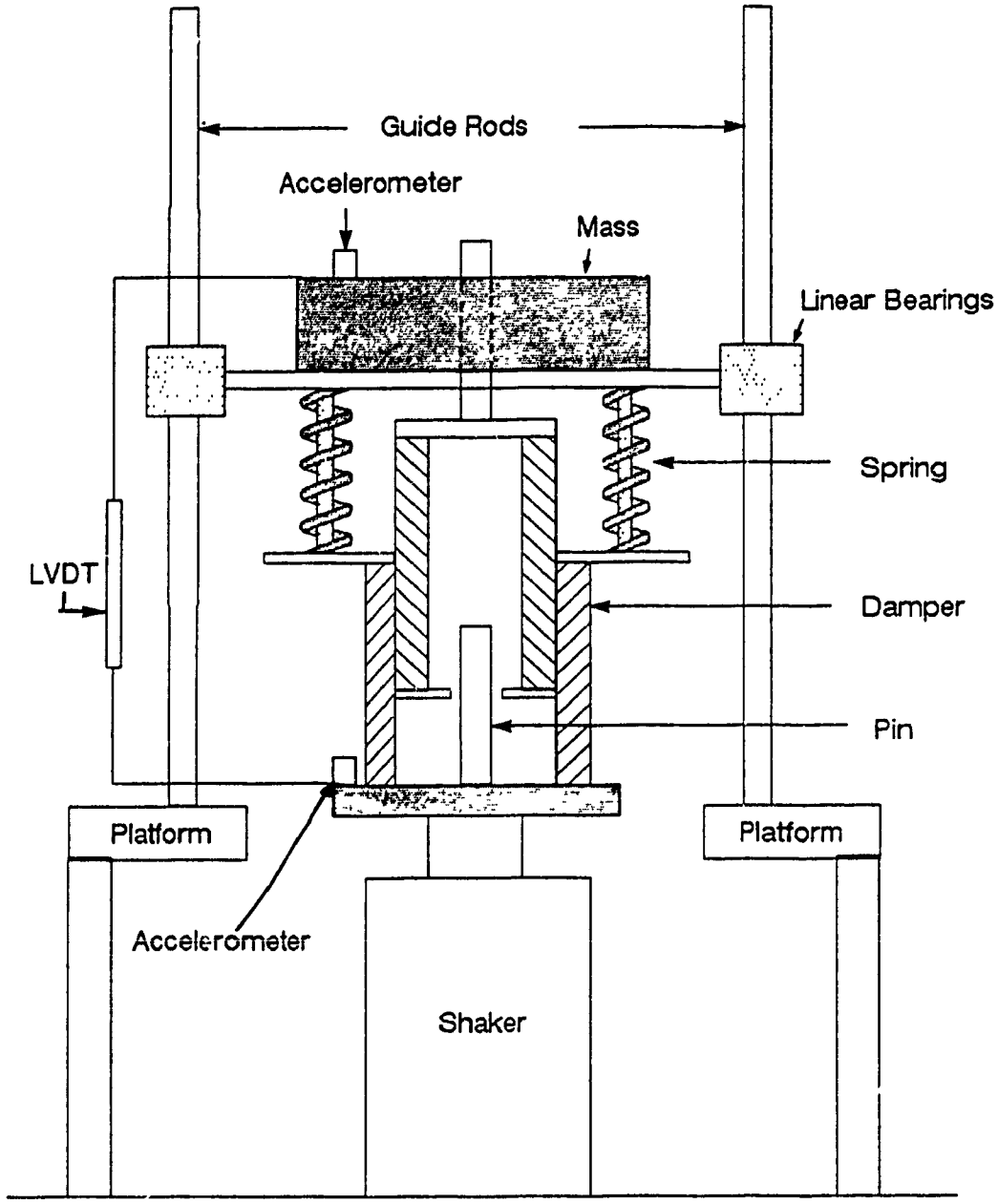

Fig.4.7 Schematic of experimental setup for phase II tests.

the damping ratio ζ, for the constant orifice dampers, in order to verify the prototype design and to carryout analytical simulation using experimental damping values. One of the convenient ways to determine the amount of damping present in a system is to measure the rate of decay of free oscillations to step displacement input. Thus, the motion of the mass was determined by means of an LVDT(which provides an electrical voltage proportional to the displacement of a moveable iron core) to step displacement input. In the experiment, the LVDT was attached between the mass and the actuator to measure the relative displacement across the damper. The decaying response was recorded on a strip chart for both extension and compression. Then, the damping ratio was calculated using the logarithmic decrement method for several runs in each case. From the response plots, it was also possible to determine the natural frequency of the system by measuring the period between either two consecutive peaks or crests and it was found that there was very good repeatability.

Table 4.1 Step displacement input results

	Damping ratio(ext)	Damping ratio(com)	Damping ratio(mean)	Damped nat. freq Hz	Undamped nat. freq Hz
Pin # 1 Low damping	0.12	0.14	0.13	2.7	2.72
Pin # 2 High damping	0.22	0 24	0 23	2.7	2.77

Table 4.1 presents the average values of ζ and f_n for both low and

high damping cases. In analytical simulation, the mean value of ζ was used.

4.4.2.2 Transmissibility Results

In the analytical studies, the results were presented in terms of transmissibility for various frequencies. Similarly, the experimental results are also presented in terms of transmissibility for various input frequencies. The transmissibility was first determined for the two constant orifice damper and then for the dual-phase damper. The frequency was varied from 0.5Hz to 5Hz in steps of 0.5Hz and for constant peak to peak amplitude of 50.8mm(2"). Transmissibilities were obtained as mass/input acceleration ratio, as well as relative displacement ratio across the damper. Figs. 4.8 and 4.9 illustrates the relative performance of low, high and dual-phase dampers. It can be observed from the experimental acceleration transmissibility results(Fig. 4.8), that constant orifice damper with low damping performs poorly in the low as well as resonant range and the maximum transmissibility value was about 4.35 around 2.7Hz. However, the performance was good beyond resonance, which indicates that low damping in a system is useful in the high frequency range. It can also be observed, that constant orifice damper with high damping performs comparatively better in the low as well as resonant range. However, the performance deteriorates beyond resonance, which indicates that high damping in a system is useful in the low and resonant frequency regions. The transmissibility plot for dual-phase damper shows that at low and resonant frequency range, the transmissibility is lower than constant

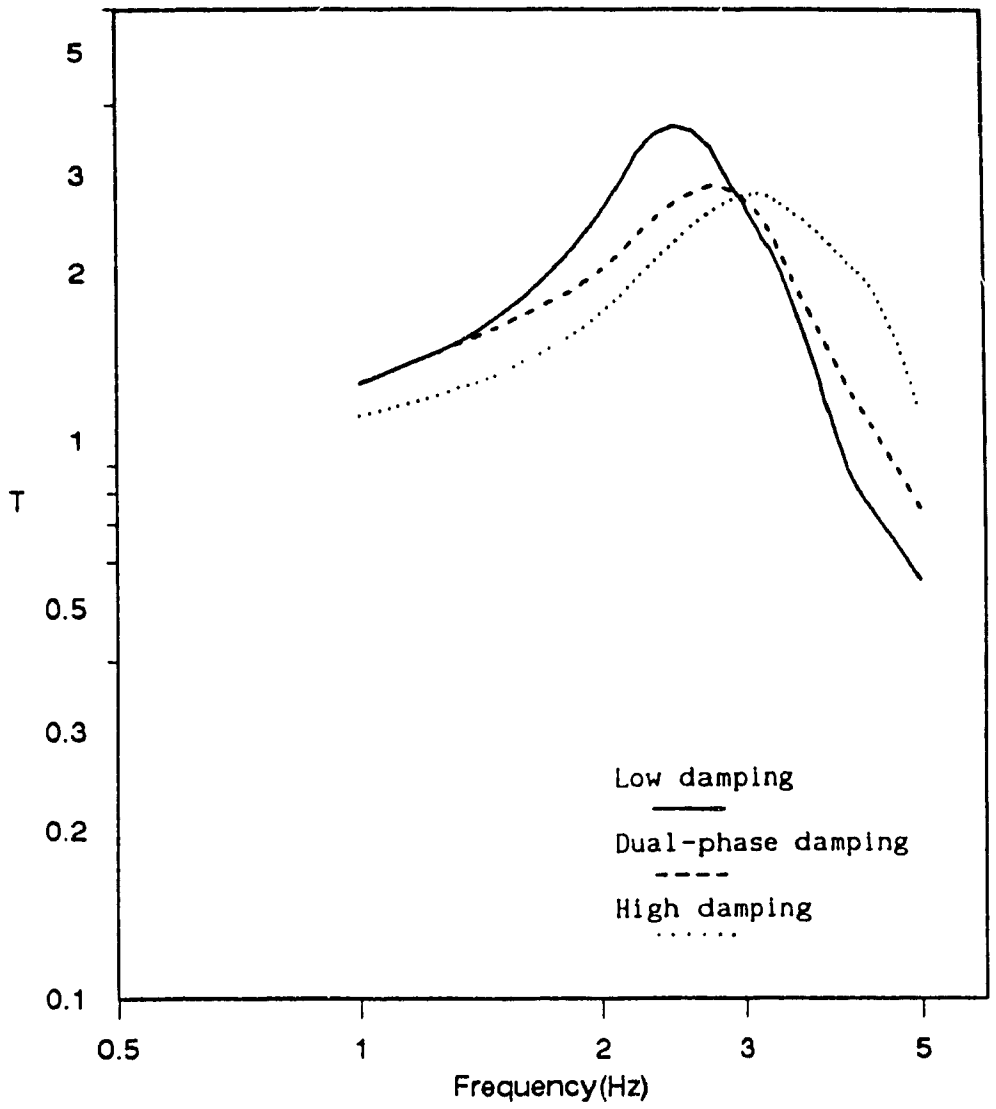

Fig.4.8 comparison of Experimental acceleration transmissibility of low, high and dual-phase dampers

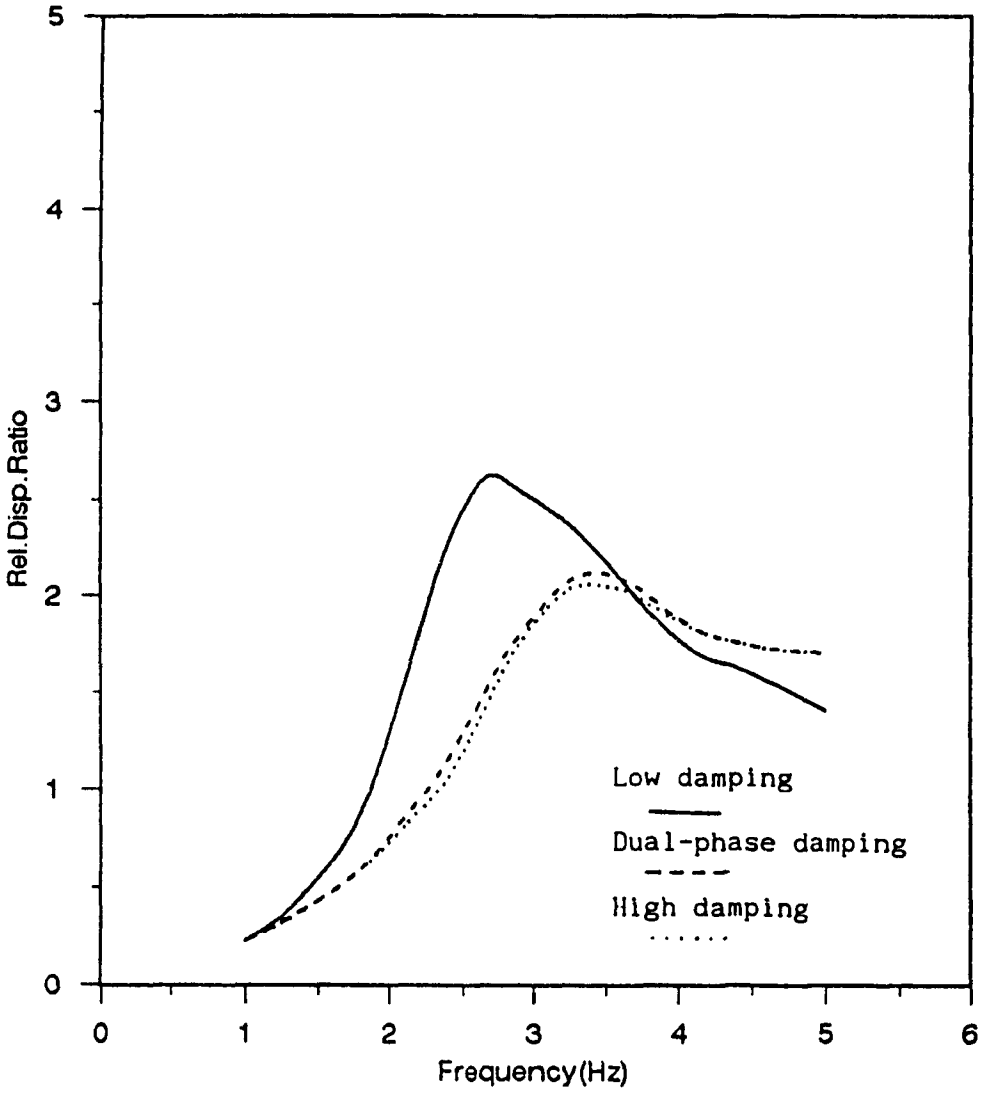

Fig.4.9 comparison of Experimental relative displacement ratio of low, high and dual-phase dampers

orifice low damping case, which is an indication that the dual-phase damper has the capability to bring down the transmissibility at resonance.

A comparison of relative displacement ratio shown in Fig.4.9 further shows that the performance of dual-phase damper is as good as that of high damping case over the entire frequency range. Hence, the improvement in transmissibility can be obtained without any loss in relative displacement performance at resonance, which is highly desirable in mount application to avoid rattle.

Using the parameters corresponding to the experiment, attempts are next made to simulate both fixed and dual-phase damping systems to compare with those of experimental findings. The following sections present such comparison for one damping case at a time.

Constant Orifice Damper(Low damping)

To begin with, the performance of the constant orifice damper with low damping was evaluated. Fig.4.10 shows the acceleration transmissibility for various input frequencies. The figure also presents the results from analytical simulation using two sets of system parameter values. In the first set, the damping ratio is assumed to be ζ=0.13 and the natural frequency to be 2.72Hz, both estimated from step response. In the second set, the damping coefficient is assumed as shown in Fig.4.6.

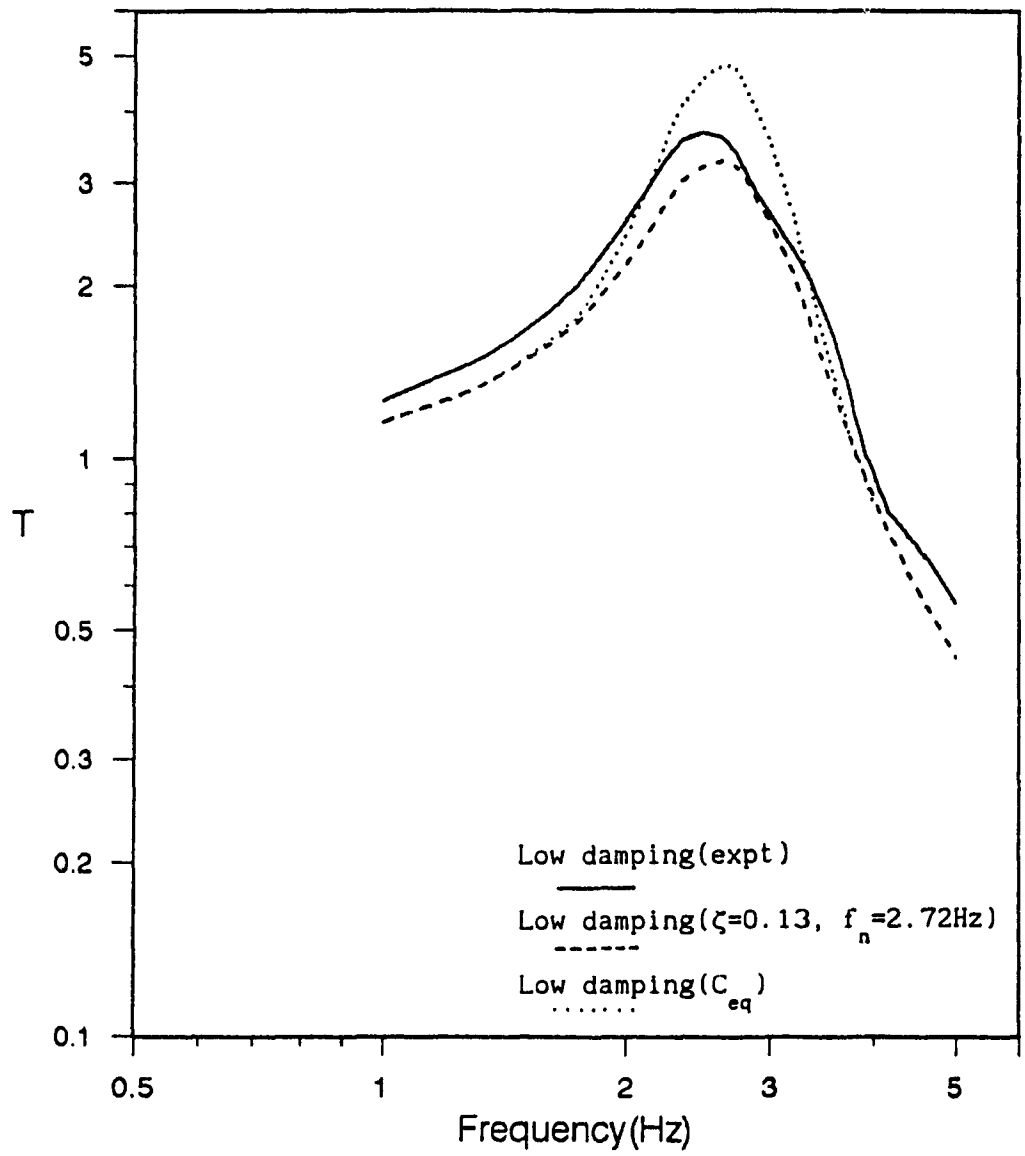

Fig.4.10 Experimental and simulation acceleration transmissibility plot for low damping

The results clearly show excellent correlation between the experimental and analytical investigation for the constant orifice damper, when undamped natural frequency of 2.72Hz was used for simulation with ζ=0.13(step response). However, when C_{eq} value(determined from the Lissajous plot) corresponding to each frequency was used in simulation, it can be seen in the figure that there is good correlation in the low as well as high frequency range. But, in the resonant region the transmissibility determined using C_{eq} value does not follow the trend set by the experimental result. This can be attributed to the fact that the damping coefficient value near the resonance is underestimated using energy equivalent method.

Similarly, the relative displacement ratio was also determined, both experimentally and analytically using constant damping ratio determined from step response and the C_{eq} value obtained from Lissajous plot. This is illustrated in Fig.4.11. Here also it can be seen that there is reasonable correlation between experimental and analytical study for constant damping ratio. However, as was mentioned earlier there is some discrepancy in the resonant region when C_{eq} value is used.

The deviations at resonance when C_{eq} from phase I of the experiment is used, results from the fact that C_{eq} was calculated for a run where displacement was fixed at 50.8mm (2") peak to peak. Where as, in the transmissibility experiment, the peak to peak displacement at resonance exceeds 127mm (5"). Since C_{eq} is a function of relative velocity for orifice damping [36], the lower value of relative displacement in obtaining C_{eq} under estimates the damping for simulation.

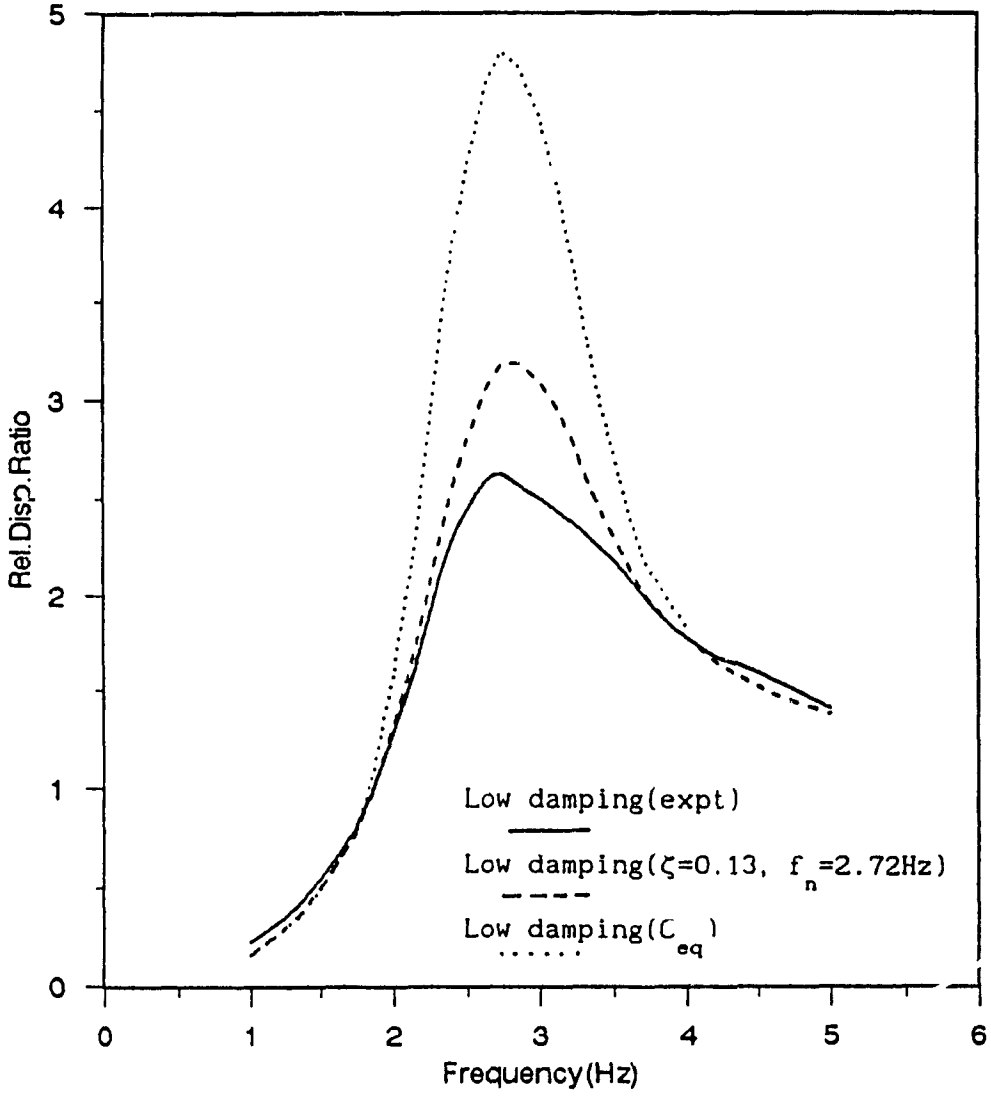

Fig.4.11 Experimental and simulation relative displacement ratio plot for low damping

Constant Orifice Damper(High damping)

The acceleration transmissibility for various input frequencies is illustrated in Fig.4.12. The figure presents the result from analytical simulation using experimentally found values: ζ = 0.23 and f_n = 2.77Hz (from step response); ζ = 0.23(from step response), f_n = 3Hz (from expt); C_{eq} (Lissajous plot), f_n = 3Hz (from expt). It can be observed from the figure that there is good correlation between experimental and analytical results in the low frequencies upto resonance. The deviation beyond resonance can be attributed to influence of non-linear air spring in the chamber and damping through the vent, asymmetric damping in the compression and extension stroke, and foaming of oil at high frequencies.

Fig.4.13 shows the relative displacement ratio from the experiment as well as analytical study for different input frequencies. Here also the analytical model follows the same trend as the experimental result, except in the case where C_{eq} value was used.

The discrepancy due to the use of C_{eq} from phase I of the test in the high damping is less than that of low damping case. The discrepancy is due to the same reason as explained for low damping results. The reason for less discrepancy in this case is due to the fact that relative displacement at resonance in the case of high damping was less than that of low damping case and closer to that of phase I test.

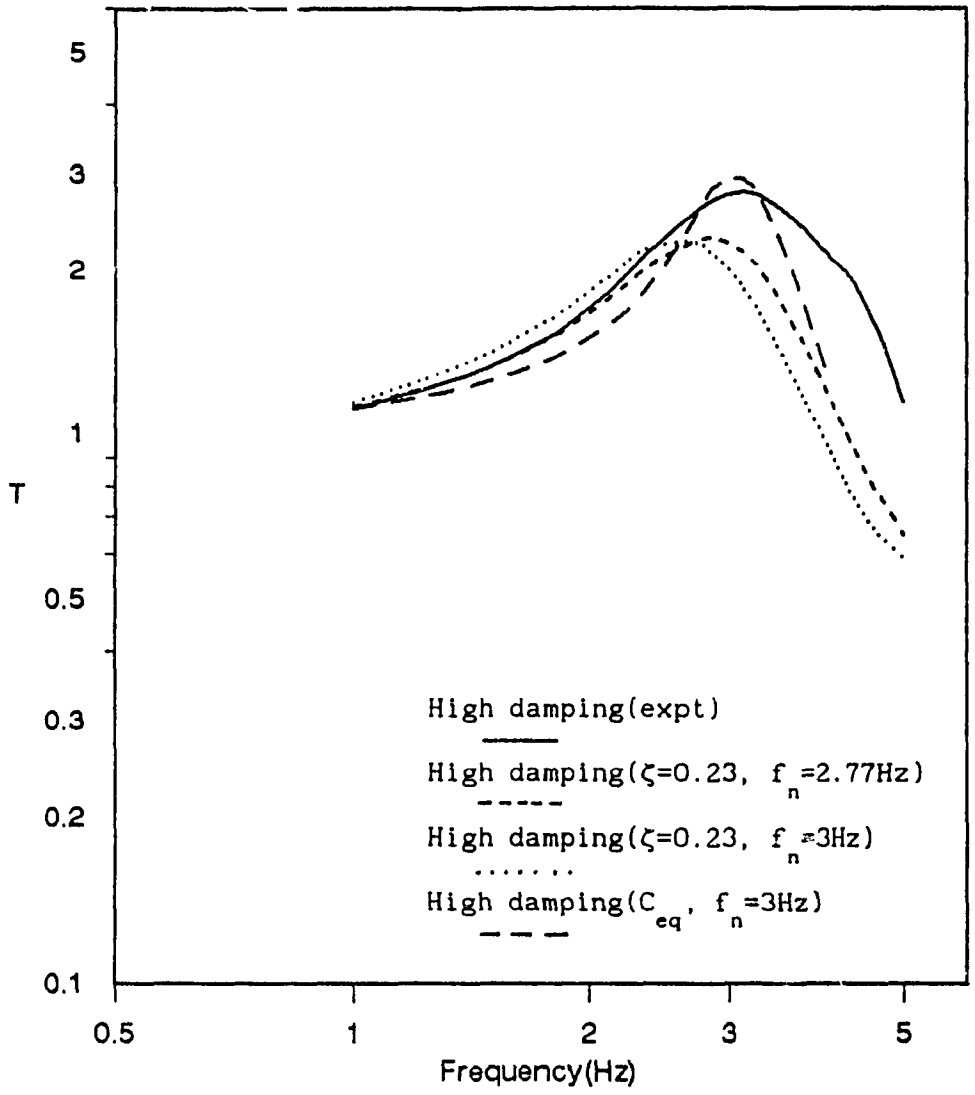

Fig.4.12 Experimental and simulation acceleration transmissibility plot for high damping

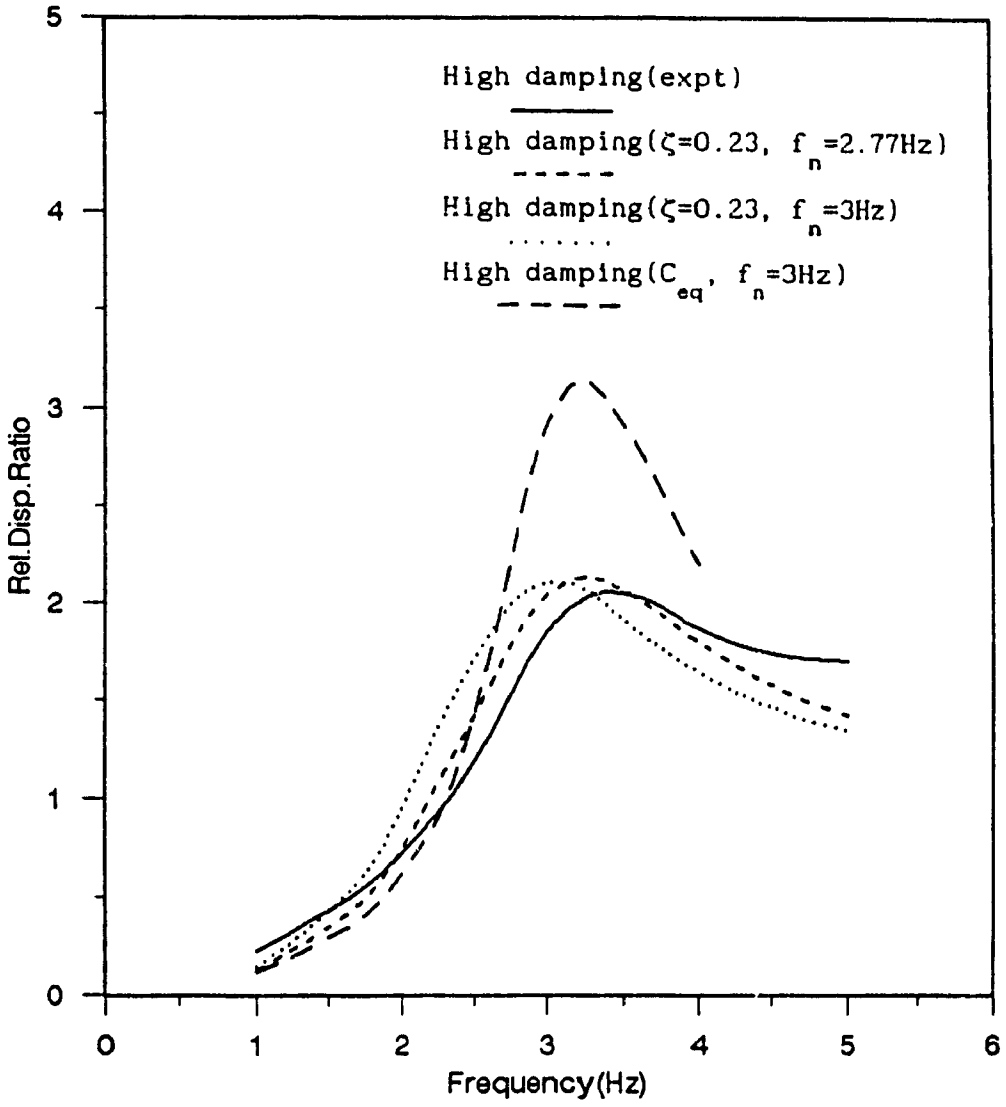

Fig.4.13 Experimental and simulation relative displacement ratio plot for high damping

Dual-Phase Damper

Similar to low and high damping cases, the result as acceleration transmissibility and as relative displacement ratio for a dual-phase damper is illustrated in Figs.4.14 and 4.15. It can be seen that there is good agreement between the experimental and analytical predictions in case of relative displacement ratio and transmissibility when $\zeta_1 = 0.13$ and $\zeta_2 = 0.23$ were used. However, there is discrepancies when C_{eq} value from Lissajous plots were used for the same reasons as those explained for low and high damping cases.

4.5 Conclusions

The objective of the experimental investigation was to develop and test a Type II dual-phase damper so that it will provide high damping in low and resonant range and low damping at high frequencies. Experimental results are presented in Figs.4.8 and 4.9 for comparison between low, dual-phase and high damping. It can be clearly seen that the acceleration transmissibility for low damping performs well in the high frequency range and similarly high damping performs well in the resonant frequency range. However, the dual-phase damper as expected performed well in the resonant range and in the high frequency range. The relative displacement ratio comparison for the three types of dampers shown in Fig.4.9, illustrates the superior performance of dual-phase damper, as it minimizes relative displacement at resonance.

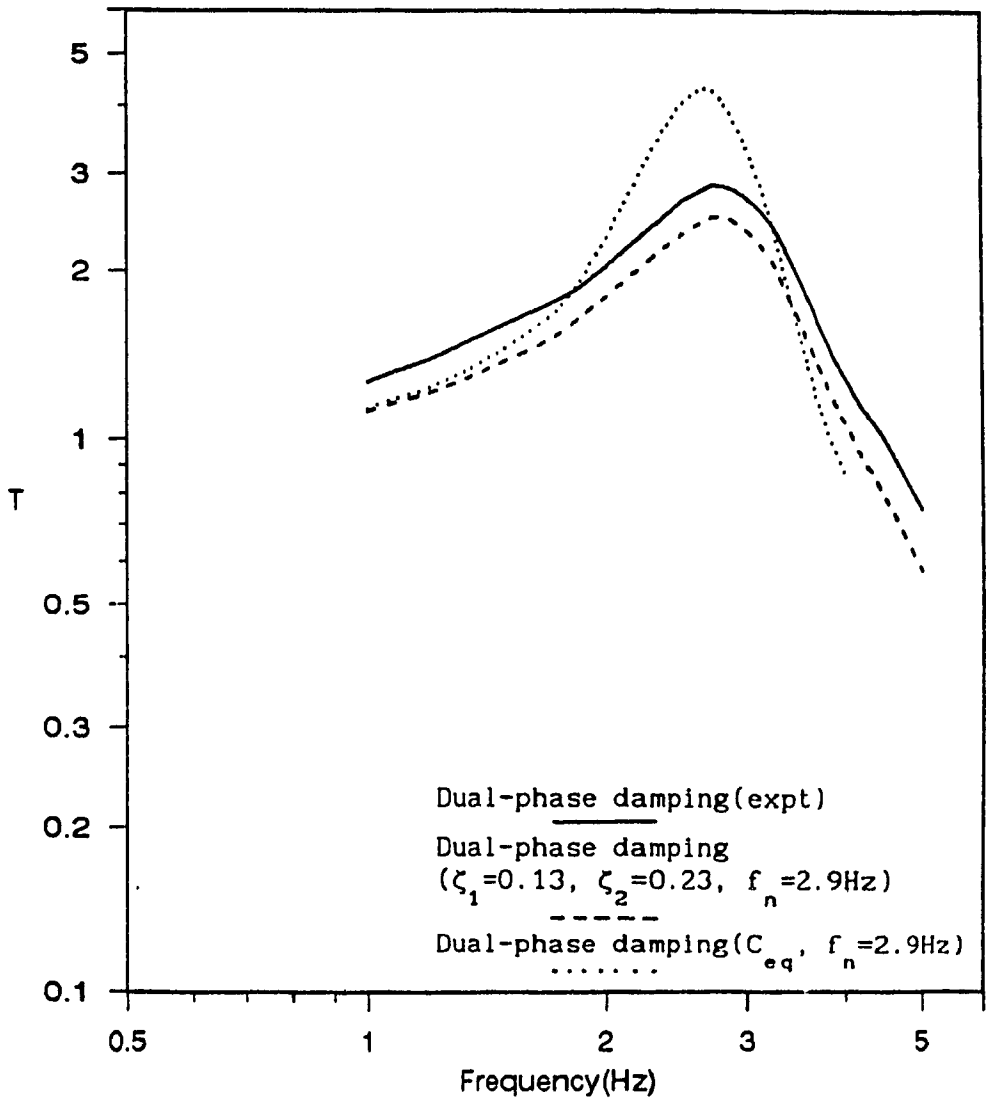

Fig.4.14 Experimental and simulation acceleration transmissibility plot for a dual-phase damper

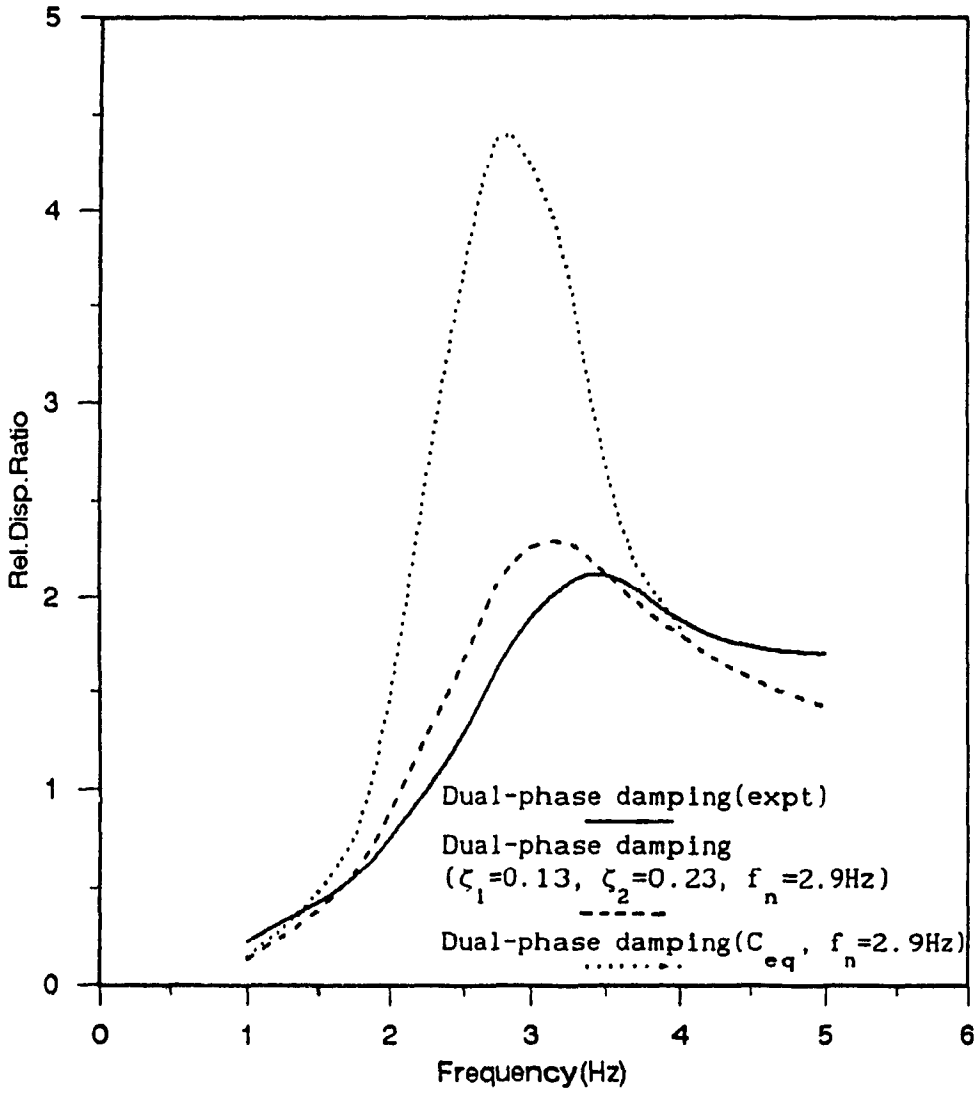

Fig.4.15 Experimental and simulation relative displacement ratio plot for a dual-phase damper

4.6 Summary

In this chapter, experimental and analytical results for low, high and dual-phase damper were presented. A prototype damper capable of simulating constant orifice and dual-phase damping was designed and tested in the laboratory. In the phase I of the experiment, the damping characteristics were first evaluated. In general, the experimental results in the form of Lissajous plot, from phase I indicate that the damping coefficient value of a dual-phase damper approaches high damping situation for low frequencies and low damping situation for high frequency.

The transmissibility ratio for a system with the prototype damper was evaluated in phase II of the experiment. The experimental results from phase II showed very good agreement with the analytical simulation (reason for discrepancy is explained). The results further showed that it is possible and feasible to develop a passive damper which has the capability to provide high damping in the low and resonant range and low damping in the high frequency range through the use of dual-phase concept. The dual-phase damper can provide a desirable compromise between a constant low or high damping devices.

CHAPTER 5

CONCLUSIONS AND RECOMMENDATIONS FOR FUTURE WORK

5.1 GENERAL

Conventional type of elastomers employed as mounts for vibration isolation do not satisfy some of the major operating requirements like providing high damping during low frequencies and low damping at high frequencies. This led to the development of passive hydraulic mounts. Even these could not satisfy the requirements because of constant orifice damping. Hence, the overall objective of this study is to investigate the possibility of utilizing a new technique to isolate vibration both in the low as well as high frequency range. The concept of dual-phase damper in place of a constant orifice damper is introduced. A dual-phase damper can provide high damping at low frequencies and low damping at high frequencies. Two different models of hydraulic mounts with two different types of dual-phase damper characteristics were analyzed with identical system parameters, and the performance was evaluated in terms of the maximum force transmitted. The advantages and disadvantages of each type of dual-phase damper are compared with hydraulic mounts having viscous damper or elasto-damper. A prototype dual-phase damper was designed, built and tested to verify the analytical model.

The major contribution of this investigation is the introduction of two types of dual-phase damping concepts for engine mount applications,

and comparing their performance with passive mounts. A further significant contribution is that, an experimental investigation with dual-phase damping is successfully conducted to validate the analytical results and to evaluate the performance of dual-phase damping concept. The results of the present investigation show that mounts with dual-phase damping concept are superior than mounts with constant orifice damping.

5.2 CONCLUSIONS

In this investigation, the dual-phase damping concept for engine vibration isolation is presented. Two major conclusions can be drawn from this research work. The first set of conclusions are from the modelling aspect and the second set of conclusions are drawn from the experimental study of Type II dual-phase damping concept.

Based on the models, the following specific conclusions are drawn:

- the two-element Type I dual-phase damping concept showed that this type of damping is applicable when one needs performance improvement primarily in the high frequency range.

- the two-element Type II dual-phase damper concept showed that this has the capability to perform well in the low as well as high frequency range. The transmissibility plots for various α_2 and β_2 values is presented and it shows that the performance either at resonance or at higher frequencies is affected when these parameters change. A

compromise is therefore needed in selecting α_2 and β_2 depending on the performance requirement.

- Of the two types of dual-phase dampers studied on four-element model, the Type I is superior than Type II in the high frequency range and Type II was superior than Type I in the low and resonant region. Moreover, the four-element model is better than either Type I or Type II two-elements model both in the low as well as high frequency regions.

An experimental study of Type II dual-phase damper was successfully carried out in this investigation. The prototype designed for this purpose was capable of simulating fixed as well as dual-phase damping. The conclusions that can be drawn from the experimental results are:

- a comparison of experimental results with that of analytical simulation showed good agreement, hence the validity of the results presented are not questionable.

- the experimental results for dual-phase damping was found to be identical to that predicted from analytical simulation. Hence it is feasible to develop a passive device with dual-phase damping to improve performance over entire frequency range.

- the improvement in acceleration transmissibility through dual-phase damping is achieved without any loss of performance in terms of relative displacement across the damper. This is highly desirable in mount application to avoid rattle.

5.3 RECOMMENDATIONS FOR FUTURE WORK

The study undertaken in this thesis is mainly to investigate the effectiveness of dual-phase damping concept in improving the engine vibration problem. Various aspects of study can be further investigated without any major modification to the model. It is with this in mind that the following recommendations are made here:

1. Study should be undertaken to analyze multi-phase damping with metering pins of various shapes in an attempt to achieve higher damping at resonance and lower damping at high frequency.

2. Future efforts should be aimed at studying a complete engine mounts system with 3 or 4 mounts utilizing dual-phase damping.

3. Optimization of dual-phase damper parameters and mount location for a complete model.

4. Attempts should be made to overcome drawbacks of the present experimental setup. They include: formation of air bubbles, air spring effect, air damping effect, etc.

5. The size of an isolator for engine mount application is restricted due to limited space. Hence, effort should be made in developing a prototype with Type II dual-phase damping to accommodate such restriction.

6. Effort should be made to develop and study models that include engine, mounts, chassis, suspension and wheels to optimize mount parameters with an objective of minimizing engine vibration effects. The study can further include combined influence of road and engine inputs.

7. With the fast advancement in the technology for active system, it may be feasible for developing semi-active and actively controlled isolation system, for mount application. However such effort should take into account the cost-performance trade-off.

REFERENCES

1. Den Hartog, J. P., Mechanical vibrations, McGraw-Hill Book Co., 4th Edition., 1956.
2. Regis V. Schimitt., and Charles, J. Leingang., "Design of Elastomeric Vibration Isolation Mounting Systems for Internal Combustion Engines", SAE Paper No 760431, 1976.
3. William, A. Fyre., "Rubber Springs", in: Shock and Vibration Handbook, C.M. Harris and C.E. Crede, Eds., McGraw -Hill Book Co., 1976, pp 35.1-35.20.
4. Charles E. Crede., Shock and Vibration Concepts in Engineering Design, Prentice-Hall Inc., Englewood Cliffs, N.J. 1965.
5. Sachs, H.K., "An Adaptive Control for Vehicle Suspensions", Vehicle System Dynamics, 12(2-3), Sept 1981, pp 201-206.
6. Karnopp, D.C., Crosby, M.J., and Harwood, R.A., "Vibration Control Using Semi-Active Force Generators", Transactions of the ASME Journal of Engineering for Industry, 6(2), May 1974, pp 619-626.
7. Margolis D.L., "Semi-active suspension for Military Ground Vehicle Under Off-Road Condition", presented at the 52nd Symposium on Shock and Vibration, New Orleans, Oct 1981.
8. Margolis D.L., "Semi-active Control of Wheel-Hop in Ground Vehicles", Vehicle System Dynamics, 12(6), Dec 1983, pp 317-330.
9. James Alanoly., "Vibration Isolation characteristics of a Class of Semi-active Suspension", Master's Thesis, Concordia University, November 1985.
10. Karnoop, D.C., "Active Damping in Road Vehicle Suspension Systems", Vehicle System Dynamics, 12(6), Dec 1983, pp 291-316.

11. Sutton, H.B., "The Potential for Active Suspension Systems" Automotive Engineer, 4(2), April-May 1979.

12 Guntur, and Sankar, S. "Fail-Safe Vibration Control Using Active Force Generators", Transactions of the ASME, Journal of Vibration, Acoustics, Stress and Reliability in Design,105(3), July 1983, pp 361-369.

13. Clark, M., "Hydraulic Engine Mount Isolation",SAE Paper NO. 851650, 1985.

14. Racca, R. Sr., "How to Select Power-Train Isolators for Good Performance and Long Service Life", SAE Paper No. 821095, 1982.

15. William G. Halvorsen., "Design of Rubber Isolation Systems", Automotive Engineer, Dec 1984.

16. Marc Bernuchon., "A New Generation of Engine Mounts", Transactions of the SAE Paper No. 840259, 1984.

17. Patrick, E. Concoran., and Gerd-Heinz Ticks., "Hydraulic Engine Mount characteristics", SAE Paper No. 840407, 1984.

18. Masaru Sugino., and Eiichi, Abe., "Optimum Application for Hydroelastic Engine Mount", SAF Paper No. 861412, 1986.

19. Wallace, C. Flower., "Understanding Hydraulic Mounts for Improved Noise, Vibration and Ride Qualities", SAE Paper No. 850975, 1985.

20. Peter, L. Graf., and Rahmat, Shoureshi., "Modelling and Implementation of Semi-Active Hydraulic Engine Mounts", Presented at ASME 87-WA/ DSC-28, Boston, Massachusetts.

21. West. J.P., "Hydraulically-Damped Engine Mounting" Automotive Engineer, March 1987.

22. "Fluidlastic mounts" The New Generation of Elastomeric Mounts, Lord Automotive Products, Lord Corporation, Erie, PA 16514, U.S.A.

23. Masaaki Mizuguchi., Takoyoshi Suda., Sunao Chikamori., and Kazuyoshi Kobayash., "Chassis Electronic Control Systems for the Mitsubishi 1984 Galant", SAE Paper No. 840258, 1984.

24. Yukihiko Hagino., Yoshiro Furishi., Yasuyuki Makigawa., Naotake Kumagi., and Makoto Yshikawa., "Active Control for Body Vibration of F.W.D. Car", SAE Paper No. 860552, 1986.

25. Robert G. Marjoram., "Pressurized Hydraulic Mounts for Cab", SAE Paper No. 852349, 1985.

26. Taylor, H.J. Jr., "The New Generation of Engine Mounts", SAE Paper No. 862052, 1986.

27. Snowdon, J.C., "Isolation from Mechanical Shock with a Mounting System Having Nonlinear Dual-Phase Damping", The Shock and Vibration Bulletin, 41(2), Dec 1970, pp 21-45.

28. Venkatesan, C., and Krishnan, R., "Harmonic Response of a Shock Mount Employing Dual-Phase Damping", Journal of Sound and Vibration, (1975), 40(3), pp 409-413.

29. Venkatesan, C., and Krishnan, R., "Dual-Phase Damping in a Landing Gear at Touch Down", J. of Aircraft, 12(10), Oct 1975, pp 847-849.

30. Guntur, R.R., and Sankar, S., "Performance of Shock Mounts Employing Different Kinds of Dual-Phase Damping", Journal of Sound and Vibration 84(2), 1982, pp 253-267.

31. Thomson, W.T., Theory of Vibration with Applications, Prentice Hall Inc., Englewood Cliffs, N.J., 1981.

32. Jacobson, L.S., and Ayre, R.S., Engineering Vibrations, McGraw-Hill, New-York, 1958, pp 226-231.

33. Ruzicka, J.E., and Derby, T.F., "Vibration Isolation with Nonlinear Damping", Transactions of the ASME, Journal of Engineering for Industry, May 1971, pp 627-635.

34. Ruzicka, J.E., and Derby, T.F., Influence of Damping in Vibration Isolation, The Shock and Vibration Information Center, Washington, D.C., 1971.

35. Mark Van Vliet., "Computer Aided Analysis and Design of Off-Road Motorcycle Suspension", Ph.D Thesis, Concordia University, October 1985.

36. Rakheja, S., Sankar. S., "Local equivalent constant representation of non-linear damping mechanisms", Engineering computations Vol 3, March 1986, pp 11-17.

APPENDIX: I

EXPERIMENTAL FORCE-DISPLACEMENT CHARACTERISTICS OF THE PROTOTYPE DAMPER

The experimental Lissajous plots are presented in this section for low, high and dual-phase damping. In all cases the peak to peak displacement was maintained to be 50.8mm(2"). The plots of force versus displacement was obtained from frequencies ranging from 0.5Hz to 4Hz in steps of 0.5Hz. In general, the plots from the low frequencies were found to be as shown below:

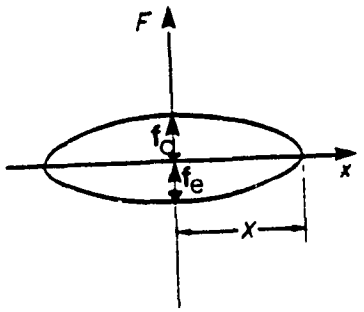

which indicates that there is neglegible stiffness at low frequency, and that peak to peak force corresponds to the damping force. Here the average damping force is equal to peak to peak damping force.

As the frequency is increased, the stiffness became apperant by the rotation of the Lissajous plots. A representation of this is shown below.

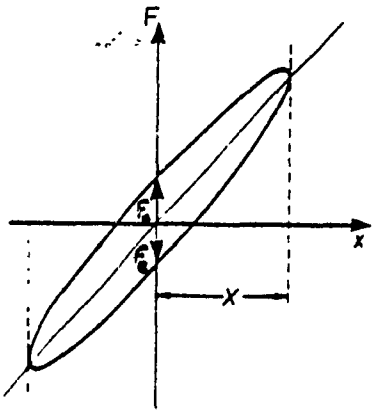

In this case the average damping force was calculated for displacement equal to zero, where average damping force:

$$F_d = \frac{f_c + f_e}{2}$$

where f_c = compression force and f_e = extension force

A table at the end of the appendix presents the sensitivities required to evaluate force and displacement from the Lissajous plots.

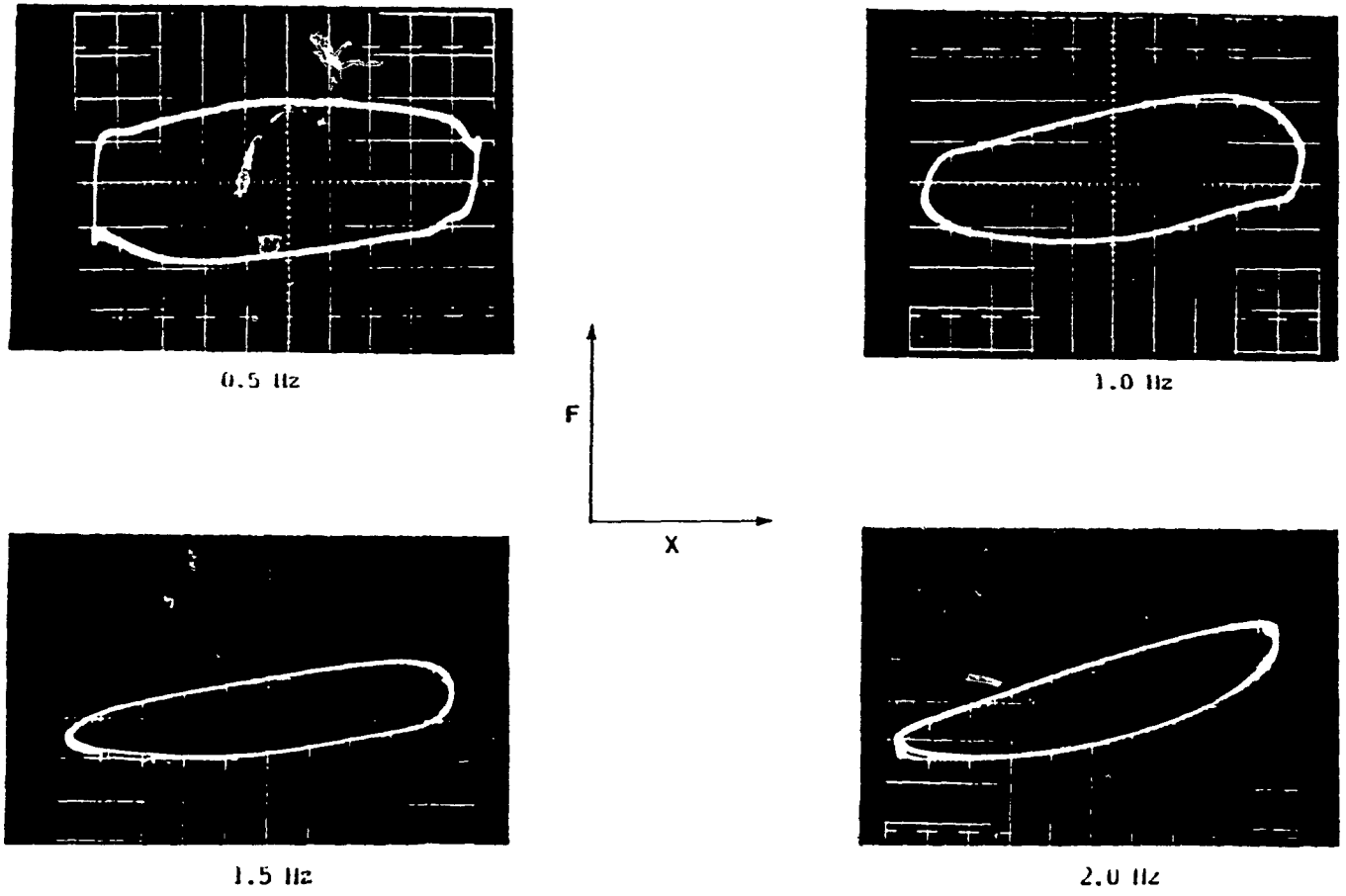

Lissajous plots - Low damping

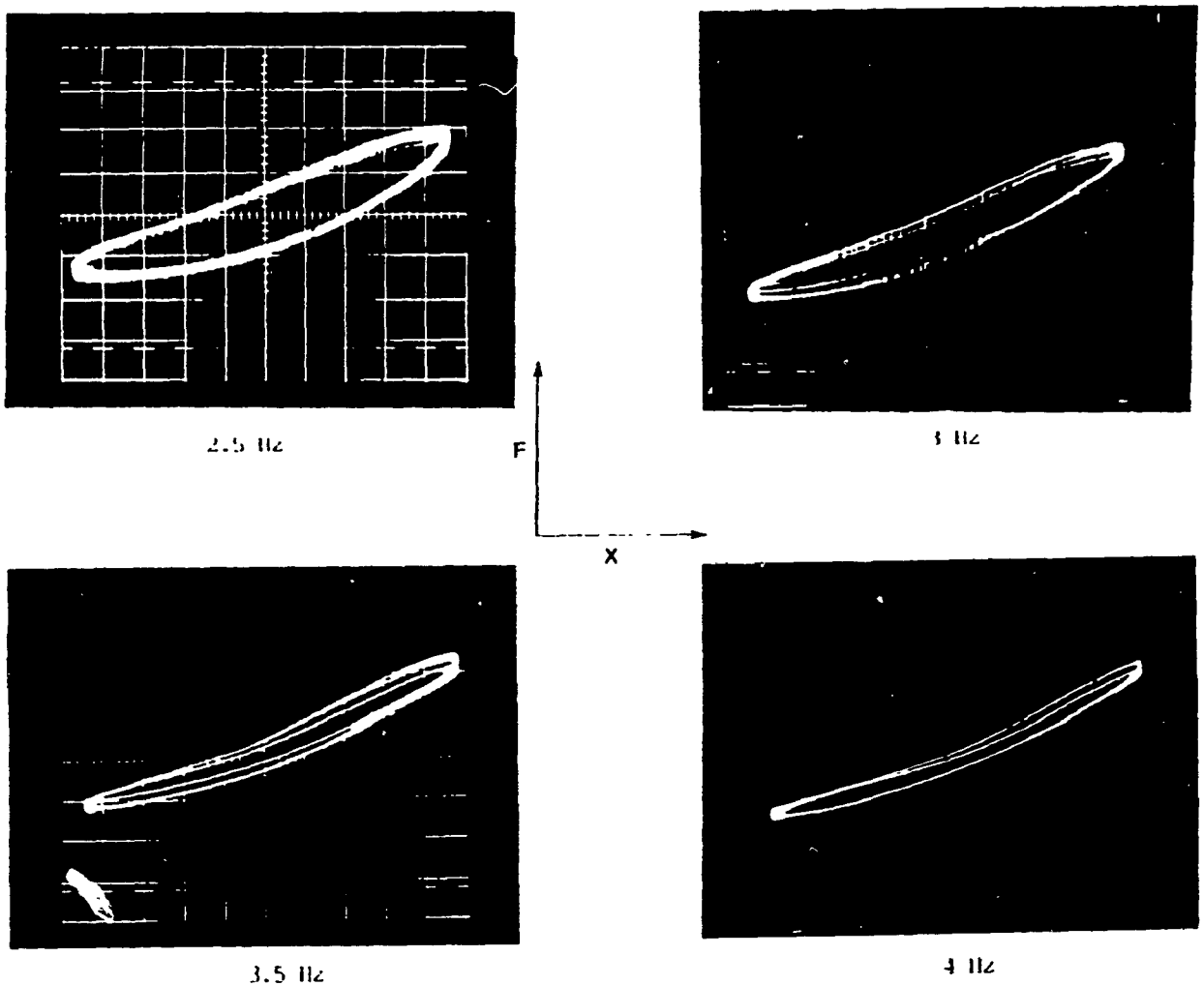

Lissajous plots - Low damping

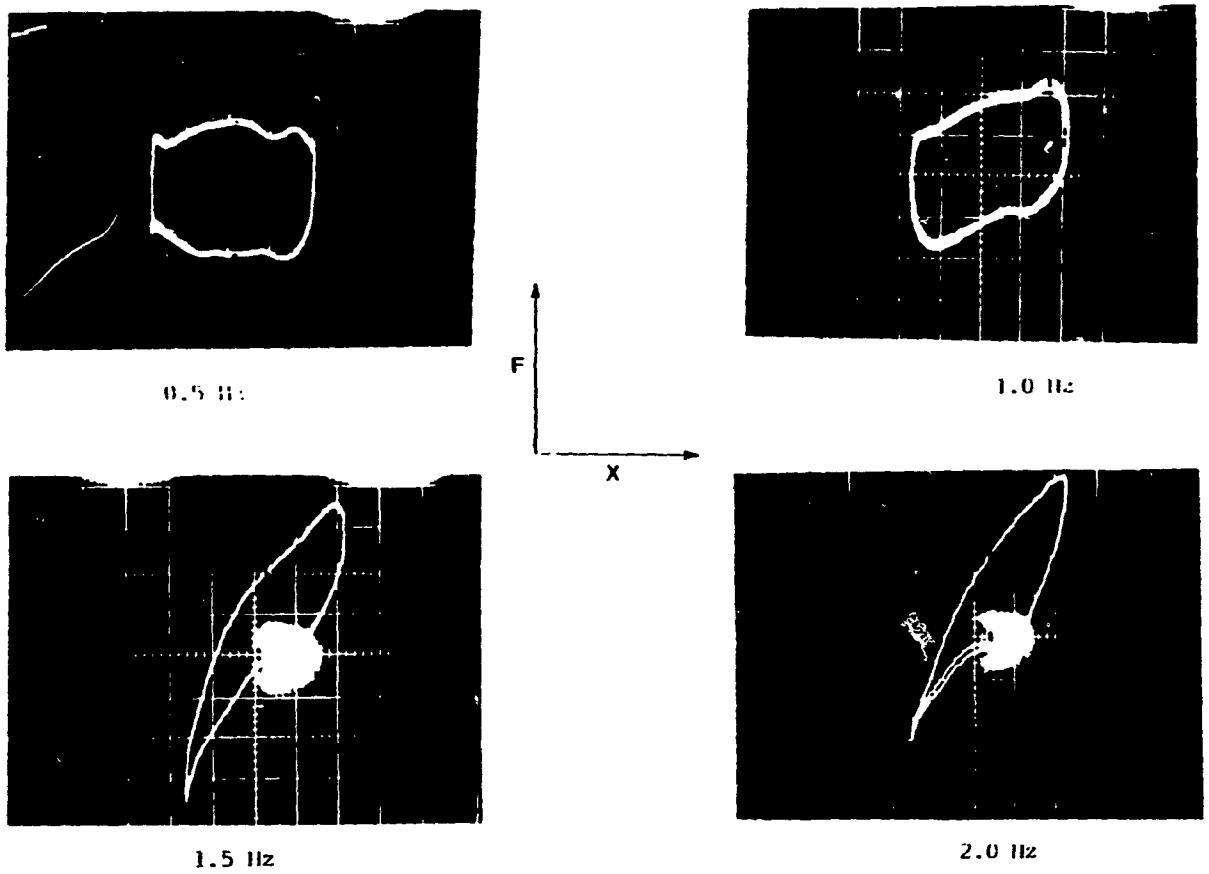

Lissajous plots - Dual-phase damping

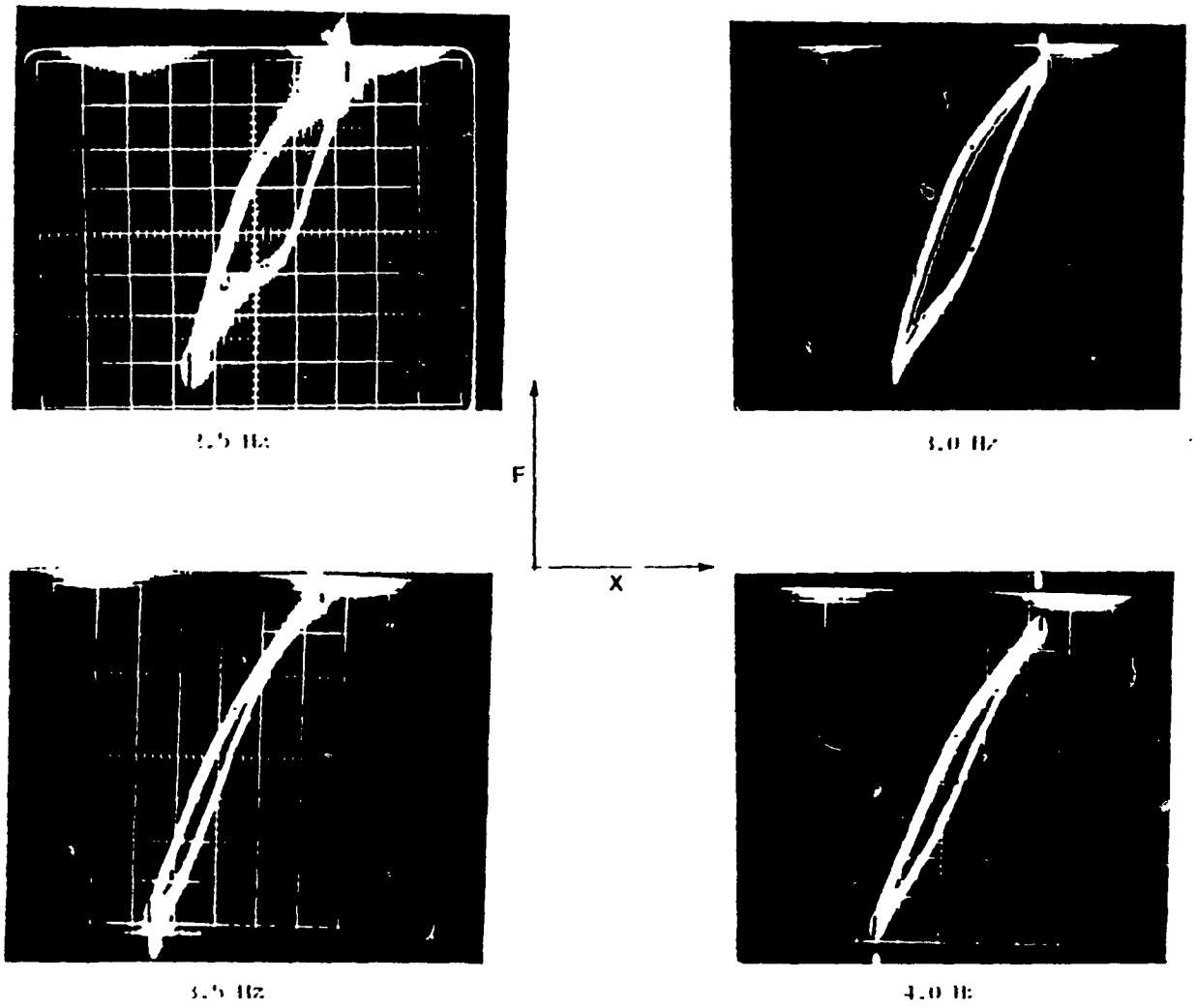

Lissajous plots - Dual-phase damping

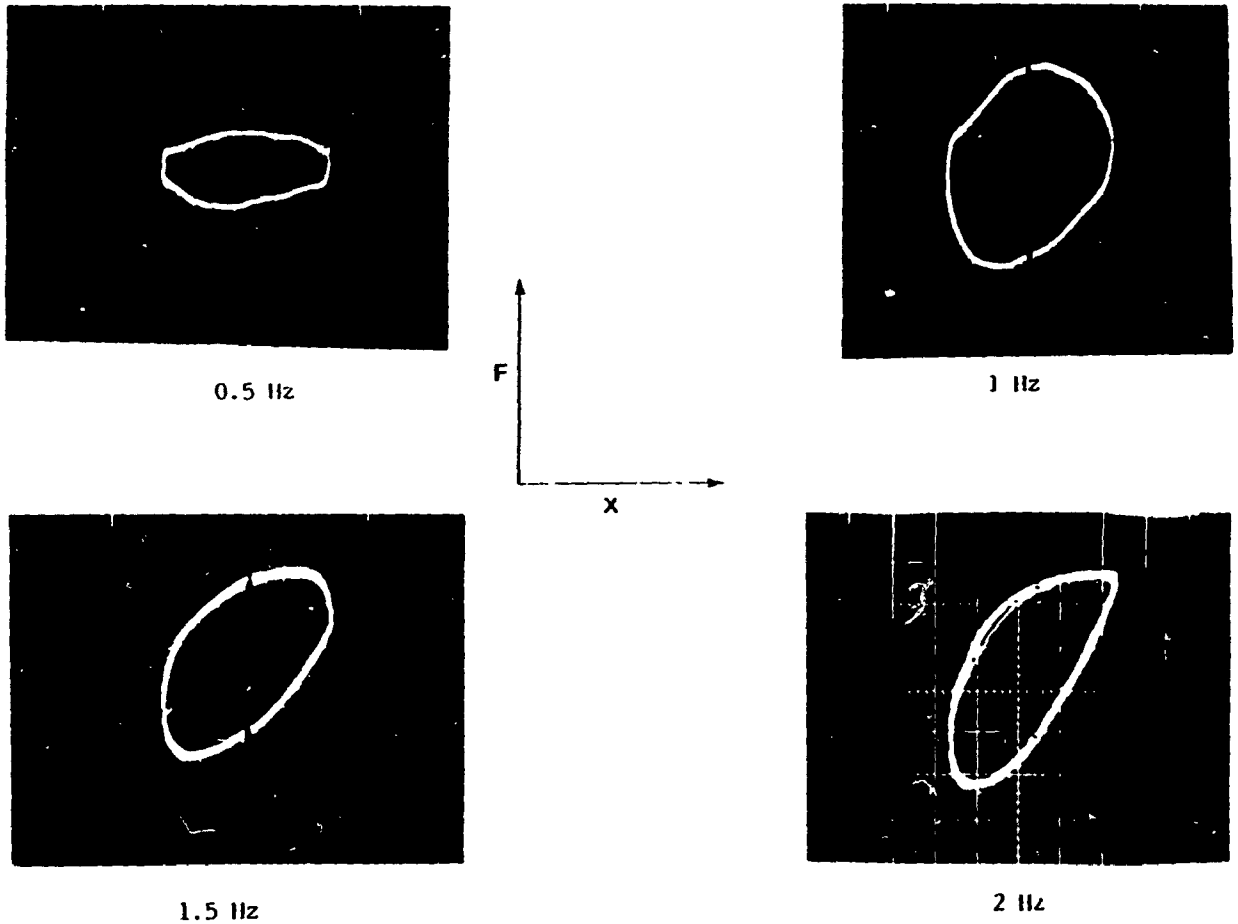

Lissajous plots - High damping

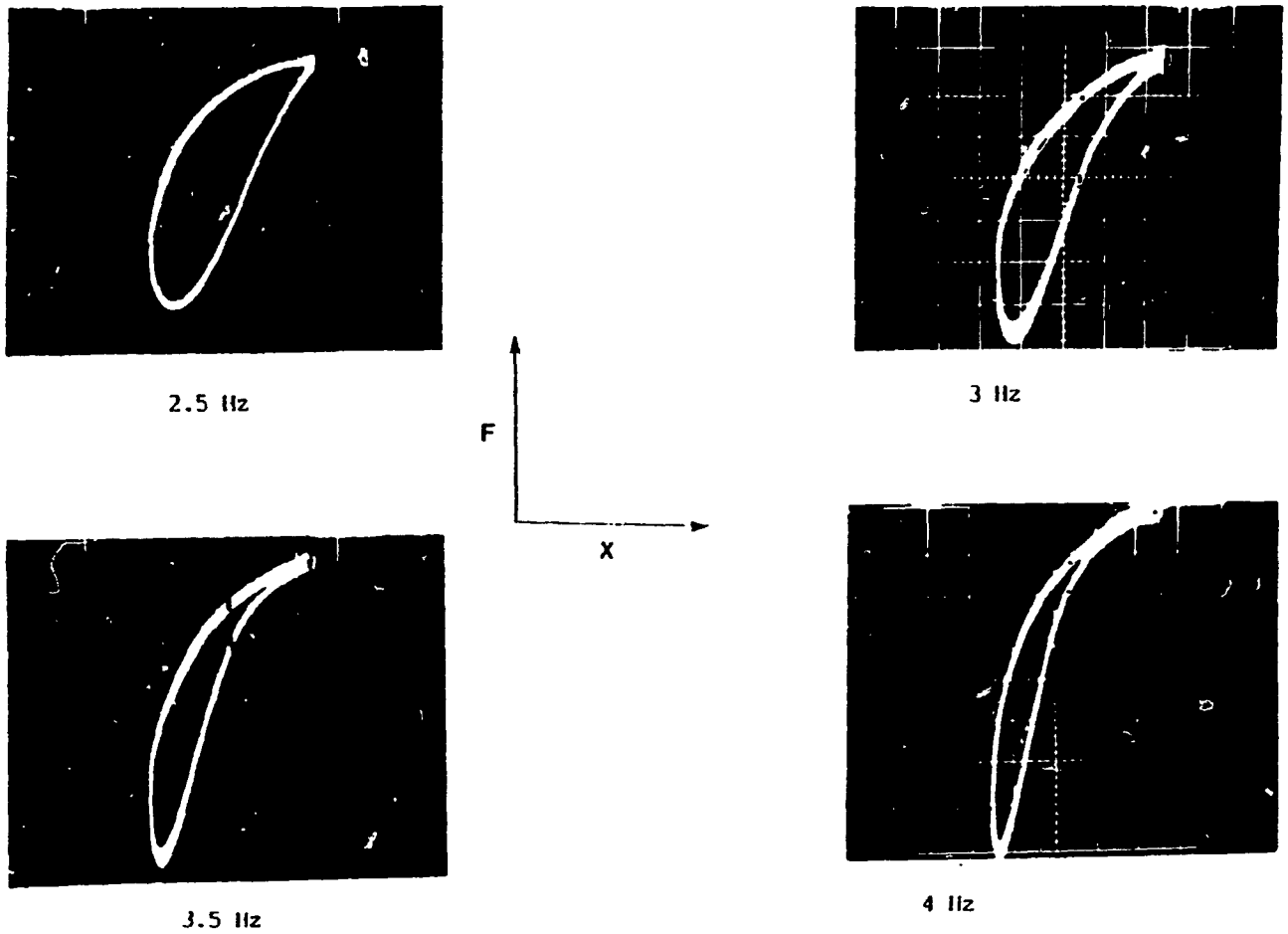

Lissajous plots - High damping

Table I.1 Lissajous plots scale

Frequency (Hz)	Displacement X-axis (V/cm)	Damping force F-axis (V/cm)
0.5	0.2	0.1
1.0	0.2	0.2
1.5	0.2	0.2
2.0	0.2	0.5
2.5	0.2	0.5
3.0	0.2	0.5
3.5	0.2	0.5
4.0	0.2	0.5

Low damping

Frequency (Hz)	Displacement X-axis (V/cm)	Damping force F-axis (V/cm)
0.5	0.5	0.2
1.0	0.5	0.5
1.5	.05	0.5
2.0	0.5	0.5
2.5	0.5	0.5
3.0	0.5	0.5
3.5	0.5	0.5
4.0	0.5	0.5

Dual-phase damping

Frequency (Hz)	Displacement X-axis (V/cm)	Damping force F-axis (V/cm)
0.5	0.5	0.5
1.0	0.5	0.5
1.5	0.5	1.0
2.0	0.5	1.0
2.5	0.5	1.0
3.0	0.5	1.0
3.5	0.5	1.0
4.0	0.5	1.0

High damping

Sensitivity: X-axis: 25.4mm = 0.92V
F-axis: 245.25N = 1.0V